Targeting the Epigenetic Lesion in MLL-Rearranged Leukemia

(Article begins on next page)

HARVARD UNIVERSITY
Graduate School of Arts and Sciences
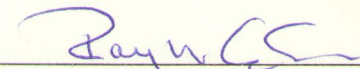
DISSERTATION ACCEPTANCE CERTIFICATE
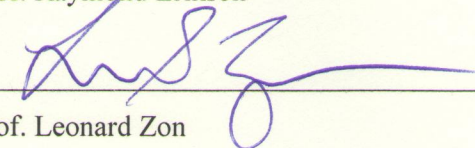
The undersigned, appointed by the

Department of Molecular and Cellular Biology

have examined a dissertation entitled

"Targeting the Epigenetic Lesion in MLL-rearranged Leukemia"

presented by Liying Michelle Chen,

candidate for the degree of Doctor of Philosophy and hereby

certify that it is worthy of acceptance.

Signature _____

Typed name: Prof. Stuart Schreiber

Signature _____

Typed name: Prof. Raymond Erikson

Signature _____

Typed name: Prof. Leonard Zon

Date: November 5, 2012

TARGETING THE EPIGENETIC LESION IN MLL-REARRANGED LEUKEMIA

A dissertation presented

by

Liying Michelle Chen

to

the Department of Molecular, Cellular and Biology

in partial fulfillment of the requirements

for the degree of

Doctor of Philosophy

in the subject of

Biochemistry

Harvard University

Cambridge, Massachusetts

December 2012

Targeting the Epigenetic Lesion in MLL-rearranged Leukemia

Abstract

It has become increasingly apparent that the misregulation of histone modification actively contributes to cancer. The histone H3 lysine 79 (H3K79) methyltransferase Dot1l has been implicated in the development of leukemias bearing translocations of the *Mixed Lineage Leukemia* (*MLL*) gene. We studied the global epigenetic profile for H3K79 dimethylation and found abnormal H3K79 dimethylation profiles exist not only in leukemias driven by MLL-fusion proteins with nuclear partners like AF9, but also in leukemia with MLL-fusions containing cytoplasmic partners like AF6. Genetic inactivation of Dot1l led to downregulation of fusion target genes and impaired both *in vitro* bone marrow transformation and *in vivo* leukemia development by MLL-AF10, CALM-AF10 as well as MLL-AF6, suggesting that aberrant H3K79 methylation by DOT1L sustains fusion-target gene expression in *MLL* rearranged leukemias and *CALM-AF10* rearranged leukemias. Pharmacological inhibition of DOT1L selectively killed MLL-AF10 and MLL-AF6 transformed cells but not Hox9/Meis1 transformed cells, pointing to DOT1L as a potential therapeutic target in *MLL*-rearranged leukemia.

We further characterized the DOT1L complex under physiological conditions from human leukemia cells and identified AF10 as a key DOT1L complex component. Given the importance of H3K79 methylation in *MLL*-rearranged leukemia, we sought to study the role of DOT1L complex component AF10 in H3K79 methylation and *MLL* leukemia. We generated conditional knockout mice in which the Dot1l-interacting octapeptide-motif leucine-zipper (OM-LZ) domain of *Af10* was flanked by *LoxP* sites. Cre induced deletion of *Af10^{OM-LZ}* is predicted to abrogate the Af10-Dot1l interaction. Our histone mass spectrometry

data demonstrated that deletion of the endogenous $Af10^{OM-LZ}$ domain abrogated global H3K79 dimethylation but retained H3K79 monomethylation. Interestingly, bone marrow transformation by MLL-AF6 and MLL-AF9 is abrogated by induced deletion of endogenous $Af10^{OM-LZ}$, while bone marrow transformation by MLL-AF10 and CALM-AF10 is not affected by deletion of endogenous $Af10^{OM-LZ}$, confirming the importance of Af10-Dot1l interaction in MLL- or CALM fusion-leukemias. Moreover, we showed $Af10^{OM-LZ}$ deletion prolonged survival of MLL-AF9 leukemia *in vivo* and led to chromotin compaction and downregulation of MLL fusion targets in MLL-AF9 leukemia. Therefore our results demonstrate a role for Af10 in the conversion of H3K79 monomethylation to dimethylation and reveal the AF10-DOT1L interaction as an attractive therapeutic target in *MLL*-rearranged leukemias.

Table of Contents

Dedicated to

My Family

Tianqing Chen & Zhen Ye

Qiguo Zhang & Quanying Zhang

Haifei Zhang, Eric Zhang, Alan Zhang, Alex Zhang

&

Children with Leukemia

Acknowledgements

I'd like to thank many people who are very special to me. It is their help and support that has made my PhD journey possible.

First of all, I am heartily thankful to my dissertation advisor, Scott A. Armstrong, whose encouragement, guidance and support from the initial to the final stage of my PhD training had made my Harvard experience a truly enjoyable one. Often I went into a meeting with Scott, feeling inadequate about my study, only to come out feeling very motivated and enthusiastic to approach the answer. During my most difficult times in the graduate school, I had doubted my ability to pursue a scientific career with my family responsibilities, but his encouragement and mentorship keep inspiring me and pushing me forward, in a very positive way. His supports enabled me to develop fully as a scientist and as a person. It has been my great honor to be his graduate student.

Special thanks are also in order for my dissertation advisory committee, Stuart Schreiber of Broad Institute, Raymond Erikson of Harvard MCB, and Leonard Zon of Harvard Medical School, and former committee member Richard Losick and Nicole Francis of Harvard MCB for their critical advice and encouragement over the past five years.

I also want to express my dearest gratitude to my colleagues and friends in the Armstrong lab, in particular Aniruddha Deshpande, Kathrin Bernt, Amit Sinha, Nan Zhu, Andrei Krivtsov, Deepti Banka, Stuart Dias, Maurizio Fazio, Joerg Farber, David Chen, Zhaohui Feng, Demetrios Kalaitzidis, Cherry Ng, Matthew Stubbs, Jennie Krasker, and Jenny Chang. They are some of the most intelligent, hard-working and fun people I have met. It has been a pleasure working alongside such an outstanding group of people.

I am especially indebted to Aniruddha Deshpande, an exceptional postdoctoral fellow in the Armstrong lab who has introduced me leukemia mouse model and guided me patiently over the last three years. I have been privileged to work with Aniruddha on the studies presented in Chapter 3-5, and I cannot give him enough credit for training me scientifically. He has been very successful as an independent investigator, and I have no doubt that he will lead a terrific group very soon.

We had the good fortune of collaborating closely with excellent scientists in other laboratories and core facilities. The large scale DOT1L complex studies in Chapter 2 were done in collaboration with Andrew Woo and Alan Cantor in Children's Hospital Boston. The complex component identification and histone modification studies were done with the help from Ross Tomaino in Harvard Medical School Taplin Biological Mass Spectrometry Facility. Renee Rubio

October 2012

Cambridge, MA

List of Figures and Tables

Chapter 5

List of Abbreviations

AEP, AF4 family/ENL family/pTEFb complex;

AF1P, ALL1 (MLL) fused gene from chromosome 1p;

AF4, ALL1 (MLL) fused gene from chromosome 4;

AF6, ALL1 (MLL) fused gene from chromosome 6;

AF9, ALL1 (MLL) fused gene from chromosome 9;

AF10, ALL1 (MLL) fused gene from chromosome 10;

AF17, ALL1 (MLL) fused gene from chromosome 17;

ALL, acute lymphoblastic leukemia;

AML, acute myeloid leukemia;

BCR-ABL, *breakpoint cluster region* gene fused with *abelson* gene;

CALM, clathrin assembly lymphoid myeloid leukemia protein;

CBP, CREB-binding protein;

CDK, cyclin dependent kinase;

ChIP, chromatin immunoprecipitation;

CLP, common lymphoid progenitor;

CMP, common myeloid progenitor;

DOT1L, disruptor of telomeric silencing 1-like;

ELL, eleven-nineteen lysine-rich leukemia;

ENL, eleven nineteen leukemia;

GMP, granulocyte monocyte progenitor;

HAT, histone acetyl transferase;

HDAC, histone deacetylase;

HMT, histone methyl transferase;

HD, homeodomain;

HOX, homeobox;

HSC, long term-hematopoietic stem cell;

L-GMP, leukemia-granulocyte monocyte progenitor;

MEIS1, myeloid ecotropic integration site 1;

MEP, megakaryocyte erythrocyte progenitor;

MLL, mixed lineage leukemia;

MOZ, monocytic leukemia zinc finger protein;

MPP, multipotent progenitor;

NPM, Nucleophosmin;

PAFc, polymerase-associated factor complex;

PHD, plant homeodomain;

SET, Su(var), Enhancer of zeste, Trithorax;

TIF2, transcription intermediary factor 2;

RNAP II, RNA polymerase II (Pol II).

Chapter 1

Introduction

Characteristics of MLL-rearranged Leukemia

Chromosomal translocations which encode fusion proteins are frequently associated with human leukemias. Current advances in biology, biochemistry and pharmacology have raised the prospects of highly targeted leukemia therapeutics that maximize efficacy and minimize systemic toxicity. One outstanding example is targeting the fusion protein BCR-ABL kinase by imatinib in chronic myeloid leukemia (1). In our lab, we focus on studying leukemia bearing translocation involving the *Mixed Lineage Leukemia (MLL)* gene on chromosome band 11q23. *MLL*-rearranged leukemia is a subset of leukemia with distinct biological and clinical characteristics (2). Despite the advances in treatments in other leukemias, leukemias bearing *MLL* rearrangement are still associated with a very poor prognosis.

Translocations involving the *MLL* gene are present in about 10% of all human leukemias, but over 70% of infant leukemias (3, 4). Since its first identification in 1991, *MLL* gene has been identified by molecular studies to be recurrently fused with a diverse array of partner genes in acute lymphoblastic leukemia (ALL), acute myeloid leukemia (AML), biphenotypic or acute mixed-lineage leukemias, and secondary leukemia after chemotherapy with Topoisomerase II inhibitors (5). Whereas children with acute leukemia that does not harbor a *MLL* translocation have an overall survival of >80%, infants diagnosed with *MLL*-rearranged leukemia fail to benefit from intensive chemotherapy, radiation therapy or allogeneic stem cell transplantation, and have an overall survival of 30-50% (6, 7). Thus new therapeutic approaches are clearly needed for patients with *MLL*-rearranged hematopoietic malignancies.

Although the oncogenic property of MLL fusion proteins has been proven by several retroviral models (8, 9) and MLL fusion knock-in mouse models (10-12), the underlying mechanisms of leukemogenesis is yet unknown. Wildtype MLL is a mammalian homolog of the *Drosophila* Trithorax protein, and it has multiple functional domains including the N terminal AT hoods that bind to DNA and the C terminal Suv39, Enhancer of Zeste, Trithorax *(*SET) domain that methylates histone H3 lysine 4 (13). In mammals,

MLL maintains the expression pattern of *Homeobox (HOX)* genes during development, and is essential for hematopoiesis (14). *Mll* knockout mice show the expression of stage-specific *Hox* genes is initiated but not maintained in the absence of *Mll*. As a result of *MLL* translocations, the N terminus of MLL fuses with the C terminus of more than 60 different partner proteins, among which AF4, AF9, ENL, AF10, AF6, ELL, AF1P, AF17 and SEPT6 are the most common (5). There are three main functional categories for MLL fusion partners. One category of fusion partners normally coexist in a P-TEFb containing transcriptional elongation complex or a histone methyltransferase Dot1l-containing complex (DotCom) (15) in the nucleus. Many MLL fusion partners, such as AF10, ENL, ELL, AF9, AF4 and AF5q31, have been identified in either DotCom or transcriptional elongation complexes called AF4, ENL, P-TEFb Complex (AEP) (16) or Super Elongation Complex (SEC) (17). It is thought that the MLL fusion protein recruits DOT1L or AEP/SEC to promote RNA polymerase II-mediated transcription of MLL target genes. The second category of fusion partners are cytoplasmic proteins important in various functions such as cellular adhesion, endocytosis, cytoskeleton organization, and signal transduction. This category includes coiled-coil domain-containing proteins such as AF6, AF1q, GAS7, EEN, and the SEPTIN family. The common feature of these cytoplasmic proteins is their ability to self-associate via the coiled-coil domains (18). It is noteworthy that these oligomerization domains are necessary and sufficient for MLL fusion mediated transformation and even MLL artificial homodimer can immortalize hematopoietic cells (18). The third category of MLL fusion partners includes transcriptional factors, such as forkhead family members AFX (19) and chromatin remodeling factors, such as histone acetyltransferase CBP and p300 (20, 21). These proteins are important for the recruitment of RNA polymerase II and the initiation of MLL target gene transcription in their respective fusion events.
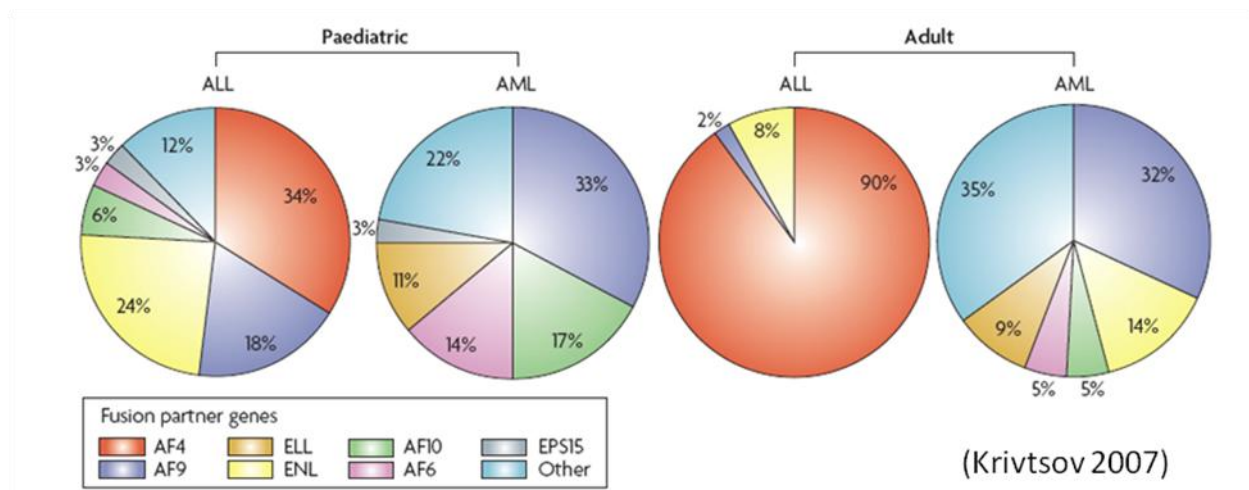
Figure 1-1 Distribution of major MLL fusion partner genes in de novo childhood and adult leukaemias.
Adapted from review (2). *AF4* is predominantly found in ALL and *AF9* and *AF10* are predominantly found in AML.

Despite the remarkably diverse MLL fusion partners, all the *MLL*-rearranged leukemias share a similar and distinct leukemogenic gene expression program, with aberrant activation of MLL target genes including *HOXA* cluster genes and *MEIS1* (2, 22). *HOX* genes are transcription factors that participate in the development of multiple organs and hematopoiesis. *HOXA* cluster genes are normally highly expressed only in early hematopoietic progenitors (23). Wildtype MLL can maintain the expression of *HOXA* cluster genes in early hematopoietic progenitors but also allow the down-regulation during normal development. However MLL fusion partners constitutively drive the expression of *HOX* genes. Strikingly, when ectopically expressed together, HOXA9 and MEIS1 can transform hematopoietic cells *in vitro* and induce leukemia in retrovial mouse models that recapitulate human *MLL*-rearranged leukemia (24). How a heterogeneous group of partner proteins leads to similar leukemia features in *MLL*-rearranged leukemia is still unclear. It is believed that MLL fusion event disrupt the normal function and gain new functions from wild-type MLL and its fusion partners. This is supported by functional studies of the minimal fusion that can transform hematopoietic cells, and clinical observation that all the MLL fusion proteins retained the open reading frame of the fusion partners, both implying the importance of fusion partner in the leukemogenesis. It is easy to understand that MLL fusion partners that reside in the nucleus recruit Pol II to the promoter regions or release Pol II from stalling at the transcriptional start sites. But it is less clear

4

why MLL fusion with cytoplasmic fusion partners that do not have transcriptional activation function and MLL N-terminal artificial homodimer can transform hematopoietic cells. Another hypothesis is that the homodimerization of MLL creates new domains with which the transcriptional elongation complexes or transcriptional coactivators interact. It was shown that MLL-AF6 does not recruit AEP/SEC or DOT1L complex, so this hypothesis still waits to be tested with more detailed biochemical studies.

Recently, we and others have demonstrated another unique characteristic of *MLL*-rearranged leukemia-the genome-wide epigenetic lesion formed by histone H3 lysine 79 (H3K79) methyltransferase Disruptor of telomeric silencing 1-like (DOT1L) (12, 16, 25). *MLL*-rearranged leukemia is a perfect example of how genetic corruption and epigenetic corruption cooperate together to initiate and maintain a disease. As discussed above, wildtype MLL is an epigenetic modifier with N-terminal DNA binding domains and C-terminal H3K4 methyltransferase domain called SET domain. Methylation of H3K4 is usually associated with positive regulation of gene expression. Interestingly, MLL always loses its SET domain after rearrangement with fusion partners, and the subtle change in H3K4 methylation profile in *MLL*-rearranged leukemia would not be able to explain the global deregulation of gene expression in *MLL*-rearranged leukemia. Through chromatin immunoprecipitation coupled with sequencing (ChIP-seq), our lab studied changes of different epigenetic marks comparing leukemia stem cells and the common progenitors from which they arose, and found aberrantly high levels of H3K79 dimethylation across the gene bodies of MLL target genes only exist in leukemia stem cells but not in the common progenitors (12). H3K79 dimethylation is ubiquitously coupled with positive regulation of gene expression in normal cells but it is remarkably more enriched in MLL target genes than in other highly expressed genes in MLL-rearranged leukemias (25). DOT1L is the sole enzyme responsible for methylation at H3K79. Interestingly, several fusion partners of MLL, for example, AF9, ENL, AF4, and AF10, are shown to bind to DOT1L either directly or indirectly (26-29). However, DOTl is not a part of AEP/SEC in MLL fusion leukemias, and recent results indicate that AF9 or ENL cannot simultaneously bind P-TEFb and DOT1L. Moreover, MLL fusion partners that normally reside in the cytoplasm cannot directly recruit DOT1L to

MLL targets. Therefore, how DOT1L is recruited to MLL target genes in *MLL*-rearranged leukemia is still a mystery.

Normal Hematopoiesis, Leukemogenesis, and Leukemia Cell of Origin

Hematopoiesis is a hierarchy where hematopoietic stem cells (HSC) possess significant self-renewal potential and their progeny cells with a restricted cell fate, have lost this potential. This developmental process is well-controlled by spacial and temporal expression of developmentally important genes, that are turned on and off by transcription factors and perhaps maintained by epigenetic mechanisms. Definitive hematopoiesis starts with HSC, which have both the ability for unlimited self-renewal and the ability to differentiate into multipotent progenitors (MPPs). MPPs have limited self-renewal ability and can differentiate into common lymphoid progenitors (CLPs) and common myeloid progenitors (CMPs). CLP can ultimately differentiate into B and T cells and CMP can differentiate into granulocyte-macrophage progenitors (GMP), which give rise to various granulocytes and macrophages, and megakaryocyte-erythrocyte progenitors (MEP), which give rise to platelets and red blood cells.

If in the journey of hematopoiesis, *MLL* rearrangement happens in hematopoietic stem cells or early hematopoietic progenitors, the mutant cells will have unlimited self-renewal potential, expand without differentiation, crowd out normal bone marrow cells and infiltrate into other organs, leading to clinical leukemia. *MLL* rearrangement breaks *MLL* in the breakpoint cluster region (BCR) region encompassing exons 5 through 11, where several topoisomerase II (topo II) cleavage sites, DNase I hypersensitive sites and scaffold attachment regions coexist and the free energy level for unwinding double strand DNA is very low (30). There is also a strong non-homologous end joining (NHEJ) repair signature including deletion, inversion and duplication in virtually all *MLL* rearrangement, suggesting *MLL*-rearrangement is caused by accidental cleavage of chromosomes and subsequent mistakes in NHEJ repair in hematopoietic cells (30).
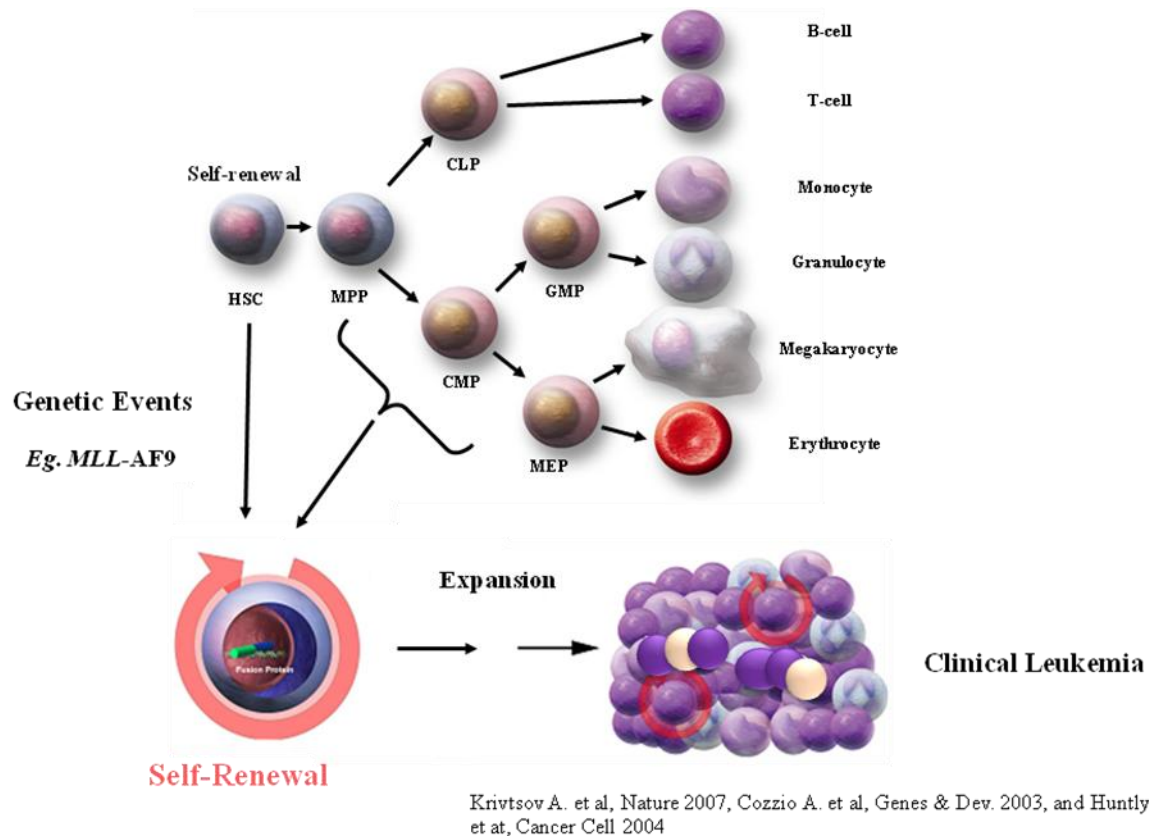
Figure 1-2 MLL rearrangement in HSC and early progenitor cells leads to clinical leukemia.

Adapted from review (2).

Mouse models provide an extremely useful tool for understanding the mechanisms of MLL-fusion-mediated leukemogenesis and for preclinical development of rational therapeutic strategies. *Mll-AF9* knock-in mouse models that constitutively express Mll-AF9 under wildtype *MLL* promoter, and *Mll-Af9* conditional knock-in mouse models that have *Mll-Af9* interchromosomal translocation in hematopoietic cells both have a propensity of developing AML (10, 11). Conditional *Mll-Enl* knock-in mouse models have rapid onset of AML, whereas conditional *Mll-CBP* knock-in model results in myelomonocytic hyperplasia that can progress to a myeloproliferative or myelodysplastic disorder only after additional chemical or radiation-induced mutagenesis (20, 31). These knock-in experiments demonstrated the

7

leukemogenic function of Mll fusions and also demonstrated that the N-terminal *Mll* knock-in alone is not leukemogenic in mice. As *MLL-ENL* and *MLL-AF9* translocations are most frequently found in acute leukemias and *MLL-CBP* translocation is most frequently found in myelodysplastic syndrome or therapeutics-induced acute leukemias, these mouse models appear to truly recapitulate the disease found in humans. Since *MLL-AF4* is the most frequent translocation found in ALL patients, it would be useful to develop an *Mll-Af4* mouse model that faithfully recapitulates human *MLL-AF4* leukemia. However, initial mouse models of constitutive *Mll-AF4* knock-in only resulted in mixed lymphoid/myeloid hyperplasia and mature B-cell neoplasms in mice (32). Conditional expression of *Mll-AF4* by interchromosomal recombination in lymphoid-specific cells produced mature B-cell lymphomas but failed to cause any ALL (32). Nevertheless, a more recently developed conditional *Mll-AF4* knock-in mouse model that specifically knock-in *Mll-AF4* in hematopoietic stem cell and progenitors, developed ALL or AML with a median latency around 100 days, and the mouse *Mll-AF4* leukemia cells share very similar global gene expression patterns and H3K79 methylation profiles with human *MLL-AF4* leukemia cells (12). This *Mll-AF4* mouse model demonstrated that *Mll-AF4* leukemia have a distinct gene expression pattern and a distinct H3K79me2 profile from *MLL*-wildtype leukemia cells. Interestingly, although MLL-fusion proteins are also expressed in other tissue like brain and kidney in the constitutive MLL-fusion knock-in mouse models, only hematopoietic related malignancies develop, suggesting that MLL-fusion proteins are only cancerous for the hematopoietic system.

Besides knock-in mouse models, mouse models based on retroviral gene transfer and bone marrow transplantation have also been a useful approach for understanding MLL fusion functions in leukemia development. In retroviral models, normal bone marrow cells are harvested from mice, transduced with a retrovirus carrying the MLL fusion gene and the cells are then analyzed *in vitro* or injected into syngenic mice to assess leukemia development *in vivo*. Using this approach, it has been shown that MLL-ENL and MLL-AF9 can induce acute leukemia from mouse bone marrow progenitors as well as human cord blood

progenitors (33, 34). Retroviral models also demonstrated that MLL-GAS7, MLL-AF9, and MOZ-TIF2, but not BCR-ABL can transform committed progenitors that have limited self-renewal potential as well as hematopoietic stem cells that have unlimited self-renewal potential (8, 35). When reprogrammed by MLL fusion genes, the committed progenitors can maintain the global identity of the progenitor from which they arose while activating a self-renewal associated program (8). This finding defines progression from normal progenitor to cancer stem cell and suggests that targeting a self-renewal program expressed in an abnormal context may be possible.

Epigenetics and Cancer Therapy

In eukaryotic cells, DNA is wrapped around a histone octamer comprised of one $(H3/H4)_2$ heterotetramer and two H2A/H2B dimers to form the nucleosome, the fundamental building block of chromatin. Genetic information is stored in the genome sequence and it serves as a bank of information for all the cells in a multicellular eukaryotic organism. During normal development or disease progression, cells change their identities, express various sets of genes and function differently. Unlike genetics, epigenetics refers to all the heritable changes of cellular status that are not related to the change of DNA sequence. Epigenetics involves DNA methylation, histone modification and chromatin remodeling and is crucial for the establishment and maintenance of gene expression patterns within any given cell type of an organism.

The histone molecules are susceptible to a variety of covalent modifications including acetylation, phosphorylation, sumoylation, ubiquitination, and methylation among others. Studies in the past decade have shown that covalent histone modifications influence chromatin structure and/or function directly or indirectly through the recruitment of effector proteins to specific chromatin regions (36-38), thus playing positive or negative roles in gene expression. Generally, histone methylation on H3K4, H3K36 and

9

H3K79 and histone lysine acetylation in H3 tails correlates with gene transcriptional activation, while histone methylation on H3K9, H3K27, and H4K20 correlates with gene transcriptional repression (38).

Interestingly, it has become increasingly apparent that the misregulation of histone modification, which is caused by the deregulation of factors that mediate the modification installation, removal and/or interpretation, actively contributes to human cancer. Recent whole genome sequencing data support the roles of epigenetic modifiers in cancer progression. For example, *UTX, JARID1A, EZH2* are frequently found mutated in cancers. In many cases, epigenetic deregulation directly drives cancer. For example, *MOZ-TIF2* is a recurrent translocation in human AML. MOZ itself is a histone acetyltransferase. The oncogenic potential of MOZ-TIF2 fusion protein is dependent on the ability of TIF2 to bind another histone acetyltransferase CBP (39). *NUP98-NSD1* is another recurrent translocation in human AML. It has been demonstrated that the H3K36 methyltransferase activity of NSD1 is essential for the activation of *Hoxa* genes and leukemogenesis in *NUP98-NSD1* leukemia (40). As mentioned in the previous sections, *MLL* rearrangement abrogates the H3K4 methyltransferase activity of MLL protein, but leads to aberrantly high H3K79 methylation in MLL target genes, possibly by directly or indirectly recruiting DOT1L to the MLL target loci (Figure 1-3).
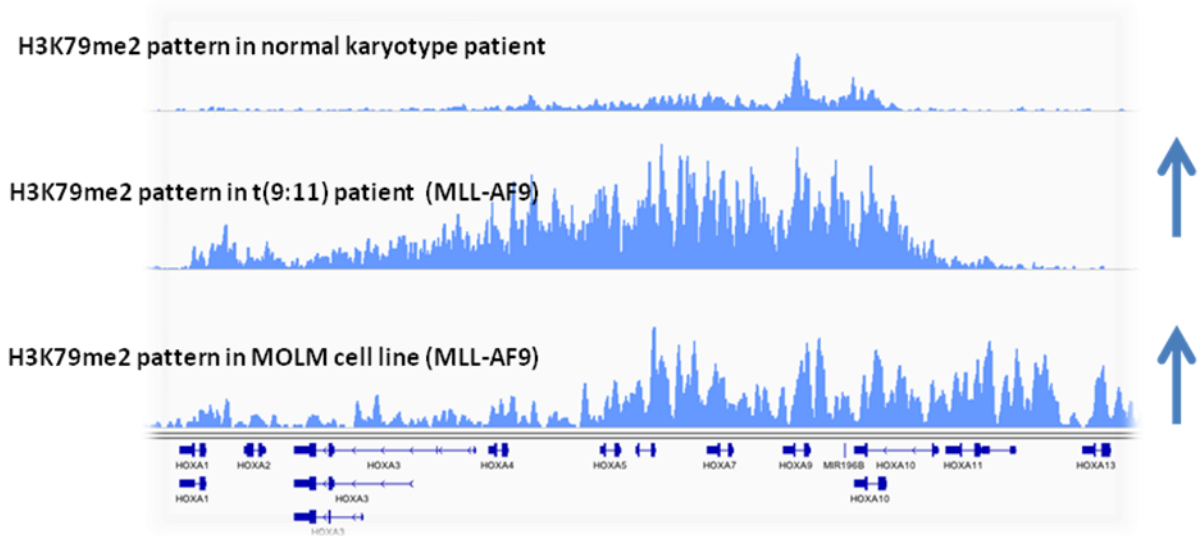
Figure 1-3 H3K79me2 is enriched in MLL target loci *HOXA6-11* in *MLL-AF9* rearranged human leukemia cell line MOLM and *MLL-AF9* rearranged human primary leukemia.

10

As a cell state, cancer is influenced by the epigenetic program that determines how chromatin is packaged and what genes are expressed and silenced. We rationalize that targeting epigenetic modifiers may correct the deregulated epigenetic program in cancer, and set the cell state back to normal. The FDA approval of DNA methyltransferase inhibitors (azacytidine and decitabine) for the treatment of myelodysplastic syndrome (41, 42), and the more recent approval of HDAC inhibitors (vorinostat and romidepsin) for use in refractory cutaneous T cell lymphoma (43) have validated epigenetic enzymes as attractive targets for pharmaceutical drug development. A number of inhibitors of histone acetyltransferases (HATs), histone methyltransferases (HMTs) and histone demethylases (HDMs) are also in various stages of preclinical development (reviewed in (44)). *MLL* rearranged leukemia is another example of how epigenetic deregulation contributes to cancer. The involvement of DOT1L enzymatic activity in leukemogenesis driven by MLL fusion proteins raises the possibility of targeting DOT1L for therapeutic intervention. In our project, we sought to answer whether H3K79 methyltransferase DOT1L is required for a subset of *MLL* rearranged leukemia and whether DOT1L and its complex components can serve as a new therapeutic target for *MLL*-rearranged leukemia.

My hypothesis is that DOT1L and its associated factors play a fundamental role in *MLL*-rearranged leukemia, and I tested this hypothesis through three specific approaches.

1. Identify DOT1L complexes in leukemic cells using biochemical approaches and study the function of DOT1L complex components in epigenetic regulation via knock-down experiments.

2. Determine whether Dot1l and aberrant H3K79 methylation is essential for MLL-AF10, CALM-AF10, or MLL-AF6 mediated leukemogenesis. MLL-AF10 represents MLL fusions with nuclear partners, and MLL-AF6 represents MLL fusions with cytoplasmic partners.

3. Assess the therapeutic potential of inhibiting the function of Dot1l complex by knock-out of a key Dot1l complex component in leukemia.

Chapter 2

Characterization of the Dot1l Complex in Leukemia

Introduction

Disruptor of Telomeric Silencing-1 (Dot1) is an evolutionarily conserved histone H3 lysine (K) 79 methyltransferase. It was discovered originally in Saccharomyces cerevisiae as a disruptor of telomeric silencing. In yeast, Dot1 mediated H3K79 methylation is associated with telomere silencing, meiotic checkpoint control, and DNA damage response. In multicellular organisms, Dot1l is essential for embryonic development, hematopoiesis, cardiac function, and the development of leukemia (reviewed in (45)).

Dot1l is a class I SAM-dependent methyltransferase. It catalyzes the mono-, di-, and tri-methylation of H3K79 in a nonprocessive manner (45, 46). Gene inactivation experiments demonstrated that Dot1l is the only H3K79 methyltransferase in yeast, flies, and mice (47-49), and despite many studies, no H3K79 demethylase has yet been reported. Unlike other histone lysine methyltransferase, the enzymatic domain of Dot1l does not belong to the Su(var)3-9, Enhancer of Zeste, and Trithorax (SET) histone lysine methyltransferase family but shares structural similarity with the histone arginine methyltransferase domain (50, 51). In contrast to other histone methyltransferases that modify the histone tails, Dot1l catalyzes the methylation of lysine in the globular domain of histone H3. Interestingly, characterization of DOT1L enzymatic activity revealed that DOT1L requires the nucleosome as its substrate (52). The fact that most histone methyltransferases have activity on structures as simple as H3 tail peptides but DOT1l has minimal activity on recombinant H3 or core histones, suggests that the activity of DOT1L may recognize other features of the nucleosome. In agreement with the substrate preference, the crystal structure of DOT1L suggested a broad interaction surface between DOT1l, DNA, H3/H4 tetramer and H2A/H2B dimer.

DOT1l was brought to the attention of oncologists by Yi Zhang's paper which revealed the interaction between DOT1l and AF10, a gene recurrently fused with MLL and CALM in AML and T-ALL patients

(29, 53). Then it was found that another MLL-fusion partner, ENL, co-purified with DOT1L (28). It was found later by several other biochemical studies that Dot1l directly or indirectly interacts with MLL fusion partner AF4, AF17 and AF9 (26, 27, 54). Indeed, the H3K79 hypermethylation associated with MLL-target genes is remarkable in MLL-AF4 and MLL-AF9 mouse leukemia and human leukemia. Like H3K4 methylation and H3K36 methylation, H3K79 methylation is usually associated with active transcribed region. However, in MLL-rearranged leukemia, H3K79 methylation, but not H3K4 or H3K36 methylation, is much higher at MLL targets than non-MLL targets that have similar gene expression levels, suggesting Dot1l and H3K79 methylation may be involved in driving the leukemia. Using a conditional knock-out mouse model, our lab as well as other labs have recently shown that Dot1l is required for transformation of murine bone marrow cells with MLL-AF9 and MLL-GAS7, but not with E2a-Pbx1(25, 55-57). One of the hypotheses is that Dot1l is attracted to MLL-fusion by the fusion partner. However, recent studies assessing the MLL-fusion complex either in its respective MLL-fusion leukemia, or in 293T overexpression system, failed to find DOT1l co-purification. Furthermore, detailed biochemical studies showed the interaction of DOT1l and ENL, and AEP and ENL, is mutually exclusive (16, 58).

To study the role of the DOT1L complex in the context of leukemia, we purified the DOT1L multiprotein complex under physiological conditions in SEMK2 leukemia cells, which represent MLL-AF4 ALL (the most common MLL rearrangement) and REH leukemia cells, which is an human ALL cell line with wildtype MLL. We aimed to characterize the DOT1L complex in leukemia, to understand the relation between super elongation complex and DOT1L complex.

Results

To understand molecular mechanisms of DOT1L function in MLL-rearranged leukemia, I started with biochemical studies of the DOT1L complex in two human pre-B cell leukemia cell lines— SEMK2,

14

which carries the most common MLL translocation MLL-AF4, and REH, which has germline MLL. In order to obtain best recovery efficiency and purity, I took advantage of a recently described technique for metabolic biotin and FLAG double tagging of protein in mammalian cells (59, 60) (Figure 2-1A). SEMK2 and REH cell lines that stably express the *E. coli* biotin ligase BirA alone (as a control), or BirA and DOT1L with a FLAG epitope followed by a 23 amino-acid BirA recognition motif have been generated. To minimize spurious association caused by overexpression, cell lines that express recombinant DOT1L at levels similar to the endogenous levels were used for subsequent nuclear protein extraction and complex characterization (Figure 2-1B). Western blot showed that H3K79 is hypermethylated when DOT1L is overexpressed, suggesting that the recombinant DOT1L is functional in vivo (Figure 2-1B). Nuclear extraction and affinity purification of FLAG-Bio-DOT1L was performed. Co-purified proteins were separated by SDS-PAGE, trypsinized and analysed by microcapillary liquid chromatography/tandem mass spectrometry. The peptide sequences were determined by matching protein or translated nucleotide databases with the acquired fragmentation pattern by the software program SEQUEST (ThermoFinnigan). Protein abundance was determined by the presence of unique peptide sequences, and proteins identified in SEM-BirA or REH-BirA cells were considered as background/noise. Together, four independent experiments were done with SEMK2 cell line, and one tandem affinity purification experiment was done with REH cell line. Figure 2-1C compared the DOT1L complex components identified in MLL-AF4 rearranged SEMK2 cells and MLL-wildtype REH cells, and Table 2-1 summarizes the functions of DOT1L complex components in SEMK2 cells and REH cells.
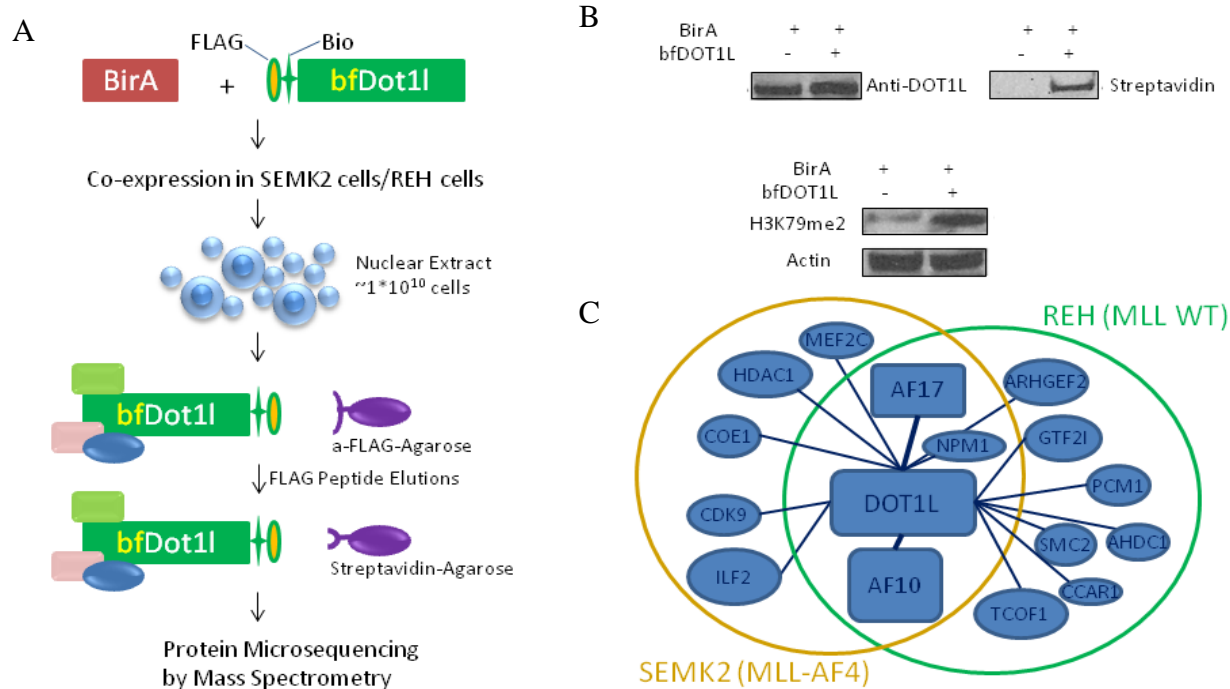
Figure 2-1 Tandem affinity purification of DOT1L-containing multiprotein complex.

(A) Schematic representation of experimental procedure. Recombinant DOT1L containing the N-terminal FLAG and the BirA recognition site was co-expressed with BirA, a biotin ligase in *E. coli*. Nuclear extraction and tandem affinity purification was followed by mass spectrometry to determine complex components. (B) Western blot analysis of nuclear extracts from SEMK2 cell lines that stably expressing BirA only (left lane) or both BirA and [Flag-Bio]DOT1L (right lane). The staining with anti-DOT1L antibody shows sub-endogenous level of DOT1L overexpression, and the staining with Streptavidin-horseradish peroxidase shows the metabolically labeled recombinant DOT1L. Lower panel showed western blot analysis of whole cell lysates from SEMK2 cell lines that stably expressing BirA only or both BirA and [Flag-Bio]DOT1L, probed with anti-di-methyl-H3K79 antibody. (C) Graph showing the components of DOT1L complex in SEMK2 (yellow circle) and REH (green circle).

As seen in Figure 2-1C and Table 2-1, mass spectrometry results demonstrated that AF10 and AF17 are two stable components in DOT1L complex in both SEMK2 and REH cells, while other proteins, such as transcription factors, histone modification factors, and scaffold proteins associate with Dot1L in a cell-type dependent manner. The interaction on the list is further verified by co-immunoprecipitation (co-IP) and reciprocal co-IP (see Figure 2-2D).

Table 2-1 Identification of DOT1L associated proteins in SEMK2 and REH cells

Dot1L complex in SEMK2 (4 experiments in total)			Dot1L complex in REH (1 experiment in total)		
Name	Average Peptide Number	Annotation	Name	Peptide Number	Annotation
Dot1L	63	H3K79 methyltransferase	Dot1L	58	H3K79 methyltransferase
AF10	16	MLL fusion partner, putative transcription factor	AF10	17	MLL fusion partner, putative transcription factor
AF17	11	MLL fusion partner, putative transcription factor	AF17	8	MLL fusion partner, putative transcription factor
ILF2	3	NFAT transcription factor	TCOF1	7	Treacher Collins-Franceschetti syndrome 1 isoform a
HDAC1	3	Histone deacetylase 1	ARHGEF2	5	Rho guanine nucleotide exchange factor 2
MEF2C	1	Transcription activator in B cells	GTF2I	2	General transcription factor II-I
COE1	(2)*[1]	Early B-cell factor	SMC2	2	Structural maintenance of chromosomes protein 2
CDK9	(1)*[2]	Transcriptional elongation factor	PCM1	2	Pericentriolar material 1 protein
NPM1	(5)*[3]	Nucleophosmin, involved in ribosome biogenesis, histone assembly, cell proliferation	NPM1	1	Nucleophosmin, involved in ribosome biogenesis, histone assembly, cell proliferation
			CCAR1	1	Cell division cycle and apoptosis regulator 1
			AHDC1	1	AT hook containing protein that may interact with MLL, ENL, AF9, AF10

Note: I performed one experiment for REH cells with tandem affinity purification and four experiments for SEMK2 cells, once with single anti-FLAG purification, twice with single strepavidin purification, and once with tandem affinity purification. All the listed proteins in SEMK2 cells have repeatedly appeared in SEM-BirA-Dot1L samples but not in SEM-BirA control except NPM1, CDK9, and COE1(see*).

*[1]: COE1 was identified once with 2 unique peptides in the tandem affinity purification in SEMK2 cells.

*[2]: CDK9 was identified once with 1 unique peptide in Streptavidin affinity purification in SEMK2 cells.

*[3]: NPM is known to be an abundant and sticky protein in the nucleus. It was detected in both SEM-BirA-Dot1L sample and SEM-BirA control in single step purifications, but it was identified only in SEM-BirA-Dot1L and REH-BirA-DOT1L samples (5 peptides and 1 peptide detected respectively) but not in SEM-BirA or REH-BirA controls using tandem affinity purification.
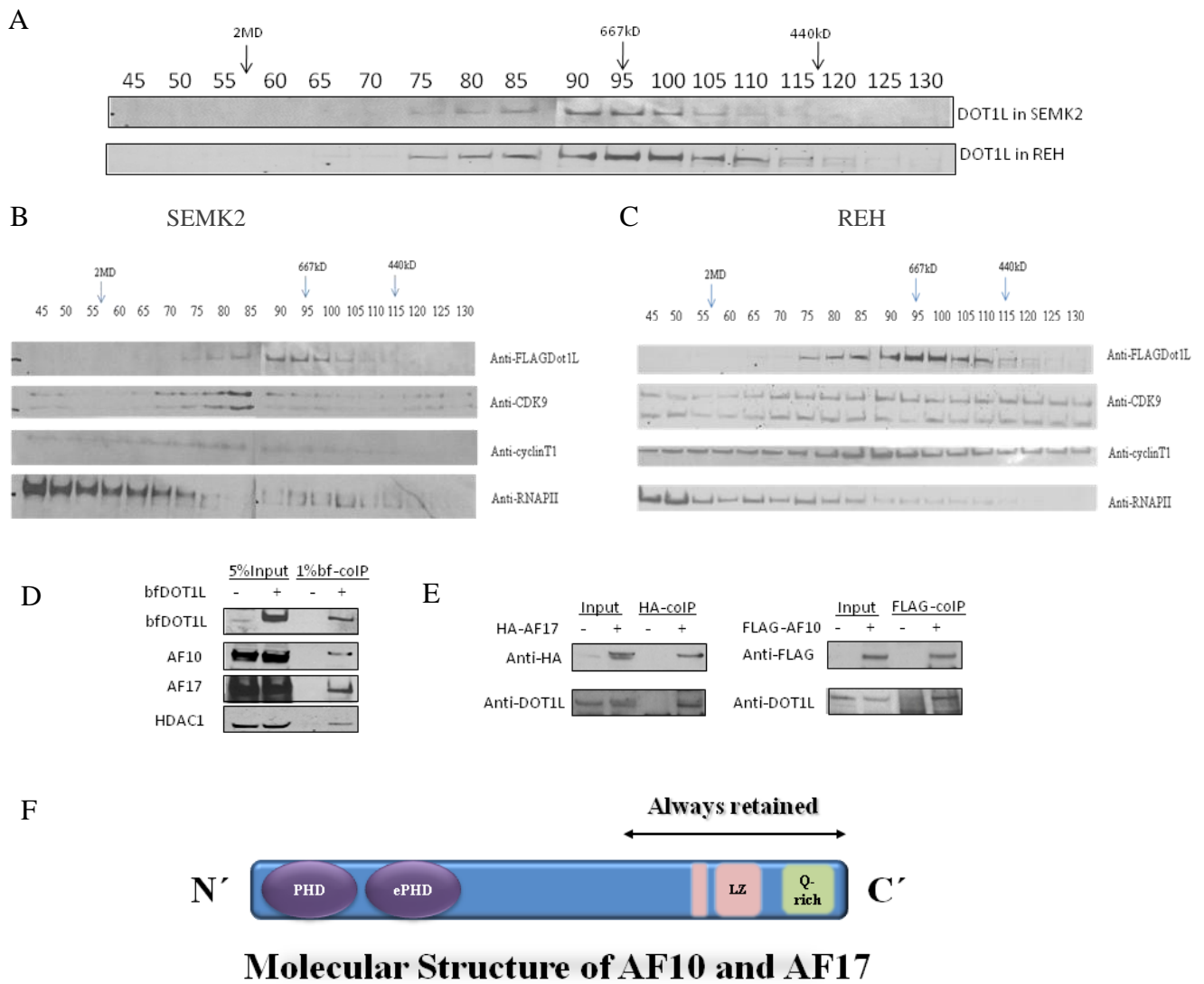
Figure 2-2 Characterization of DOT1L complex in leukemia cells.

(A-C) Size exclusion chromatography of crude nuclear extracts from SEMK2 (A and B) and REH (A and C) cells showed that DOT1L complexes elute at the size around 670kD (fractions 90-95) while P-TEFb elute at a broader range (enriched infractions 65-95) . Western blot was performed with antibodies against Dot1l, CDK9, cyclinT1 and RNAPII CTD, respectively. (D) The interaction between DOT1L and AF10/AF17/HDAC1 was confirmed by immunoprecipitation. (E) Reciprocal co-IP showed AF10 and AF17 interact with DOT1L in vivo. (F) The molecular structure of AF10 and AF17.

To further characterize DOT1L complex, I performed gel filtration on nuclear extracts from SEMK2 and REH cells. As shown in Figure 2-2, the DOT1L complex was eluted as a sharp peak about 670kDa in both SEMK2 cells and REH cells. In contrast, RNA polymerase II (RNAPII), CDK9 and cyclin T1 were all eluted as very broad peaks, consistent with the diversity of RNAPII and P-TEFb containing complexes. In our study, RNAPII and P-TEFb subunits were mainly co-eluted at sizes above 1MDa, in agreement with recent papers that showed the Pol II elongation complex AEP or SEC at the size of about 1.5MDa (17).

There are several important points raised by this study. First, though SEMK2 cells have *MLL-AF4* translocation, neither MLL or AF4 is found to interact with DOT1L, suggesting that DOT1L is not recruited to MLL target loci through direct association with MLL-AF4 fusion protein or that the association is weak or transcient. Second, except CDK9, none of the DOT1L complex components identified in leukemic cells appears in AEP or SEC, and the DOT1L complex was eluted at different sizes than AEP or SEC, suggesting that the DOT1L complex and AEP or SEC are two distinct complexes. Third, proteins that only associate with DOT1L in SEMK2 or REH cells may have biological relevance. For example, it has been shown that transcription activator MEF2C is highly expressed in MLL-rearranged AML and its up-regulation may be responsible for the aggressive nature of MLL-rearranged AML (61). DOT1L may cooperate with MEF2C to promote homing and invasiveness of MLL-rearranged leukemic cells.

As shown in Figure 2-2, the two most stable DOT1L interacting partners are AF10 and AF17. AF10 and AF17 were both identified as MLL fusion partners in acute myeloid leukemias. They are highly homologous proteins with similar N-terminal plant homeodomain (PHD) fingers, and C-terminal Leucine Zipper (LZ) domain. What are their functions in DOT1L complex? Why does nature evolve two similar proteins? We hypothesized that the two proteins serve different functions in vivo. To characterize the

19

function of AF10 and AF17, I started with shRNA-mediated knock-down experiments in human acute leukemia cell lines. Five shRNAs against human AF10 and five shRNAs against human AF17 were tested, among which shAF10.1 and shAF17.7 showed consistent knock-down in leukemia cell lines (Figure 2-3A and 2-3B) and no toxicity in 293T cells.
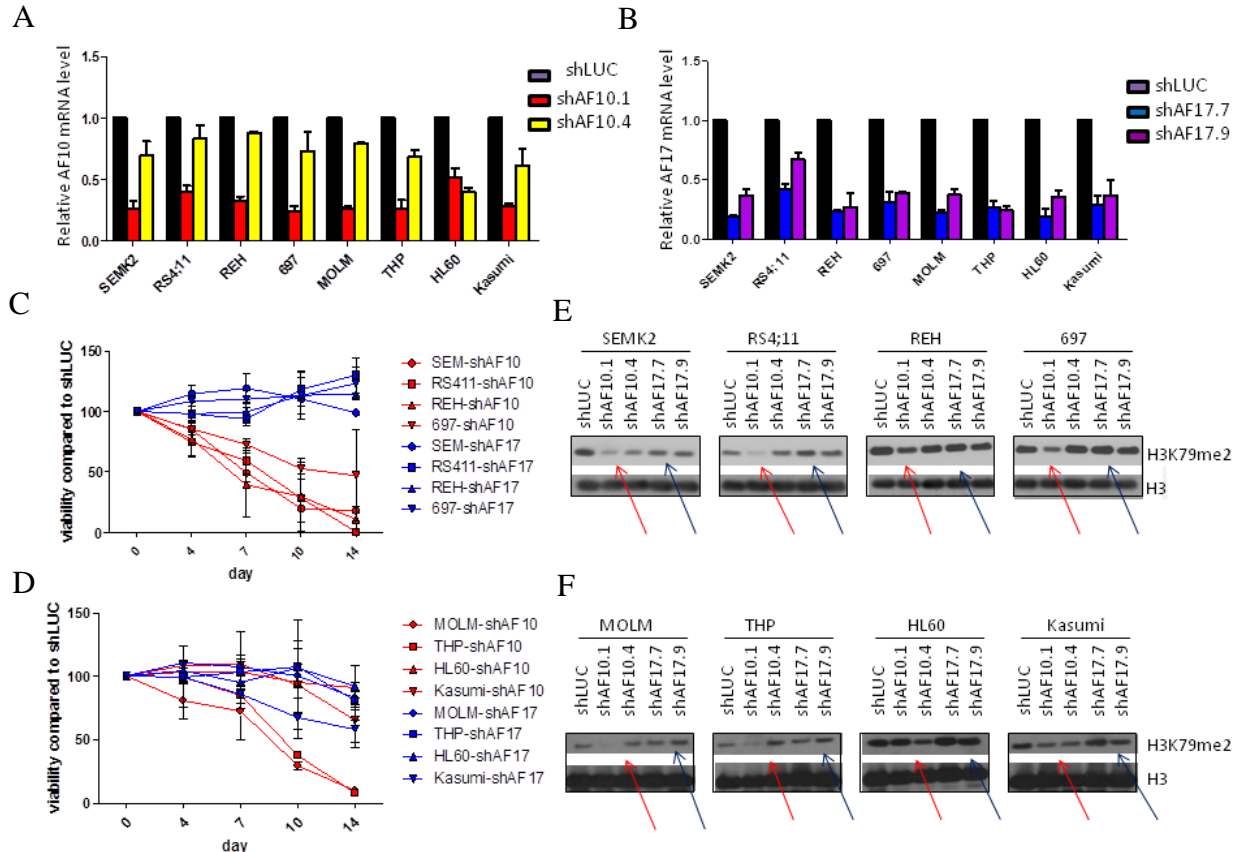
Figure 2-3 Suppression of AF10 and AF17 have different phenotypes in leukemia.

(A-B). Reverse transcription and q-PCR showing effective knock-down of AF10 (A) and AF17 (B) 4 days after transduction with lentivirus carrying shRNA construct. AF10 and AF17 expression levels were normalized to GAPDH and expressed relative to control cells which were transduced with lentivirus carrying shRNA against Luciferase gene (shLUC, set to 100%). (C) Growth of human ALL cell line SEM (MLL-AF4) and RS4;11(MLL-AF4), REH (non-MLL-rearranged), and 693 (non-MLL-rearranged) cells after transduction with shAF10.1 and shAF17.7. Viable cells were counted every 3 to 4 days, and cell numbers after transduction with shLUC were set as 100%. Result is representative of 3 indipendent experiments. (D) Growth of human AML cell line MOLM (MLL-AF9) and THP (MLL-AF9), HL60 (non-MLL-rearranged), and Kasumi (non-MLL-rearranged) cells after transduction with shAF10.1 and shAF17.7. Viable cells were counted every 3 to 4 days, and cell numbers after transduction with shLUC were set as 100%. Result is representative of 3 indipendent experiments. Western blot showing AF17 protein level after shRNA-mediated knock-down. (E-F) Western blot showing H3K79me2 level 9 days after transduction with shRNA (red arrows points to reduced H3K79me2 level) in 4 ALL cell lines (E) and 4 AML cell lines (F).

Knock-down of *AF10* in human leukemia cell lines led to a global decrease of H3K79me2 9 days after introduction of shRNA by lentivirus (red arrows, Figure 2-3E and 2-3F), while knock-down of *AF17* did not significantly affect H3K79me2 level. In addition, *AF10* knock-down affected cell viability of *MLL*-rearranged leukemia cell line SEM, RS4;11, MOLM, and THP, while *AF17* knock-down does not affect cell viability (Figure 2-3C and 2-3D). Therefore, AF10 and AF17 may function differently and AF10 is more important regarding H3K79 dimethylation by Dot1l. In Chapter 5, I focus more on the role of AF10 in MLL leukemogenesis.

Discussion

The diversity of MLL fusion partners poses a challenge to developing a unified mechanistic model for MLL leukemias. However, gene expression signatures of *MLL* rearranged leukemias are remarkably similar and can be reliably used to distinguish leukemias with *MLL* rearrangements from other subtypes. Our lab has shown that *MLL* rearranged leukemias with nuclear fusion partners (12, 25) and with cytoplasmic fusion partners (see Chapter 4) both have aberrantly high histone methylation at H3K79 in MLL target genes. Thus this epigenetic lesion may be involved in driving the gene expression signatures in *MLL* leukemias. The development of molecular therapies to specifically target epigenetic modifiers is a promising new field. In this project, I sought to study the requirement of DOT1L complex in several MLL rearranged leukemias with dismal prognosis. To understand the function of DOT1L in leukemia and to suggest new therapeutic strategies, however, requires information about the DOT1L complex in the right context. Therefore we purified DOT1L complex in human acute leukemia cells with the most common *MLL* rearrangement, *MLL-AF4*, or without *MLL* rearrangement. Our mass spectrometry data showed AF10 and AF17 are the two most stable DOT1L-interacting proteins in leukemia cells. Moreover, shRNA mediated knock-down of *AF10* in human acute leukemia cell lines diminished global H3K79 methylation

level and affected the survival of MLL-rearranged leukemia cells, while knock-down of *AF17* showed no effect on global H3K79 methylation or *in vitro* leukemia cell survival.

In our study, we purified the DOT1L complex under physiological conditions from human acute leukemia cells. While we further characterized the functions of DOT1L complex components, Ali Shilatifard group published the first paper describing Dot1l complex, which they called DotCom. In their study, they overexpressed FLAG-tagged Dot1l in 293T cells and performed mass spectrometry after one-step affinity purification. Similar to our study, they also identified AF10 and AF17 in the complex. Besides AF10 and AF17, they found two more MLL fusion partner AF9 and ENL, and a scaffolding protein TRRAP in DotCom. There are some possibilities to explain the discrepancy between the two studies. First, while the human kidney fibroblast cell line 293T is a useful mammalian system to study protein-protein interaction, it is known for overexpression of recombinant proteins at an artificially high level, which may pick up false interactions that do not happen under the physiological protein concentration. Second, human kidney fibroblast cells and human leukemia cells express different sets of proteins. The difference in the cellular proteome may explain the difference of DOT1L/Dot1l interacting network in the two studies. The interaction between DOT1L and MEF2C or ILF2 may have important functions in hematopoietic malignancy, but MEF2C and ILF2 may not be expressed at a detectable level in kidney fibroblasts. It is possible that AF9 and ENL are less abundant in human acute lymphoblastic cells than in 293T cells, therefore even if they interact with DOT1L *in vivo*, they will not be identified in our study with human ALL cell lines.

Our study brought the function of the AF10-DOT1L complex into sharp focus, leading us to study its role in the epigenetic activation of gene expression and involvement in MLL rearranged leukemias. The interaction between AF10 and DOT1L was first discovered in yeast-two-hybrid screen by Yi Zhang's group. They also demonstrated that the C-terminal octapeptide motif-leucine zipper (OM-LZ) domain of AF10, which is required for association with DOT1L, is the "minimal" fusion domain necessary and

sufficient for bone marrow transformation by MLL-AF10 and CALM-AF10. The PHD finger, 50-80 amino acids in length, is a common domain that reads histone modifications. It is found in many human proteins and is involved in chromatin-mediated gene regulation. For example, the PHD finger in ING2 and NURF binds to H3K4me3, and the PHD finger in JARID1C binds to H3K9me3. Many histone modifying enzymes have well characterized chromatin binding domains, DOT1L, however, does not have any known domain to read histone modifications. Although our study with H3 tail peptide binding assay failed to identify the histone modification AF10 may read (data not shown), it is still possible that AF10 completes DOT1L complex function by targeting DOT1L to specific histone modifications.

One straight-forward hypothesis for MLL rearranged leukemia would be that the MLL-fusion partner attracts Dot1l to MLL targets, promotes H3K79 methylation and gene transcription. This hypothesis could explain the mechanisms of MLL-AF10, and possibly MLL-AF9 and MLL-ENL. However, our study of DOT1L complex in MLL-AF4 expressing cells did not find AF4 or MLL by mass spectrometry. The DotCom identified by Ali Shilartifard group also does not include other common MLL fusion partners like AF4, CBP, GAS7 or AF6. Moreover, recently it was revealed that AF4, AFF4, AF9 and ENL, all of which are MLL fusion partners that exist in the nucleus, form a higher-order transcriptional elongation complex called AEP or SEC, with the positive transcription elongation factor (P-TEFb). It was demonstrated that AEP or SEC was hijacked to MLL targets in the context of MLL-fusion leukemia, contributing to leukemogenesis. Consistent with our study, their studies also showed Dot1l is not part of the MLL-fusion-AEP/SEC complex, although H3K79 methylation is aberrantly high at MLL targets. The detailed structure-function study revealed that although ENL binds to Dot1l, the binding of Dot1l and ENL or AEP and ENL is mutual exclusive. (16, 17) Therefore, how DOT1L is recruited to MLL targets in MLL-rearranged leukemias remains elusive and more detailed studies about the functions of DOT1L interacting proteins need to be done.

It is intriguing that two homologous proteins AF10 and AF17 serve different functions in vivo. Knock-down of AF10 affects global H3K79 dimethylation level and cellular survival, while AF17 does not. When we were characterizing the function of AF10 with knock-out mouse model, a AF17 knock-out mouse model was reported (62, 63). In agreement with our knock-down study, AF17 knock-out has minimal effect on H3K79 methylation and hematopoiesis, but plays a role in sodium homeostasis and blood pressure control.

Material and Methods

Generation of Dot1l expressing human leukemia cell lines

pEF-BirA-V5-His, MSCV-BirA-V5-His, pEF-FLAG-Bio-puro, and MSCV-FLAG-Bio-puro were gifts from Orkin lab. pEF-FLAG-Bio-DOT1L-puro was generated by amplifying DOT1L cDNA using 5'-ATT GGA TCC TGG GGG AGA AGC TGG AGC TGA GAC TGA AG-3' (forward primers) and 5'-TAT AGC TAG CGA ATT CTA GTT ACC TCC AAC TGT GCC GCC TGC CAC CCC-3' (reverse primer), and inserting the cDNA into the BamHI/XbaI sites of pEF-FLAG-Bio-puro vector. MSCV-FLAG-Bio-DOT1L-puro was assembled by ligating the DOT1L cDNA fragment and the MSCV-FLAG-Bio-puro vector at the EcoRI site. Packaging plasmids VSV.G and M57 gag/pol were used with MSCV plasmids to make amphotropic retrovirus carrying BirA and DOT1L. And packaging plasmids pMD2.G and psPAX2 were used with pLKO plasmids to make lentivirus carrying shRNA. Coding region human AF10, AF17 and control shRNA in pLKO.1-lentiviral vectors were kindly synthesized by the Harvard/MIT Broad Institute RNA consortium (http://www.broad.mit.edu/rnai/trc). A shRNA targeting Luciferase served as control.

Cell culture

24

The following human cell lines were obtained from *American Type Culture collection*:

MLL-AF4 rearranged ALL cell line RS4;11 (ATCC CRL-1873),

MLL wildtype ALL cell line REH (ATCC CRL-8286),

MLL-AF9 rearranged AML cell line THP-1 (ATCC TIB-202),

MLL wildtype AML cell line HL-60 (ATCC CCL-240).

The following cell lines were purchased from the *Deutsche Sammlung von Mikroorganismen und Zellkulturen* (DSMZ, Germany):

MLL-AF9 rearranged AML cell line MOLM-14 (DMSZ ACC 554),

MLL wildtype AML cell line KASUMI-1 (DMSZ ACC 220).

MLL wildtype ALL cell line 697 cells were provided by Dr. Kimberly Stegmaier (Dana Farber Cancer Institute).

MLL-AF4 rearranged ALL cell line SEMK2-M1 are previously described (Faber et al., 2009).

All the leukemia cell lines were maintained in RPMI-1640 media (Invitrogen) supplemented with heat-inactivated 10% fetal bovine serum, 2 mM L-glutamine and non-essential amino acids and 50 U/ml Penicillin/Streptomycin (all Gibco, Invitrogen, Carlsbad, CA). 293T cells were cultured in DMEM media (Invitrogen) supplemented with heat-inactivated 10% fetal bovine serum, 2 mM L-glutamine and non-essential amino acids and 50 U/ml Penicillin/Streptomycin. All cells were cultured in the appropriate medium in a humidified incubator at 37°C in 5% CO_2.

Lentiviral shRNA experiment

The knock-down efficiency of different shRNAs against AF10 and AF17 was tested by q-PCR and western blotting in 293T and human cell lines. The two most efficient shRNAs among the five were selected for further experiments. Human leukemia cell lines were transduced with pLKO.1 puro lentiviral shRNA against AF10, AF17, or luciferase. Lentiviral particles were produced by cotransfection of 293T cells with pLKO.1 constructs and packaging plasmids pMD2.G and psPAX2. Transfections were carried out with FuGENE 6 (Roche Diagnostics), and virus was harvested 48 and 72 hr after transfection.

Polybrene (Sigma-Aldrich, St Louis, MO) was added to a final concentration of 7 μg/ml, and cells were overlaid with viral supernatant. Spinocculation was performed at 2250 rpm for 90 minutes at 37°C. 12 hours after the transduction, media was replaced. 24 hours after transducation, infected cells were selected with 2 μg/ml puromycin. Media was replaced with fresh media with 2 μg/ml puromycin and the number of viable cells was counted with trypan blue stain under the microscope every 3 days.

Generation of human leukemia cell lines stably expressing BirA with and without DOT1L

Amphotropic retroviral supernatants were produced by cotransfection of 293T cells with VSV.G, M57 gag/pol, and the plasmid of interest using FuGENE6 (Roche Molecular Biochemicals, Indianapolis, IN). Virus containing supernatant medium was collected 2-3 days after the transfection. For transduction, 2,000,000 cells/well were plated into 6 well plates in the appropriate culture media. Polybrene (Sigma-Aldrich, St Louis, MO) was added to a final concentration of 7 μg/ml, and cells were overlaid with viral supernatant. Spinocculation was performed at 2250 rpm for 90 minutes at 37°C. 12 hours after the transduction, media was replaced with 2 ml of the appropriate fresh culture media. 24 hrs after the transduction, cells were selected with 0.5 mg/ml G418 for one week (for establishing BirA expressing cells first) or in 0.5 mg/ml G418 and 5 μg/ml puromycin (Sigma-Aldrich) for three days (for establishing DOT1L expressing cells based on BirA expressing cells), and maintained in 0.5 mg/ml G418 alone (for BirA expressing cells without DOT1L) or 0.5 mg/ml G418 and 2.5 μg/ml puromycin (for BirA expressing cells with DOT1L) throughout the remainder of the observation period. Stably transfected cells that express lower level of DOT1L were cloned by limiting dilution.

Large-scale purification of DOT1L complex and proteomic analysis

Nuclear extracts are prepared simultaneously from BirA expressing cells with and without tagged DOT1L, and affinity purification is processed simultaneously. Cell culture were scaled up to 5-10 liter in 850ml roller bottles (BD falcon) and kept in a rolling incubator at 37°C in 5% CO_2. Crude nuclear extracts were

26

prepared from ~1 × 1010 cells essentially as described previously (60). Briefly, cells were collected by centrifugation at 2400g for 5 mins and washed with ice-cold 1X PBS twice. Cells were rapidly resuspended with ~5X packed cell volume (PCV) of ice-cold Hypotonic Buffer (10 mM HEPES [pH 7.9], 1.5 mM MgCl2, 10 mM KCl, 0.5 mM DTT, 0.2 mM PMSF, 1:100 mammalian protease inhibitor cocktail [Sigma]), and centrifuged at 3000 rpm at 4oC for 5 mins. Cells were then resuspended in 3X PCV of ice-cold hypotonic buffer and incubated on ice for 10 mins to swell cells. And then cells were transfered to glass Dounce Homogenizer and slowly homogenized up and down 12 times with type B pestle. Cells were checked for cell lysis by examinzation of small aliquot in tyypan blue stain under microscope. Homogenate was centrifuged at 4000 rpm at 3300g at 4oC and supernatant was removed. Nuclei was resuspended by first adding ½ packed nuclear volume of ice cold low-salt buffer (20 mM HEPES [pH 7.9], 25% glycerol (v/v), 1.5 mM MgCl2, 0.02 M KCl, 0.2 mM EDTA, 0.5 mM DTT, 0.2 mM PMSF, 1:100 mammalian protease inhibitor cocktail [Sigma]) and then adding ½ packed nuclear volume of ice-cold high-salt buffer (20 mM HEPES [pH 7.9], 25% glycerol [v/v], 1.5 mM MgCl2, 1.5 M KCl, 0.2 mM EDTA, 0.5 mM DTT, 0.2 mM PMSF, 1:100 mammalian protease inhibitor cocktail [Sigma]). Nuclei suspension was incubated on a rotating wheel for 30 mins at 4oC, and centrifuged at 25,000 g for 30 mins at 4oC. The supernatant (nuclear extract) was transferred to fresh tubes and the centrifugation was repeated to remove any insoluble material.

Nuclear extracts were immediately dialyzed against 50 volumes of BC139K buffer (139 mM KCl, 12 mM NaCl, 0.8 M MgCl$_2$, 20 mM Tris-HCl [pH 7.9], 0.5% NP-40, 0.2 mM EDTA, 20% [v/v] glycerol, 1 mM dithiothreitol, 0.2 mM phenylmethylsulfonyl fluoride, 0.1% mammalian protease inhibitor cocktail) at 4°C using a 10,000-molecular-weight-cutoff dialysis cassette (Pierce). The dialysate was centrifuged twice at 25,000 × *g* for 30 min at 4°C. Between 50 and 120 mg of total nuclear protein was then precleared with protein A/G beads (Roche) for 1 h on a rotating wheel at 4°C. The precleared supernatant was incubated with anti-FLAG M2-agarose beads (Sigma) overnight (14 to 16 h) on a rotating wheel. The beads were collected by centrifugation and washed four times with cold BC139K buffer on a rotating

27

wheel at 4°C for 15 min each. Bound material was eluted by incubating beads in BC139K containing 0.1 mg/ml FLAG peptide (Sigma) for 90 min at 4°C on a rotating wheel. Material from four successive elutions was pooled and incubated with streptavidin-agarose beads (Invitrogen) for 14 to 16 h at 4°C on a rotating wheel. The beads were washed as described above, transferred into BC139 K buffer in which NaCl was substituted for KCl, and heated at 95°C to 100°C in Laemmli sodium dodecyl sulfate (SDS) sample buffer for 5 min. The eluted material was concentrated using a YM-10 Centricon (Millipore) device and resolved by SDS-polyacrylamide gel electrophoresis (PAGE) on 10% acrylamide gels running 2.5 cm into the separating gel. Proteins were visualized with colloidal Coomassie blue stain (Invitrogen), and the lanes were divided into three sections as "low Molecular Weight (MW)", "medium MW", and "high MW".

Excised acrylamide gel sections were cut into approximately 1-mm^3 pieces. Gel pieces were then subjected to a modified in-gel trypsin digestion procedure (64). Gel pieces were washed and dehydrated with acetonitrile for 10 min, followed by the removal of acetonitrile. Pieces were then completely dried in a Speed-Vac. Rehydration of the gel pieces was done with 50 mM ammonium bicarbonate solution containing 12.5 ng/µl modified sequencing-grade trypsin (Promega) at 4°C. After 45 min, excess trypsin solution was removed and replaced with 50 mM ammonium bicarbonate solution to just cover the gel pieces. Samples were then placed in a 37°C room overnight. Peptides were later extracted by removing the ammonium bicarbonate solution, followed by one wash with a solution containing 50% acetonitrile and 5% acetic acid. The extracts were dried in a Speed-Vac (~1 h) and then stored at 4°C until analysis. On the day of analysis, the samples were reconstituted in 5 to 10 µl of high-performance liquid chromatography solvent A (2.5% acetonitrile, 0.1% formic acid). A nanoscale reverse-phase high-performance liquid chromatography capillary column was created by packing 5-µm C18 spherical silica beads into a fused silica capillary (100-µm inner diameter by ~12-cm length) with a flame-drawn tip (65). After equilibrating the column, each sample was loaded onto the column via a Famos autosampler (LC Packings). A gradient was formed, and peptides were eluted with increasing concentrations of solvent B

28

(97.5% acetonitrile, 0.1% formic acid). As each peptide was eluted, they were subjected to electrospray ionization and fed into an LTQ linear ion-trap mass spectrometer (ThermoFinnigan). Eluting peptides were detected, isolated, and fragmented to produce a tandem mass spectrum of specific fragment ions for each peptide. Peptide sequences (and, hence, protein identity) were determined by matching protein or translated nucleotide databases with the acquired fragmentation pattern by the software program SEQUEST (ThermoFinnigan) (66).

Sephacryl S400 gel filtration chromatography

Crude nuclear extracts were prepared from human leukemia cells as described above and dialyzed against 50 volumes of cold BC100 buffer (100 mM KCl, 12 mM NaCl, 0.8 M $MgCl_2$, 20 mM Tris-HCl [pH 7.9], 0.2 mM EDTA, 20% [vol/vol] glycerol, 1 mM dithiothreitol, 0.2 mM phenylmethylsulfonyl fluoride, 0.1% protease inhibitor cocktail [Sigma]). The dialysate was centrifuged twice at $25,000 \times g$ for 30 min at 4°C. The final supernatant (~15 mg of total protein) was injected into a 5-ml loop of a DuoFlow (Bio-Rad) fast protein liquid chromatography apparatus and run over a HiPrep Sephacryl S400 26/60 column (Amersham Pharmacia Biotech) in cold BC100 buffer at 0.5 ml/min with collection of 1-ml fractions. Molecular mass standards were aldolase (177 kDa), catalase (240 kDa), ferritin (438 kDa), thyroglobulin (670 kDa), and blue dextran (2 MDa).

Chapter 3

MLL-AF10 and CALM-AF10 Require Dot1l in Leukemia Initiation and Maintanence

Addendum:

This chapter is adapted from the original article:

L. Chen, A. Deshpande, D. Banka, K. M. Bernt, S. Dias, C. Buske, S. R. Daigle, V. M. Richon, R. M. Pollock, S. A. Armstrong. Abrogation of MLL-AF10 and CALM-AF10-mediated transformation through genetic inactivation or pharmacological inhibition of the H3K79 methyltransferase Dot1l. *Leukemia*. Dec 4, 2012; PMID: 23138183.

Liying Chen, Aniruddha Deshpande, and Scott Armstrong designed the experiments. Liying Chen, Stuart Dias and Aniruddha Deshpande performed the genetic experiments. Liying Chen and Deepti Banka performed the pharmacological experiments.

Introduction

Chromosomal translocations which encode fusion proteins are frequently associated with human leukemias. The t(10;11)(p12;q23) translocation, which encodes the MLL-AF10 fusion protein, is a recurrent chromosomal rearrangement observed mainly in patients with acute myelogenous leukemia (AML) (67, 68). Another translocation involving *AF10*, the t(10;11)(p12;q14) translocation, encodes a CALM-AF10 fusion protein and is observed in AML, acute lymphoblastic leukemia (ALL) and precursor T lymphoblastic lymphoma (69). Patients with AML harboring either *MLL-AF10* or *CALM-AF10* rearrangements have a particularly poor outcome compared to patients whose leukemia cells do not harbor these translocations (70). Thus new therapeutic approaches are clearly needed for patients with AF10-rearranged hematopoietic malignancies.

While similar motifs in the AF10 portion are retained in both MLL-AF10 as well as CALM-AF10 oncoproteins motifs, MLL and CALM are quite dissimilar proteins. The wild-type MLL (Mixed Lineage Leukemia) protein positively regulates expression of homeobox (*Hox*) genes, and is essential for hematopoietic development (14, 71). MLL possesses multiple N-terminal domains required for target gene recognition (72-74), which are retained in the oncogenic MLL-AF10 fusion protein. MLL also possesses a C-terminal H3 lysine 4 (H3K4) methyltransferase domain (75, 76), which activates *Hox* gene expression during normal development but is absent in the fusion protein. On the other hand, wild-type CALM (Clathrin Assembly Lymphoid Myeloid leukemia) protein, primarily localized in the cytoplasm, is involved in clathrin-mediated endocytosis and has been shown to be involved in erythropoiesis and iron metabolism (77, 78). The clathrin binding domain on the C-terminus of CALM is always retained in the CALM-AF10 fusion proteins and is sufficient for leukemogenesis when fused with AF10 (79). As a fusion partner of both MLL and CALM, wild-type AF10 (*ALL-1* fused gene from chromosome 10) is a putative transcription factor containing N-terminal Plant Homeodomain (PHD) zinc finger motifs and a C-terminal octapeptide motif-leucine zipper (OM-LZ) domain (80). The AF10 OM-LZ domain is always

31

retained in the MLL-AF10 and CALM-AF10 fusion proteins and has been identified as a domain that interacts with the histone H3 lysine 79 (H3K79)-specific methyltransferase DOT1L(15, 29). Although the mechanism by which the leukemogenic AF10 fusions transform hematopoietic cells has not been fully elucidated, it has been suggested that Dot1l interaction with the AF10 OM-LZ domain is critical for oncogenesis (29, 53).

H3K79 methylation, catalyzed solely by Dot1l, is a chromatin modification ubiquitously associated with actively transcribed genes (81, 82). In human and mouse MLL-AF10 and CALM-AF10 leukemia cells, dimethylated H3K79 is typically enriched in the promoter regions of leukemogenic genes, including the posterior *Hoxa* cluster genes (29, 53). Furthermore, the epigenetic deregulation of these specific leukemogenic genes correlates with aberrant overexpression in leukemia cells (29, 53, 79). Therefore, while DOT1L has not been found to be genetically altered in leukemia, its aberrant recruitment and/or activity may lead to epigenetic deregulation and overexpression of crucial fusion protein target genes.

Consistent with this model, it has been shown that hematopoietic progenitor cells cannot be transformed by MLL-AF10 after being treated with shRNA against Dot1l for one week (29). Moreover, bone marrow cells could not be transformed by CALM-AF10 when a dominant negative form of Dot1l was overexpressed (53). Although the knock-down and over-expression approaches have some limitations, these results raise the possibility that DOT1L may be a relevant therapeutic target for MLL-AF10 and CALM-AF10 leukemia. To determine whether inhibition of DOT1L represents a valid approach to treat MLL-AF10 and CALM-AF10 leukemias, we assessed the effects of genetic deletion and pharmacological inhibition of Dot1l in murine bone marrow cells immortalized by MLL-AF10 and CALM-AF10 oncoproteins. Using genetically defined models of human leukemia that bear specific epigenetic perturbations, our study demonstrates that such abnormal chromatin modifications can be specifically targeted using a small-molecule inhibitor. These observations are of particular interest in the light of mounting evidence for specific epigenetic alterations in several human tumors.

Results

H3K79me2 Is Abrogated by Genetic Inactivation of Dot1L in MLL-AF10 and CALM-AF10 Transformed Bone Marrow Cells.

We used a *Dot1l* conditional knockout mouse model, in which the exon encoding the active site of Dot1l is flanked by *LoxP* sites (25), to determine whether Dot1l and H3K79 methylation are indeed required for transformation driven by MLL-AF10 and CALM-AF10. We sorted HSC-enriched Lin$^-$Sca1$^+$cKit$^+$ (LSK) cells from *Dot1l*$^{+/+}$ and *Dot1l*$^{f/f}$ mouse bone marrow cells, and transformed sorted cells with FLAG-MLL-AF10 or the FLAG-CALM-AF10 minimal fusion (79). The expression of MLL-AF10 and CALM-AF10 in transformed bone marrow cells was confirmed by western blotting using an antibody against the N-terminus of MLL and FLAG respectively (Figure 3-1B). Cells were then plated in cytokine-supplemented methylcellulose and expanded for 1-2 weeks. The MLL-AF10 or CALM-AF10 expressing cells were subsequently transduced with retroviruses encoding either the Cre-Mi-Tomato (Cre) or the control Mi-Tomato (MIT), sorted for tdTomato positive cells 2 days after transduction, and plated in methylcellulose (see Figure 3-1A). Genotyping of tdTomato$^+$ cells right after sorting showed a complete deletion of *Dot1l* in cells transduced with Cre (Figure 3-2D). Consistent with deletion of *Dot1l*, H3K79 di-methylation was diminished in MLL-AF10 and CALM-AF10 transformed bone marrow cells after transduction with Cre (Figure 3-1C and 3-2C).
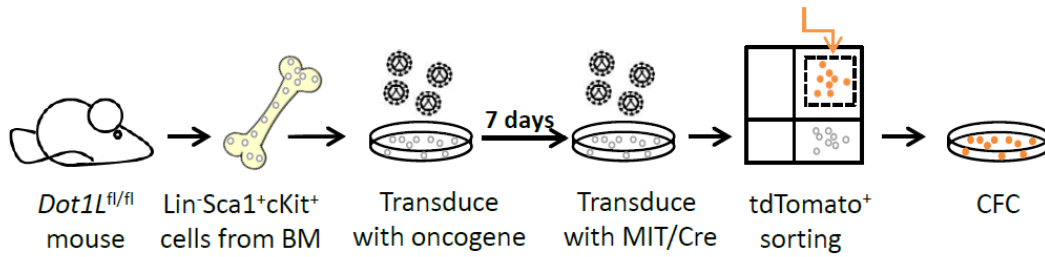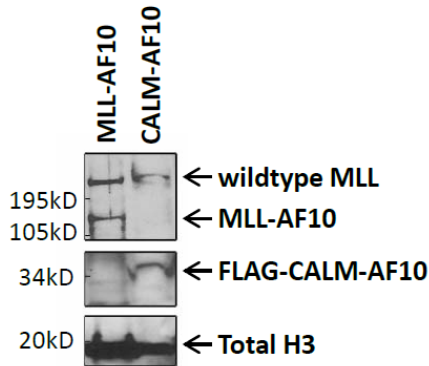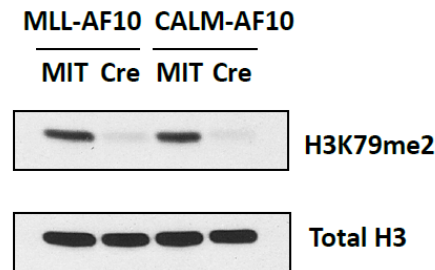
Figure 3-1 Cre-mediated deletion of *Dot1l* leads to loss of H3K79me2 in MLL-AF10 and CALM-AF10 immortalized murine bone marrow cells

(A) Schematic representation of experimental design. (B) Western blot showing the expression of MLL-AF10 using anti-MLL antibody and FLAG-CALM-AF10 using anti-FLAG antibody in transformed bone marrow cells. Total H3 was used as a control. (C) Western blot showing the loss of H3K79 methylation 7 days after transduction with Cre or MIT.

Loss of Dot1l Inhibits Transformation by MLL-AF10 or CALM-AF10

We next evaluated the effects of genetic deletion of *Dot1l* on LSK cells transformed by MLL-AF10 or CALM-AF10. Deletion of *Dot1l* significantly reduced the colony forming potential in both cases (Figure 3-2A). The number of colonies was significantly decreased in the first week. In addition, *Dot1l*$^{-/-}$ colonies were morphologically distinct. While the majority of cells after transduction with MIT formed "blast-like" compact and hypercellular colonies, cells after transduction with Cre formed smaller and more diffuse colonies (Figure 3-2B). Moreover, Wright-Giemsa staining showed that the Cre-transduced cells have a larger cytoplasm and smaller nucleus, consistent with myeloid differentiation. We then verified the

status of the *Dot1l* locus in the remaining cells harvested at different time points after Cre transduction. Figure 3-2D demonstrates that 3 days after transduction only the excised allele can be detected. However, at the end of the first round of plating (day 9), the surviving cells have various degree of deletion, and at the end of the second round of plating (day 16), only the non-deleted allele can be detected. The fact that a small number of non-deleted cells outgrew in two weeks demonstrates a high selective pressure against *Dot1l* deleted cells.

We then assessed changes in expression of select MLL-fusion target genes in MLL-AF10 transformed bone marrow cells after the loss of Dot1l. The N-terminus of MLL binds to leukemogenic genes, including 5' *Hoxa* cluster genes and *Meis1*, and the binding property is retained in MLL-AF10 fusion proteins (72, 73). The overexpression of MLL-fusion targets is a key feature of MLL-AF10 leukemia and the suppression of these leukemogenic genes, such as *Hoxa9*, is sufficient to abolish the leukemia (29, 53). As shown in Figure 3-2C, targets of MLL-AF10 were down-regulated after Cre-mediated deletion of *Dot1l*, while the expression of a gene that is not an MLL-fusion target, *Hoxb4*, is not changed. This finding demonstrates that Dot1l is required for continued expression of MLL-AF10 target genes which further supports the requirement of Dot1l in MLL-AF10 leukemia. We also assessed the expression changes of leukemia-related genes in CALM-AF10 transformed LSK cells after loss of Dot1l. It has been shown that leukemogenic genes, including 5' *Hoxa* cluster genes and *Meis1* are overexpressed in both CALM-AF10 mouse leukemias and CALM-AF10 positive patient leukemias (83, 84). The suppression of these leukemogenic genes, such as *Hoxa5*, is sufficient to abolish CALM-AF10 leukemia (53). As shown in Figure 3-2C, *Hoxa5*, *Hoxa7*, *Hoxa9*, *Hoxa10*, and *Meis1* were all down-regulated after Cre-mediated deletion of *Dot1l*, while the expression of a control gene, *Hoxb4*, did not change. This finding demonstrates that Dot1l is required for maintenance of the transformed phenotype in cells expressing the CALM-AF10.

Figure 3-2 Loss of Dot1l leads to decreased colony forming potential and increased differentiation of MLL-AF10 or CALM-AF10 transformed cells.

(A) Blast and differentiated colony count of *Dot1l*-deleted MLL-AF10 (left) or CALM-AF10 (right) transformed cells in methylcellulose 9 days after transduction with Cre in comparison to controls (n=3 independent experiments). (B) Morphologic changes (10X image of colony morphology in methylcellulose, 40X image of Wright-Giemsa stain) and H3K79me2 immunofluorescence (20X image, Alexa 674-H3K79me2 and DAPI nuclear stain) in MLL-AF10 (left) or CALM-AF10 (right) transformedpreleukemia cells 9 days after transduction with Cre. (C) Relative expression levels of *Hoxa5*, *Hoxa7*, *Hoxa9*, *Hoxa10*, *Meis1*, and *Hoxb4* on cells 5 days after transduction with Cre or MIT. Expression levels were normalized to *Gapdh* and expressed relative to MIT-transduced cells (set to 100%). Error bars indicate the SEM (n=3 independent experiments). (D) Genotyping of transduced bone marrow cells on day 3, day 9, and day 16 after transduction of Cre. f: floxed allele. Δ: deleted allele.

Figure 3-2 (Continued)
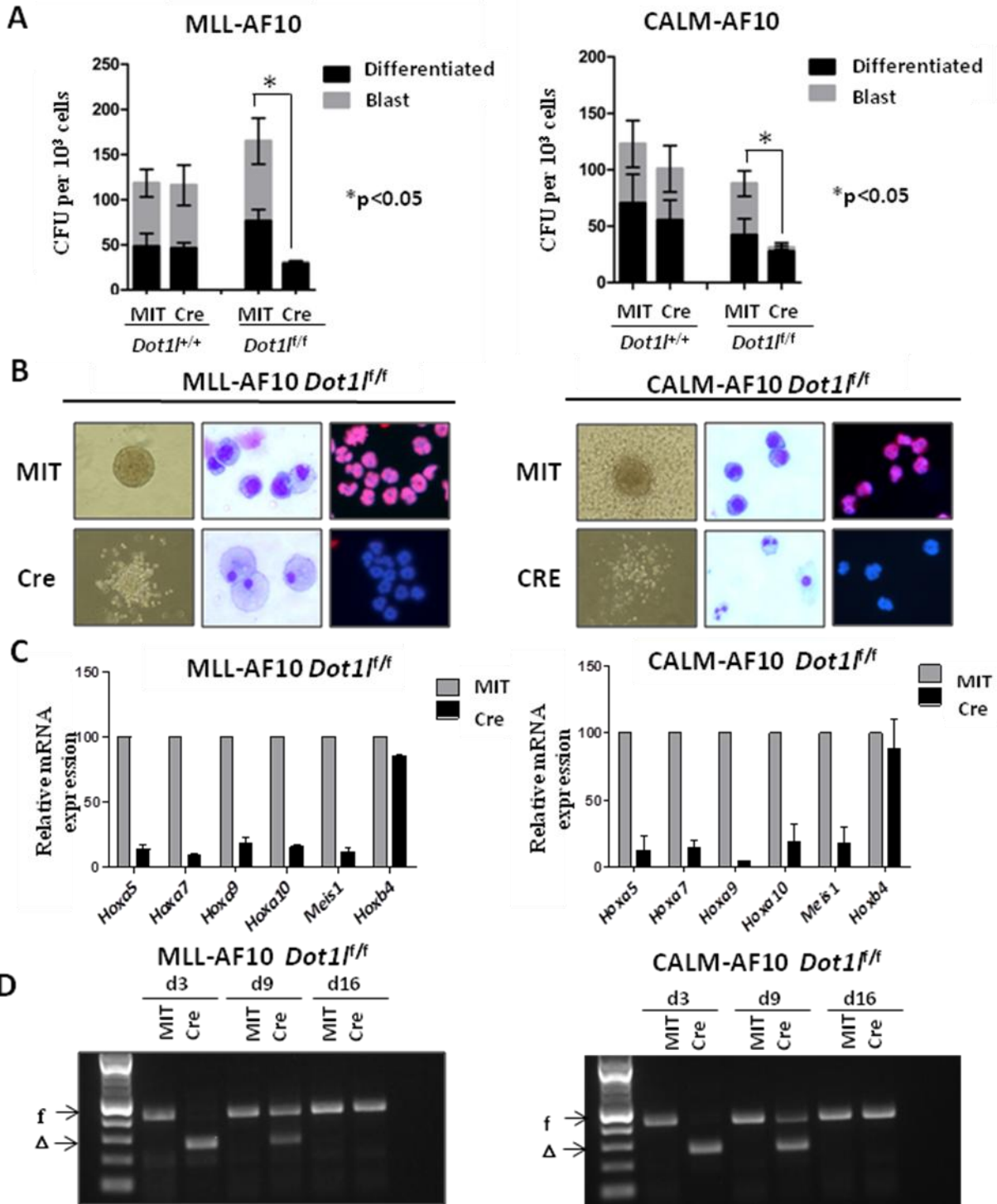
Selective Anti-Proliferative Effect of MLL-AF10 and CALM-AF10 Transformed Cells by the Dot1l Inhibitor EPZ004777

Having established that genetic inactivation of Dot1l inhibits H3K79 methylation and clonogenic potential of MLL-AF10 or CALM-AF10 transformed cells, we investigated the efficacy of Dot1l inhibitors against MLL-AF10 and CALM-AF10 transformed murine bone marrow cells. Recently it has been shown that the Dot1l inhibitor EPZ004777 selectively kills MLL-rearranged leukemia cells, including an MLL-AF4 leukemia cell line MV4-11 and an MLL-AF9 leukemia cell line MOLM13, but not MLL-germline leukemia cells, including Jurkat and HL-60 (85). However, the response of MLL-AF10 leukemia cells to a Dot1l inhibitor has not yet been evaluated, and the CALM-AF10 leukemia cell line U937 surprisingly showed minimal response to the inhibitor (85). Therefore, we performed proliferation assays over several days with three independently-transformed mouse LSK cell populations with MLL-AF10 or CALM-AF10 in the presence of increasing concentrations of EPZ004777 (up to 10 μM) or DMSO vehicle control. MLL-AF9 transformed cells were included as a positive control, and HoxA9 and Meis1 co-transformed (HoxA9/Meis1) cells were included as a non-MLL-rearranged cell line control which has been shown to be refractory to Dot1l inhibition (25). As shown in Figure 3-3A, the growth of MLL-AF10 and CALM-AF10 cells, as well as MLL-AF9 cells, was dramatically inhibited by EPZ004777, while the growth of HoxA9/Meis1 cells was unaffected. The anti-proliferative effect was dose-dependent, with an IC50 between 0.1 μM to 1 μM for MLL-AF10 and CALM-AF10 (Figure 3-3B). Similar to previous findings with human MLL-AF9 and MLL-AF4 leukemia cell lines, the anti-proliferative effect against MLL-AF10 and CALM-AF10-transformed primary murine hematopoietic progenitor cells only became apparent after 7 days. Nevertheless, when exposed to EPZ004777 longer, MLL-AF10 and CALM-AF10 transformed cells showed a dramatic decrease in cell number, while proliferation of the Hoxa9/Meis1 transformed cells was unaffected. Consistent with the proliferation and viability curve, Western blots showed a dose-dependent reduction of H3K79 dimethylation in all cell lines after incubation with the Dot1l inhibitor EPZ004777 (Figure 3-3E).
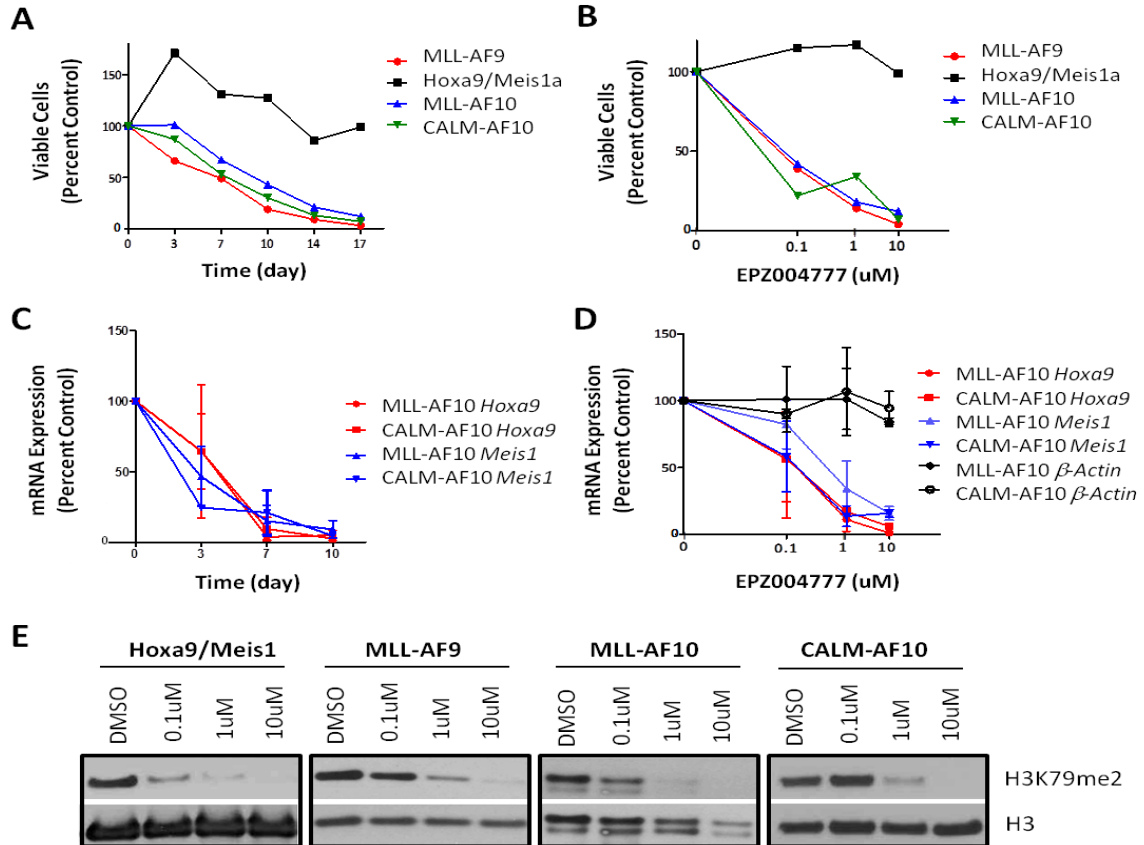
Figure 3-3 EPZ004777 selectively inhibits proliferation of MLL-AF10 and CALM-AF10 transformed murine bone marrow cells

(A) Growth of MLL-AF10, CALM-AF10, MLL-AF9, and Hoxa9/Meis1a transformed bone marrow cells during several days' incubation with 10 μM EPZ004777. Viable cells were counted and replated at equal cell numbers in fresh media with fresh compound every 3–4 days. Results were plotted as percentage of split-adjusted viable cells in the presence of 10 μM EPZ004777 compared to DMSO vehicle control. Results are representative of three independent experiments. (B) Dosage effect of EPZ004777 treatment on MLL-AF10, CALM-AF10, MLL-AF9, and HoxA9/Meis1a transformed bone marrow cells. Cells were counted and replated at equal cell numbers in fresh media with fresh compound every 3–4 days. Results were plotted as percentage of split-adjusted viable cells on day 17 in media with 0.1 μM, 1 μM, 10 μM of EPZ004777 compared to DMSO control (set as 100%). Results are representative of three independent experiments. (C) Time course of *Hoxa9* and *Meis1* mRNA expression in MLL-AF10 and CALM-AF10 transformed cells over 10 days of incubation with 10 μM EPZ004777 as measured by quantitative real-time PCR. Expression levels were normalized to *Gapdh* and expressed relative to those at day 0 (set to 100%). Error bars indicate the SEM (n=3 independent experiments). (D) Quantitative real-time PCR analysis of *Hoxa9*, *Meis1*, and *β-Actin* mRNA levels in MLL-AF10 and CALM-AF10 transformed cells following 7 days of incubation with EPZ004777. Relative mRNA expression levels are plotted as a percentage of those in vehicle-treated control cells. Error bars represent SEM (n=3 independent experiments). (E) Inhibition of cellular H3K79me2 levels in MLL-AF10, CALM-AF10, MLL-AF9 or Hoxa9-Meis1a transformed bone marrow cells following 7 days of treatment with the indicated concentrations of EPZ004777 as measured by immunoblot analysis of extracted histones with an anti-H3K79me2 antibody.

We next tested whether the expression of MLL-AF10 and CALM-AF10 target genes was affected after EPZ004777 treatment. *Hoxa9* and *Meis1* overexpression is a hallmark of both MLL-AF10 and CALM-AF10 leukemia (29, 83, 84). We performed quantitative real-time PCR to examine the effect of EPZ004777 on *Hoxa9* and *Meis1* mRNA expression levels in MLL-AF10 and CALM-AF10 transformed cells. The mRNA expression levels of *Hoxa9* and *Meis1* started to decrease within 3 days and became significantly lower within 7 days' treatment with 10 μM EPZ004777 (Figure 3-3C). Analysis of cells on day 7 of EPZ004777 treatment showed a concentration-dependent decrease of mRNA levels of *Hoxa9* and *Meis1*, but not *β-actin*, which shows that the decrease in *Hoxa9* and *Meis1* expression is not caused by a general inhibition of gene expression.

Next we determined if the decrease in cell number for EPZ004777 treated MLL-AF10 or CALM-AF10 transformed cells was due mostly to inhibition of cell proliferation or induction of apoptosis. Dot1l inhibition reduced the number of actively proliferating MLL-AF10 cells, with an increase in the percentage of cells in the G1 or sub G1fractions after 4 days of incubation with 10 μM EPZ004777 (Figure 3-4A). Moreover, a significant increase in the percentage of apoptotic cells after inhibition of Dot1l was observed in MLL-AF10 transformed cells compared to DMSO control on day 10 (Figure 3-4B). Similarly, Dot1l inhibition reduced the number of CALM-AF10 cells in S-phase, with the majority of cells found in G1 after 4 days of incubation with 10 μM EPZ004777 (Figure 3-4C). Interestingly, there was only a minimal increase in apoptotic cells throughout the length of this experiment (Figure 3-4D), suggesting the effect on CALM-AF10 may be more of a cell cycle arrest whereas MLL-AF10 cells respond with cell cycle arrest and more pronounced apoptosis.
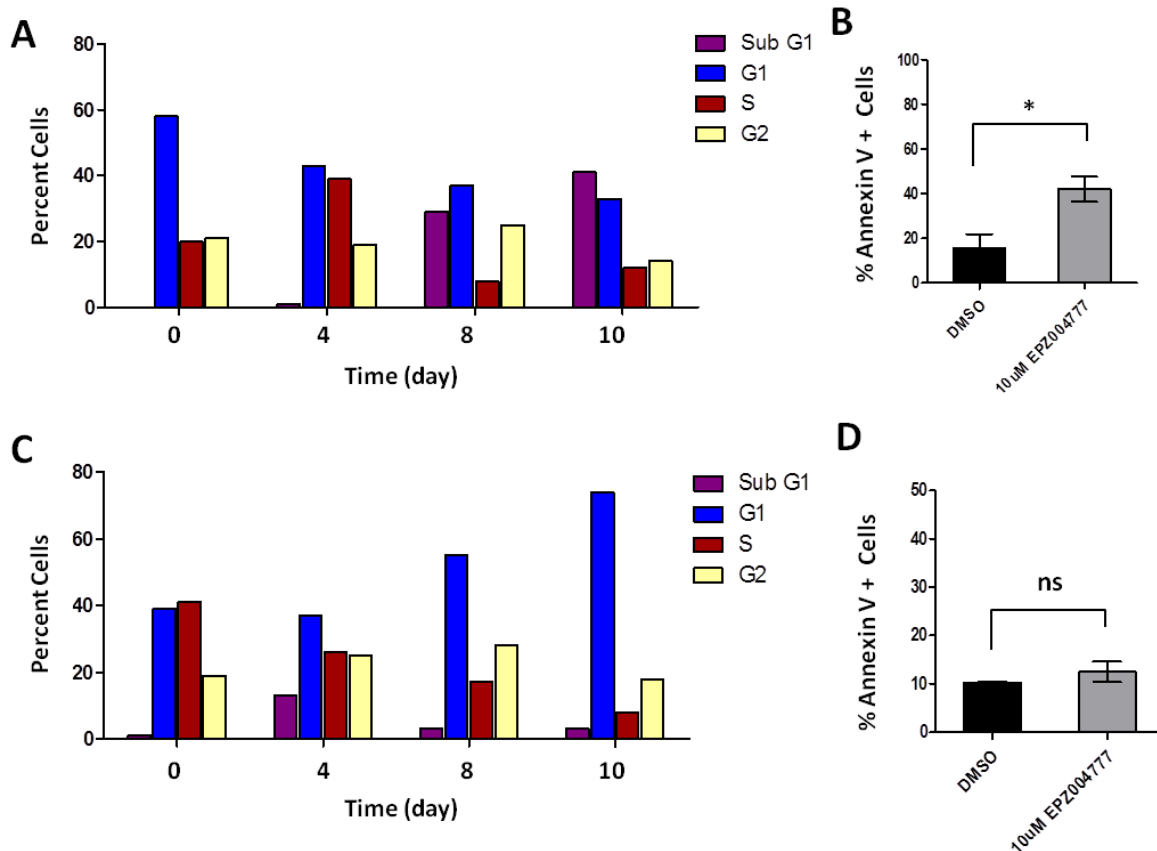
Figure 3-4 EPZ004777 causes cell cycle arrest and apoptosis in MLL-AF10 and CALM-AF10 transformed bone marrow cells

(A) Cell cycle changes (BrdU/7-AAD flow cytometry) in MLL-AF10 transformed bone marrow cells after being treated with 10 μM EPZ004777 for 0, 4, 8, or 10 days. Results are representative of two independent experiments. (B) Annexin V staining in MLL-AF10 transformed bone marrow cells 10 days after treatment with 10 μM EPZ004777 or DMSO control (n = 2 independent experiments). Error bars represent standard error of the mean (SEM). (C) Cell cycle changes (BrdU/7-AAD flow cytometry) in CALM-AF10 transformed bone marrow cells after being treated with 10 μM EPZ004777 for 0, 4, 8, or 10 days. Results are representative of two independent experiments. (D) Annexin V staining in CALM-AF10 transformed bone marrow cells 10 days after treatment with 10μM EPZ004777 or DMSO control (n = 2 independent experiments). Error bars represent standard error of the mean (SEM).

We went on to test whether EPZ004777 treatment affects the colony forming ability and serial replating

capacity of MLL-AF10 and CALM-AF10 transformed LSK cells in *in vitro* CFC assays. We cultured

MLL-AF10 or CALM-AF10 transformed mouse bone marrow cells in methylcellulose based medium

containing DMSO or 10μM EZP004777. MLL-AF10 or CALM-AF10 transformed cells formed large,

highly clonogenic compact blast-like colonies in methylcellulose based medium containing DMSO. However, MLL-AF10 or CALM-AF10 transformed cells formed significantly fewer compact colonies in medium containing 10μM EZP004777 starting from the first week (Figure 3-5A). The clonogenic potential of MLL-AF10 or CALM-AF10 transformed cells was abrogated after two weeks culture in the presence of inhibitor. Cytospin at the end of the first week showed that the majority of EPZ004777-treated cells have large cytoplasm and small or fragmented nucleus, consistent with myeloid differentiation.

To study the effect of pharmacological inhibition of Dot1l *in vivo*, we pretreated MLL-AF10 and CALM-AF10 transformed cells in liquid culture with either DMSO or 10μM EPZ004777 for 8 days before injecting into lethally irradiated recipients (Figure 3-5C). Two weeks after injection, we assessed the spleen-colony forming ability with CFU-S assay. MLL-AF10 or CALM-AF10 transformed cells without inhibitor treatment formed >10 large spleen colonies in two weeks. In contrast, cells pretreated with inhibitor failed to form any large spleen colonies, and instead formed several small and diffuse foci, similar to the colonies observed in the *in vitro* methylcellulose based cultures. These effects on the CFU-S forming activity suggest that EPZ004777 may show *in vivo* efficacy against AF10-fusion transformed cells (Figure 3-5D).

Figure 3-5 EPZ004777 decreased the colony forming potential and induced differentiation in MLL-AF10 and CALM-AF10 transformed bone marrow cells *in vitro* and EPZ004777 pretreatment diminished spleen-colony forming potential *in vivo*

(A) Blast and differentiated colony count of MLL-AF10 or CALM-AF10 transformed cells cultured in methylcellulose based medium in the presence of 10uM EPZ004777 or DMSO vehicle control at the end of 1 week or 2 weeks (n=2 independent experiments). (B) Morphologic changes (10X image of colony morphology in methylcellulose, 40X image of Wright-Giemsa stain) in MLL-AF10 (left) or CALM-AF10 (right) transformed cells cultured in methylcellulose based medium containing EPZ004777 for 7 days. (C) Schematic representation of CFU-S experimental design. (D) The morphology of spleen dissected from mice injected with pretreated MLL-AF10 or CALM-AF10 transformed cells.

Figure 3-5 (Continued)
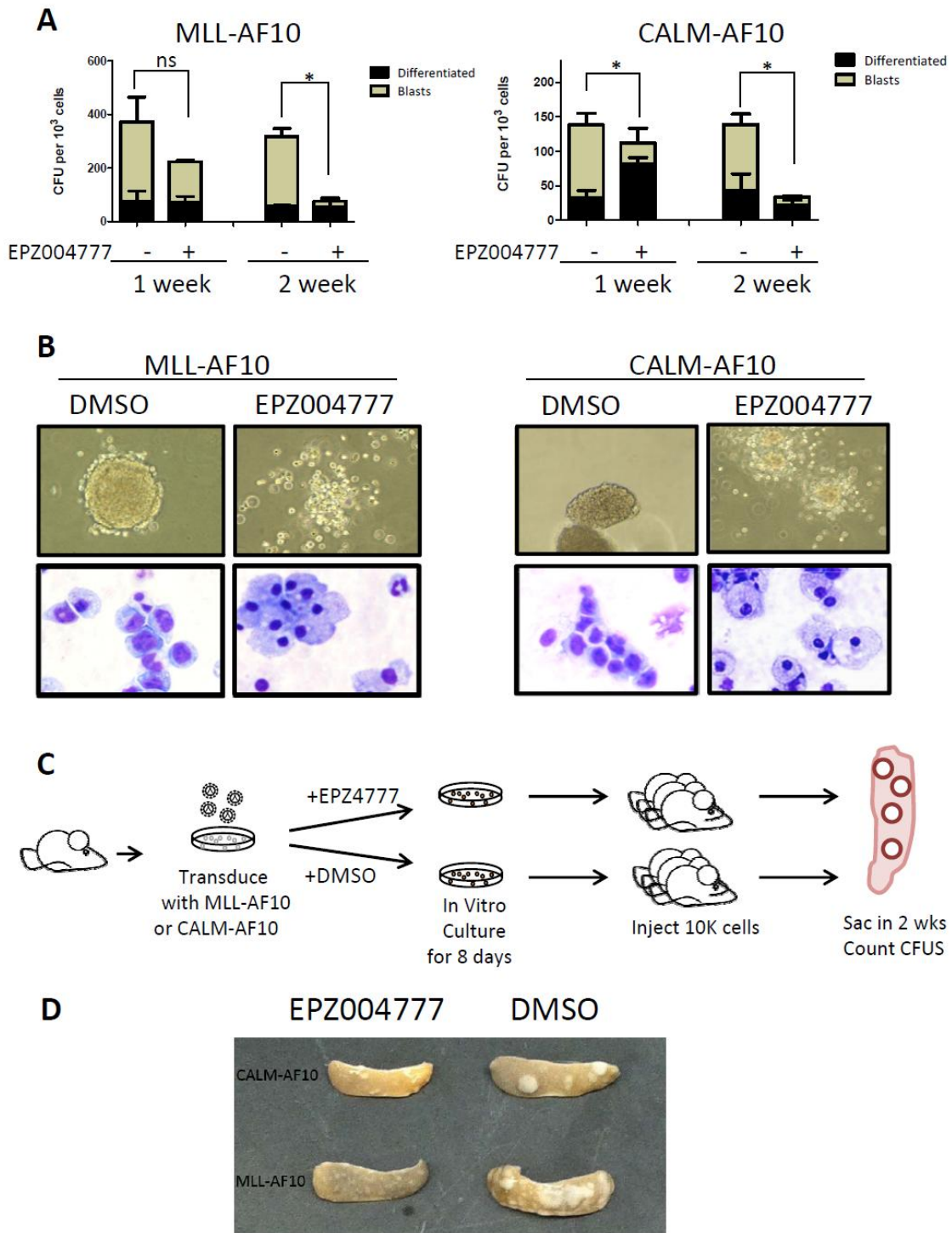
Dot1l is Indispensible for the Initiation and the Maintenance of MLL-AF10 or CALM-AF10 Leukemia Cells *In Vivo*

Since CFU-S activity does not directly test whether Dot1l inactivation impacts full-blown leukemogenesis, we sought to assess the impact of *Dot1l* deletion on *in vivo* leukemia initiation and maintenance by the leukemogenic AF10 fusions. *Dot1l*$^{f/f}$ bone marrow cells were transformed using retroviral MLL-AF10 or CALM-AF10. In two to three days, Dot1l was deleted in preleukemic-transformed cells through retroviral delivery of Cre-recombinase. Two days after MIT or Cre transduction, GFP$^+$tdTomato$^+$ cells were sorted and injected into sublethally irradiated recipients at 5×10^5 cells/mouse. Flow cytometric analysis of mouse peripheral blood 102 days after injection showed the propagation of *Dot1l*$^{f/f}$ MLL-AF10-transformed cells but not *Dot1l*$^{-/-}$ MLL-AF10-transformed cells in recipients (Figure 3-6F). Mice injected with preleukemic MLL-AF10-transformed *Dot1l*$^{f/f}$ cells all developed myeloid leukemia with a median of 112 days. However, no leukemia could be generated in mice injected with same doses of MLL-AF10-transformed Dot1l$^{-/-}$ cells (Figure 3-6A). Similar to MLL-AF10, preleukemic CALM-AF10-transformed *Dot1l*$^{f/f}$ cells represented an increasing population of GFP$^+$tdTomato$^+$ cells in recipients' peripheral blood and ultimately caused myeloid leukemia in recipients (Figure 3-7A and B), while CALM-AF10-transformed *Dot1l*$^{-/-}$ cells disappeared from the peripheral blood within 2 months (data not shown). This result shows that Dot1l is required for *in vivo* leukemogenesis of mouse bone marrow cells transformed by MLL-AF10 as well as CALM-AF10.

We then checked the effect of *Dot1l* deletion on established mouse leukemia cells. We collected bone marrow cells from primary MLL-AF10 or CALM-AF10 leukemia mice, performed MIT or Cre transduction, and sorted GFP$^+$tdTomato$^+$ cells for injection into mice. *Dot1l*$^{f/f}$ MLL-AF10 leukemic cells caused Mac1$^+$Gr1$^+$ secondary myeloid leukemia with a median of 81 days after transplantation, while MLL-AF10 leukemic cells lacking Dot1l failed to cause any leukemia in mice (Figure 3-6B and 3-6C).

Histopathology study showed massive organ infiltration of leukemic cells in mice injected with $Dot1l^{f/f}$ MLL-AF10 (Figure 3-6E). The spleen weight of mice injected with $Dot1l^{f/f}$ MLL-AF10 was significantly higher than that of mice injected with $Dot1l^{-/-}$ MLL-AF10 (p<0.01, Figure 3-6D). Similar to MLL-AF10, $Dot1l^{f/f}$ CALM-AF10 leukemic cells resulted in an increasing population of GFP$^+$tdTomato$^+$ cells in recipients' peripheral blood and ultimately caused myeloid leukemia in recipients, while $Dot1l^{-/-}$ CALM-AF10 leukemic cells appeared in peripheral blood initially, but disappeared from peripheral blood within 38 days (Figure 3-7C). This result shows that Dot1l is also required for the maintenance of MLL-AF10 or CALM-AF10 leukemia *in vivo*.

Figure 3-6 Dot1l is required for initiation and maintenance of MLL-AF10-driven leukemia *in vivo*

(A) Survival curves for mice injected with $5X10^5$ MLL-AF10 transformed bone marrow cells 2 days after transduction with Cre or MIT-control retrovirus and sorting for GFP$^+$/tdTomato$^+$ cells. (B) Survival curves for secondary recipient mice that received $2X10^5$ MLL-AF10 leukemia cells 2 days after transduction with Cre or MIT and sorting for GFP$^+$/tdTomato$^+$ cells. (C) Immunophenotype of spleen cells from MIT-transduced secondary MLL-AF10 leukemic mice (a typical AML phenotype: Mac1$^+$Gr1$^+$CD3$^-$B220$^-$). (D) Spleen picture and spleen size in mice injected with Cre or MIT transduced *Dot1l $^{f/f}$* MLL-AF10 cells (n=5.*: p<0.01). (E) Morphology of peripheral blood smear (40X image of Wright-Giemsa stain) and pathology of organs from MIT transduced secondary MLL-AF10 leukemic mice (10X H&E stain). (F) Peripheral blood chimerism in mice 102 days after injection of MIT or Cre transduced MLL-AF10 preleukemic cells. Donor cells are GFP$^+$/tdTomato$^+$ and recipient cells are GFP$^-$/tdTomato$^-$.

Figure 3-6 (continued)

A MLL-AF10 primary leukemia survival curve

B MLL-AF10 secondary leukemia survival curve

C

D

E Liver Spleen Kidney Peripheral Blood

F

MIT

Cre
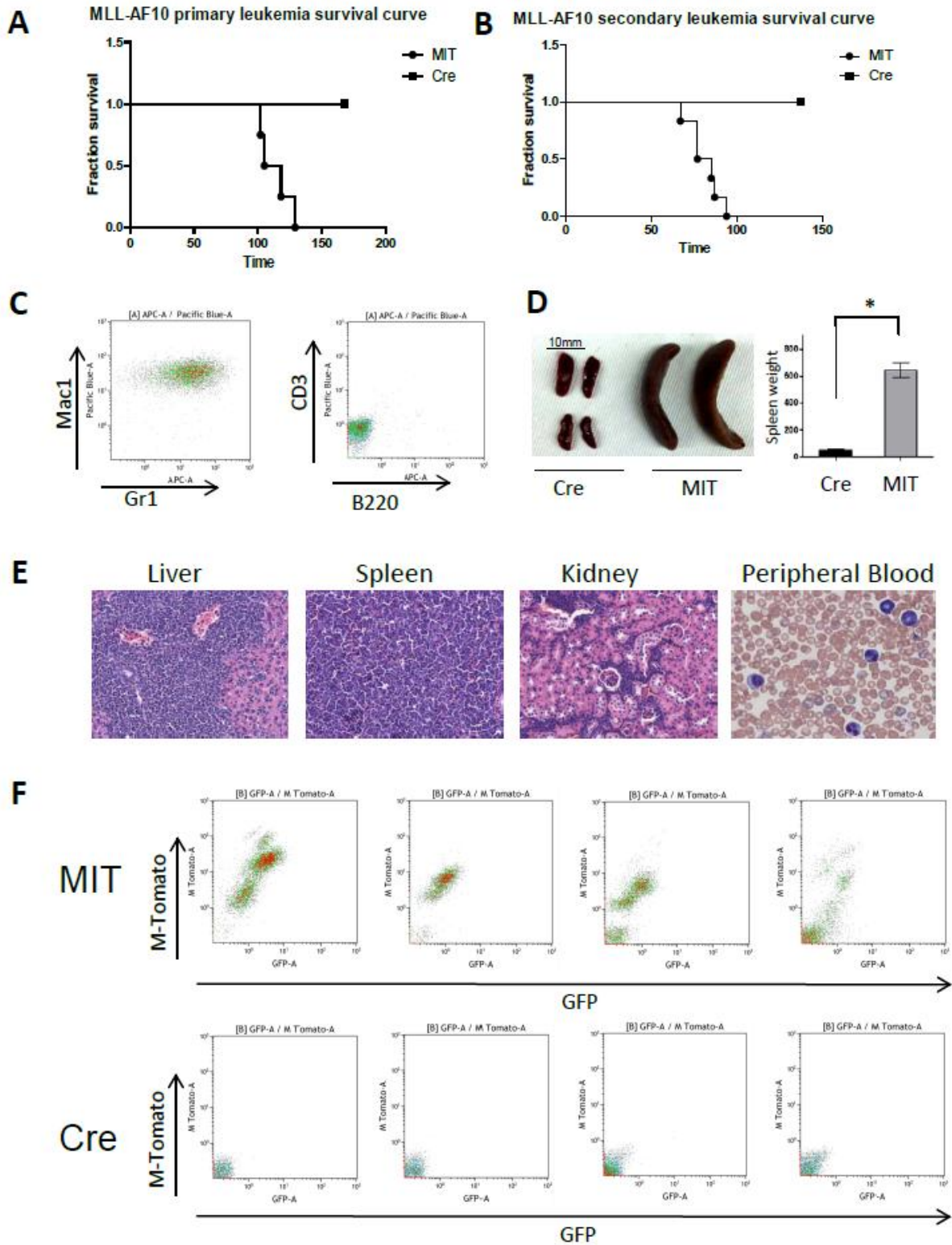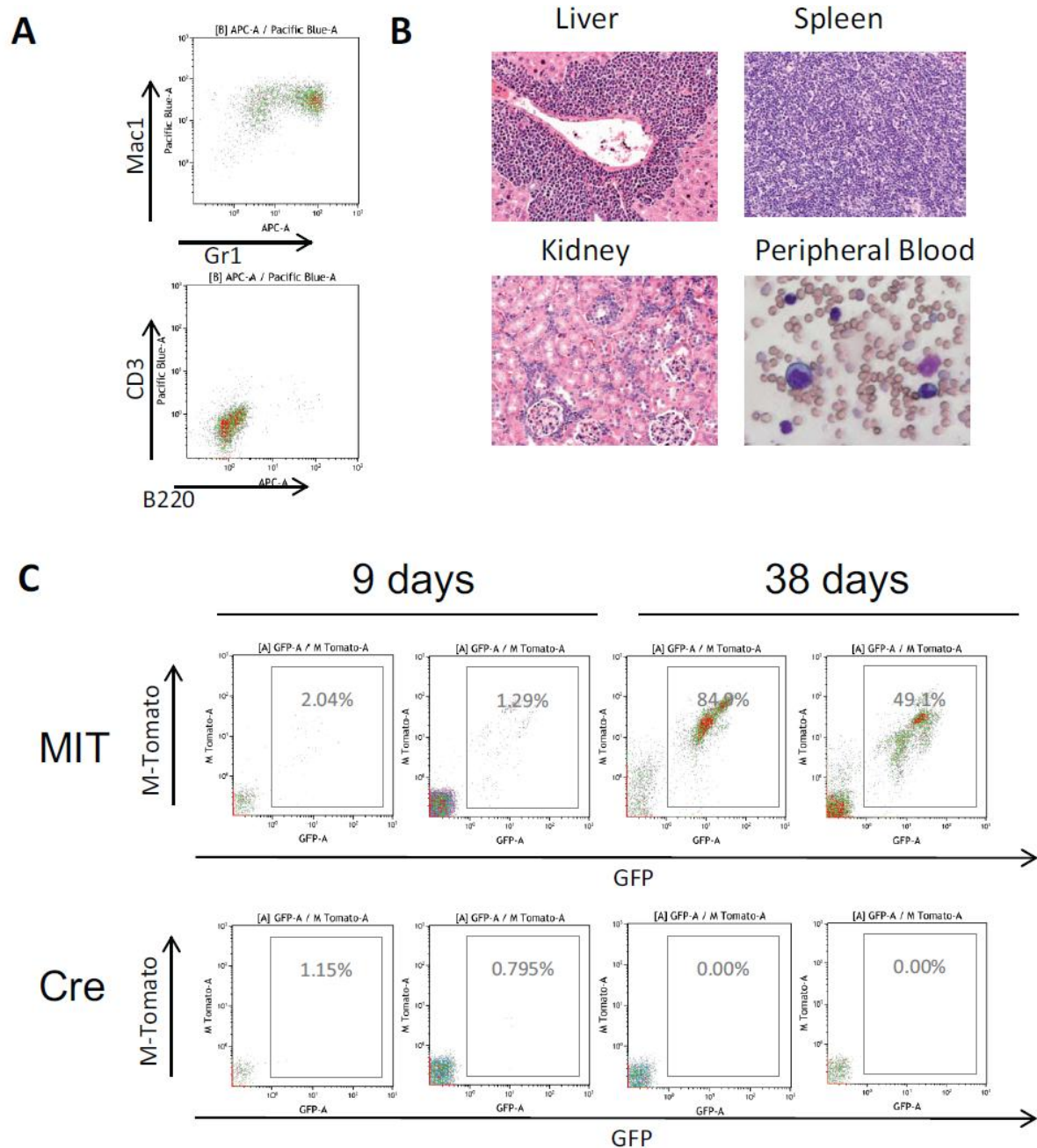
Figure 3-7 *Dot1l* deleted CALM-AF10 leukemic cells failed to repopulate in secondary recipients.

(A) Immunophenotype of spleen cells from MIT transduced *Dot1l*$^{f/f}$ CALM-AF10 leukemic mice (majority of cells in the spleen displays an AML immunophenotype: Mac1$^+$Gr1$^+$CD3$^-$B220$^-$). (B) Morphology of peripheral blood smear (40X image of Wright-Giemsa stain) and pathology of organs from moribund mice that were injected with MIT transduced *Dot1l*$^{f/f}$ CALM-AF10 cells (10X H&E stain). (C) Peripheral blood chimerism in secondary recipients 9 days or 38 days after injection of MIT or Cre transduced *Dot1l*$^{f/f}$ CALM-AF10 leukemic cells. Donor cells are GFP$^+$/tdTomato$^+$ and recipient cells are GFP$^-$/tdTomato$^-$.

Discussion

A number of studies have recently demonstrated that DOT1L and H3K79 methylation plays an important role in MLL-AF9 (25, 45, 56, 57), MLL-GAS7 (56), and possibly MLL-AFX (56) transformation. In this study, we show that loss of Dot1l abrogates *in vitro* as well as *in vivo* transformation in MLL-AF10 and CALM-AF10 immortalized cells. This genetic approach circumvented the drawbacks of knock-down and overexpression approaches, such as off-target effects and problems of non-physiologic protein expression, thus strengthening the case for targeting Dot1l therapeutically in leukemias involving AF10 fusions.

Current advances in biology, biochemistry and pharmacology have raised the prospects of highly targeted therapeutics that maximize efficacy and minimize systemic toxicity. One outstanding example is targeting the fusion protein BCR-ABL kinase by imatinib in chronic myeloid leukemia (86). In our study, we tested the efficacy of targeting Dot1l in MLL-AF10 and CALM-AF10 leukemia. We show that the small-molecular inhibitor of Dot1l EPZ004777 selectively inhibits the proliferation of MLL-AF10 and CALM-AF10 transformed mouse bone marrow cells but has no effect on HoxA9/Meis1 transformed mouse bone marrow cells. The fact that Dot1l is dispensable for transformation driven by ectopically-expressed HoxA9 and Meis1 is in agreement with the model that the OM-LZ domain of AF10 present in leukemic AF10 fusions recruits Dot1l and activates *Hox-Meis* target genes through aberrant H3K79 methylation. Cells ectopically expressing retrovirally introduced *HoxA9* and *Meis1* genes are therefore immune to loss of H3K79 methylation. It not only demonstrates a strong rationale for inhibiting Dot1l as a strategy to target the *AF10* rearranged leukemias, but also is in agreement with previous data that Dot1l is not absolutely required for cell proliferation (25). Recent studies showed that although conditional knockout of Dot1l leads to pancytopenia and failure of hematopoietic homeostasis in adult mice, the toxicity did not develop until 7-8 weeks after Dot1l inactivation (57). More importantly, *in vivo* administration of EPZ004777 for 2 weeks leads to extension of survival in a mouse MLL xenograft model with minimal

hematopoietic side effects (85). These data provide further support for the continued development of DOT1L inhibitors as a potential therapeutic modality for MLL-rearranged and CALM-AF10 leukemias.

Interestingly, Daigle et al. recently demonstrated that the leukemia cell line U937, which harbors the CALM-AF10 fusion, was insensitive to EPZ004777 (85). The U937 cell line is a monocytic leukemia cell line in which the CALM-AF10 translocation was first identified in 1996 and it is the only readily available human leukemia cell line that carries the CALM-AF10 translocation (87). The long latency of CALM-AF10 leukemia in the murine bone marrow transplantation model and incomplete penetrance in the transgenic CALM-AF10 model strongly hints at additional collaborating mutations that need to be accumulated for CALM-AF10 leukemogenesis (83, 88). It is possible that the U937 cell line has accumulated other mutations, either during in-vivo leukemogenesis or during in-vitro passages, which may enable cells to circumvent the requirement of DOT1L for leukemia maintenance in vitro. The insensitivity of U937 to DOT1L inhibition is intriguing since both circumstantial evidence from human leukemias as well as experimental evidence presented here and from other studies points to a key role for the DOT1L methyltransferase in *AF10* rearranged leukemias. The DOT1L interacting OM-LZ domain is consistently retained in both CALM-AF10 as well as MLL-AF10 patients, and the exclusion of the OM-LZ domain completely inhibits transforming activity of both the CALM –AF10 as well as MLL-AF10 fusions in murine models (29, 53). Moreover, the OM-LZ domain is also the minimal portion of AF10 required for the leukemogenesis for both the aforementioned AF10 fusions (79, 89). Importantly, our studies showing that Dot1l gene ablation as well as pharmacologic Dot1l inhibition demonstrates anti-leukemic activity demonstrate that DOT1L inhibition could be an attractive therapeutic target in human *AF10* rearranged leukemias. Therefore, development of a panel of other *AF10* rearranged cell lines or primary human xenograft models would appear to be warranted to assess the efficacy of DOT1L inhibition on human *AF10* rearranged leukemia.

We and others have recently demonstrated that leukemogenesis mediated by a number of MLL fusions is dependent on abnormal H3K79 methylation (25, 29, 45, 56, 57). It was shown that the Dot1l inhibition in these MLL leukemias specifically interfered with the constitutive activation of MLL-target genes, resulting in abrogation of leukemogenesis mediated by these MLL-fusions. Interestingly, even though the CALM-AF10 fusion does not involve MLL as a fusion partner, gene expression studies have shown that the transcriptional profiles of CALM-AF10 patient samples bear strong similarities to those of MLL patient samples (84, 90). A simplistic explanation for this similarity could be the shared dependence of these fusions on aberrant H3K79 methylation for the activation of oncogenic programs. The relation between H3K79 methylation and *AF10*-rearranged leukemias is, however, more complicated. On one hand, aberrant H3K79 hypermethylation in MLL-AF10 and CALM-AF10 targets are required for activation of leukemogenic transcriptional programs and the maintenance of leukemia. On the other hand, MLL-AF10 and CALM-AF10 patient samples show a global hypomethylation of H3K79, possibly because the AF10 fusions disrupt normal AF10 function (91). Further studies will focus on the mechanisms of how abnormal H3K79 methylation patterns are established and how deregulation of a single epigenetic modification may act as a driver of leukemias with *AF10* rearrangements.

Our observation that MLL-AF10 and CALM-AF10 fusions require Dot1l for initiation as well as maintenance of leukemia, strongly indicates that pharmacologic inhibition of aberrant H3K79 methylation could be of potential clinical benefit in the *AF10*-rearranged leukemias. Future studies will determine the effect of pharmacologic DOT1L inhibition on *in vivo* AF10-rearranged leukemias using syngenic or xenogenic leukemia models. At the moment, such studies are precluded by the poor pharmacokinetic properties of the DOT1L inhibitor used in our studies (24). These results could help inform future clinical trials with DOT1L inhibitors.

Materials and Methods

Mutant Mice

Mice engineered to harbour *LoxP* sites flanking exon 5 of *Dot1l* were generated in our laboratory and have been described previously (25). Bone marrow cells from 7-10 week old mice in *Dot1l* wild-type or homozygous floxed (*Dot1l*^f/f) backgrounds were used for transformation assays and subsequent biochemical experiments.

Generation of Transformed Murine Cells and Leukemia

The MSCV based MLL-AF9-IRES-GFP, HoxA9-IRES-GFP, and Meis1a-PGK-Puromycin constructs were described previously (25). The FLAG-CALM-AF10 minimal fusion construct has been described in detail earlier (79) and the FLAG-MLL-AF10 construct was generated by fusing amino acids 1-1430 of MLL to amino acid 625-1027 of AF10 in an MSCV-IRES-GFP vector. The MSCV-IRES-Tomato (MiTomato, or MIT) plasmid was a kind gift from the lab of Hassan Jumaa (Max Planck Institute, Freiburg). The cDNA for Cre recombinase was sub-cloned into the MIT plasmid to generate the MSCV-Cre-IRES-Tomato (Cre-MiTomato, or Cre) construct. Retroviral supernatants were collected from 293-T cells separately transfected with the plasmids using standard protocols and used for retroviral spin infections. Sorted Lin^-Sca^-1^+cKit^+ (LSK) cells from mouse bone marrow were used for retroviral transduction experiments. The LSK cells were transduced with viruses carrying MLL-AF10, CALM-AF10, MLL-AF9, or HoxA9 and Meis1, and expanded for 2-5 days in methylcellulose M3234 (StemCell Technologies, Vancouver, Canada) supplemented with cytokines (6ng/ml IL3, 10ng/ml IL6 and 20ng/ml SCF). MLL-AF10 or CALM-AF10 transformed cells were then transduced with Cre or MIT and expanded in methylcellulose M3234 supplemented with cytokines. After two days, GFP^+Tomato^+ cells were sorted for in vitro colony forming assays, or sorted and transplanted into B6/129 syngeneic sublethally irradiated (550 rad) recipients at 5×10^5 cells/mouse. For secondary transplants, whole-bone marrow from leukemic mice was isolated and transduced with Cre or MIT on the same day; GFP^+Tomato^+ cells were sorted in two days, and transplanted into sublethally irradiated (550 rad) B6/129

53

syngeneic recipients at 5×10^5 cells/mouse for generation of secondary CALM-AF10 leukemia, or non-irradiated severe combined immunodeficiency (SCID) recipients at 2×10^5 cells/mouse for generation of secondary MLL-AF10 leukemia.

Colony Forming Assays

Colony forming cell (CFC) assays were performed by plating 1000 cells per ml of methylcellulose M3234 supplemented with cytokines (6ng/ml IL3, 10ng/ml IL6 and 20ng/ml SCF). On day 6-7 after plating, colonies were scored using a Nikon Eclipse TS100 microscope (Nikon, Tokyo, Japan) and classified into two categories - compact and hypercellular blast-like colonies or small and diffuse differentiated-type colonies. Colonies were then pooled and used for biochemical assays or replated for assessment of secondary replating potential at the same concentration. Cytospin preparations were performed from 50-100,000 cells. Pictures of colonies and Wright-Giemsa stained cytospin preparations were taken using a Nikon Eclipse E400 microscope (Nikon, Tokyo, Japan) and a SPOT RT color digital camera (Diagnostic Instruments, Sterling Heights, MI, USA).

EPZ004777

EPZ004777 was synthesized by Epizyme (Cambridge, MA). 50 mM stock solutions were prepared in DMSO and stored at -20 °C. Serial dilutions of stock solutions were carried out just prior to use in each experiment and final DMSO concentrations were kept at, or below 0.02%.

Cell Proliferation,Viability Assay and Colony-Forming Unit-Spleen (CFU-S) Assay

For assessment of cell proliferation and viability, cells from three independent transductions for each virus were plated, in duplicate, in 96-well plates at a density of 1.5×10^4 cells/well in a final volume of 150 μl. Cells were incubated in the presence of increasing concentrations of EPZ004777 up to 10 μM. Viable

cell number was counted every 3–4 days for up to 17 days using Trypan blue staining. On days of cell counts, growth media and EPZ004777 were replaced and cells split to a density of 1.5×10^4 cells/well. Results were plotted as the percentage of split-adjusted viable cells in the presence of EPZ004777 compared to DMSO vehicle control. For CFU-S assays, cells from two independent transductions for each virus were plated in 24-well plates at a density of 1.5×10^4 cells/well with 10 μM EPZ004777 or DMSO control. Growth media and EPZ004777 were replaced on day 4. On day 8, viable cells were counted and injected into lethally irradiated (550rad twice) syngeneic recipients at 10^4 cells/mouse. After two weeks, mice were euthanized and spleens were collected and fixed using standard protocols.

Cell Cycle and Apoptosis Assays

MLL-AF10 and CALM-AF10 transformed bone marrow cells were plated in 12-well plates at a density of 2×10^5 cells/ml. Cells were incubated with 10 μM EPZ004777 or DMSO vehicle control in a final volume of 1 ml for up to 10 days during which media with inhibitor were changed every 3 to 4 days. Cell cycle analysis was performed after 30 min. of BrdU labeling using BrdU-APC/7AAD kit from BD-Pharmingen (San Jose, CA, USA) on day 0, day 4, day 8, and day10. Data was acquired on a 4-color Becton-Dickinson FACSCalibur flow cytometer and analyzed using BD FACS Diva (San Jose, CA, USA) and Modfit LT (Verity Software House, Topsham, ME, USA). Annexin V apoptosis assays were performed on day 10. Cells incubated with 10μM EPZ004777 or DMSO vehicle control were washed in PBS, resuspended in Ca/HEPES buffer (10 mM HEPES, pH7.4; 140 mM NaCl; 2.5 mM $CaCl_2$) and incubated with Annexin V-PE (BioVision Inc., Mountain View, CA) for 20 mins. Data was acquired on a 4-color Becton-Dickinson FACSCalibur flow cytometer and analyzed using BD FACS Diva.

Western Blotting and Immunofluorescence

Histone purification was performed with triton extraction (1×PBS, 0.5% TritonX100 and 2 mM phenylmethylsulfonylfluoride) followed by acid extraction with 0.2 N HCl as previously described (25). Whole cell protein extracts were prepared for detection of MLL-AF10 and CALM-AF10 fusion proteins (see supplemental data for detailed protocol). Immunofluorescence was done following a previously established protocol (21). The following antibodies were used for detection: anti-H3K79me2 antibody ab3594 (Abcam, Cambridge, MA, USA), anti-total H3 antibody ab1791 (Abcam, Cambridge, MA, USA), anti-MLL antibody A300-086A (Bethyl Laboratories, Montgomery, Texas, USA), anti-FLAG m2 antibody F1804 (Sigma-Aldrich); secondary antibodies used: sheep anti-mouse ECL horseradish peroxidase linked NA931V, donkey anti-rabbit ECL horseradish peroxidase linked NA934V (GE healthcare UK limited, Little Chalfont Buckinghamshire, UK), and Alexa 594 conjugated goat anti-rabbit antibody A11072 (Invitrogen, Carlsbad, CA, USA).

Reverse transcription and Real Time PCR

Total RNA was isolated using Trizol (Invitrogen, Carlsbad, CA, USA) according to the manufacturer's instruction. The resultant cDNA was generated using the Tetro cDNA synthesis kit (Bioline, Taunton, MA, USA). Real time PCR was performed using Taqman probes (Applied Biosystems) on the ABI 7700 Sequence Detection System (Applied Biosystems). Expression levels (average values and standard deviations of triplicate determinations) were normalized to housekeeping gene GAPDH. All experiments were performed with technical duplicates from three individual experiments.

Chapter 4

Leukemic Transformation by the MLL-AF6 Fusion Requires Dot1l

Introduction

In *MLL*-rearranged leukemias, the *MLL* gene is fused to one of more than 60 different partner genes, resulting in the formation of oncogenic MLL fusion proteins (2, 5, 92). The partners of MLL are nuclear, cytoplasmic or membrane associated proteins involved in diverse functional processes ranging from chromatin modification and transcriptional elongation to cellular adhesion, endocytosis, cytoskeleton organization, and signal transduction (reviewed in (5)). A number of MLL fusion partners, especially nuclear proteins such as AF4, AF9, ENL, ELL, and AF10 – fusions of which together account for the vast majority of MLL patients – are components of large multi-subunit that control gene expression. Several such complexes have been identified including the transcriptional elongation complex called super elongation complex (SEC) (17) or the AF4/ENL/p-Tefb complex (AEP) (16), and the chromatin modifying Dot1l complex (see Chapter 2 and (15)). In *MLL*-rearranged leukemias, constitutive recruitment of one or more of these complexes by chimeric MLL fusion proteins is believed to facilitate sustained expression of MLL target genes, resulting in leukemic transformation. These complexes represent possible targets for pharmacologic inhibition, with several studies demonstrating the importance of different components of these complexes to MLL fusion mediated transformation (reviewed in (92)). One such promising candidate for therapeutic intervention is the histone methyltransferase Dot1l. Dot1l is the only known enzyme catalyzing the methylation of histone H3K79. Studies using various human *MLL*-rearranged leukemia cells demonstrate high levels of H3K79 methylation on MLL-fusion target genes suggesting that Dot1l may play an important role in leukemia driven by a variety of MLL-fusion proteins (12, 25, 55-57, 93). Moreover, a specific small-molecule inhibitor of DOT1L has been shown to have selective activity against *MLL*-rearranged human leukemia cell lines (85) raising hopes for therapeutic inhibition of Dot1l as a novel strategy for patients with *MLL*-rearranged leukemias.

Leukemias with t(6;11)(q27;q23) which encodes the MLL-AF6 fusion protein, constitute the largest subgroup of *MLL*-rearranged leukemias in which MLL is fused with a predominantly cytoplasmic protein (2). Retrospective studies have shown that presence of the t(6;11)(q27;q23) predicts a particularly poor prognosis (94, 95), and thus new therapeutic approaches are clearly needed. Given the recent studies demonstrating an important role for Dot1l in leukemias driven by various MLL-fusion proteins and the development of small molecule Dot1L inhibitors, we wondered if the MLL-AF6 fusion protein, where the MLL fusion partner is normally cytoplasmic and thus unlikely to be associated with transcriptional complexes, also requires Dot1L to maintain the oncogenic transcription program. MLL-AF6 leukemias have been modeled in mice, where it was recently shown that the MLL-AF6 fusion can transform hematopoietic progenitors *in vitro* and *in vivo*, a process dependent on the dimerization activity of the Ras-association (RA) domain of AF6 (96). We sought to analyze a potential role for H3K79 methylation by conducting a genome-wide analysis of H3K79 dimethylation in MLL-AF6 leukemia cells. We also assessed whether transformation by the MLL-AF6 fusion oncogene was dependent on aberrant H3K79 methylation by genetic or pharmacologic inhibition of the Dot1l histone methyltransferase.

Results

Elevated H3K79 dimethylation is found on MLL-fusion target genes in murine MLL-AF6 leukemias

The presence of abnormally high levels of H3K79 dimethylation (H3K79me2) at MLL-fusion target genes has been shown to be a characteristic of cells bearing MLL fusions with predominantly nuclear proteins such as AF9 and AF4. In 2011, Yokoyama et al., demonstrated the co-occurrence of the AEP complex, H3K79me2 as well as the MLL-AF6 fusion protein at the chromatin of select MLL target genes in the MLL-AF6 positive cell line ML2. We decided to probe genome wide H3K79me2 in MLL-AF6 transformed leukemia cells in order to assess whether H3K79 methylation might be involved in driving MLL target gene expression more broadly in MLL-AF6 leukemias. We established MLL-AF6 driven

leukemias using a bone marrow transplantation model in which Lin$^-$ Sca-1$^+$ Kit$^+$ (LSK) cells were transformed with the *MLL-AF6* fusion gene. MLL-AF6 expression was confirmed by Western blot following overexpression in 293-T cells (Figure 4-1B). All mice that developed leukemia were found to have AML with more than 90% of cells expressing the Gr-1 and Mac-1 myeloid markers in the bone marrow and spleen (Figure 4-1C), and a concomitant depletion of cells expressing lymphoid surface markers (data not shown). Genome wide analysis of H3K79me2 by ChIP-seq using H3K79me2 specific antibodies showed high levels of H3K79me2 at well-characterized MLL-target genes (Figure 4-1E). To analyze whether MLL-target loci possessed higher relative levels of H3K79me2 than other highly expressed genes, we compared the average distribution of H3K79me2 on a set of previously defined MLL-core target genes (25) and a randomly chosen set of highly expressed genes as control. We observed consistently higher deposition of H3K79me2 associated with MLL-fusion core target genes as compared to controls (Figure 4-1F).
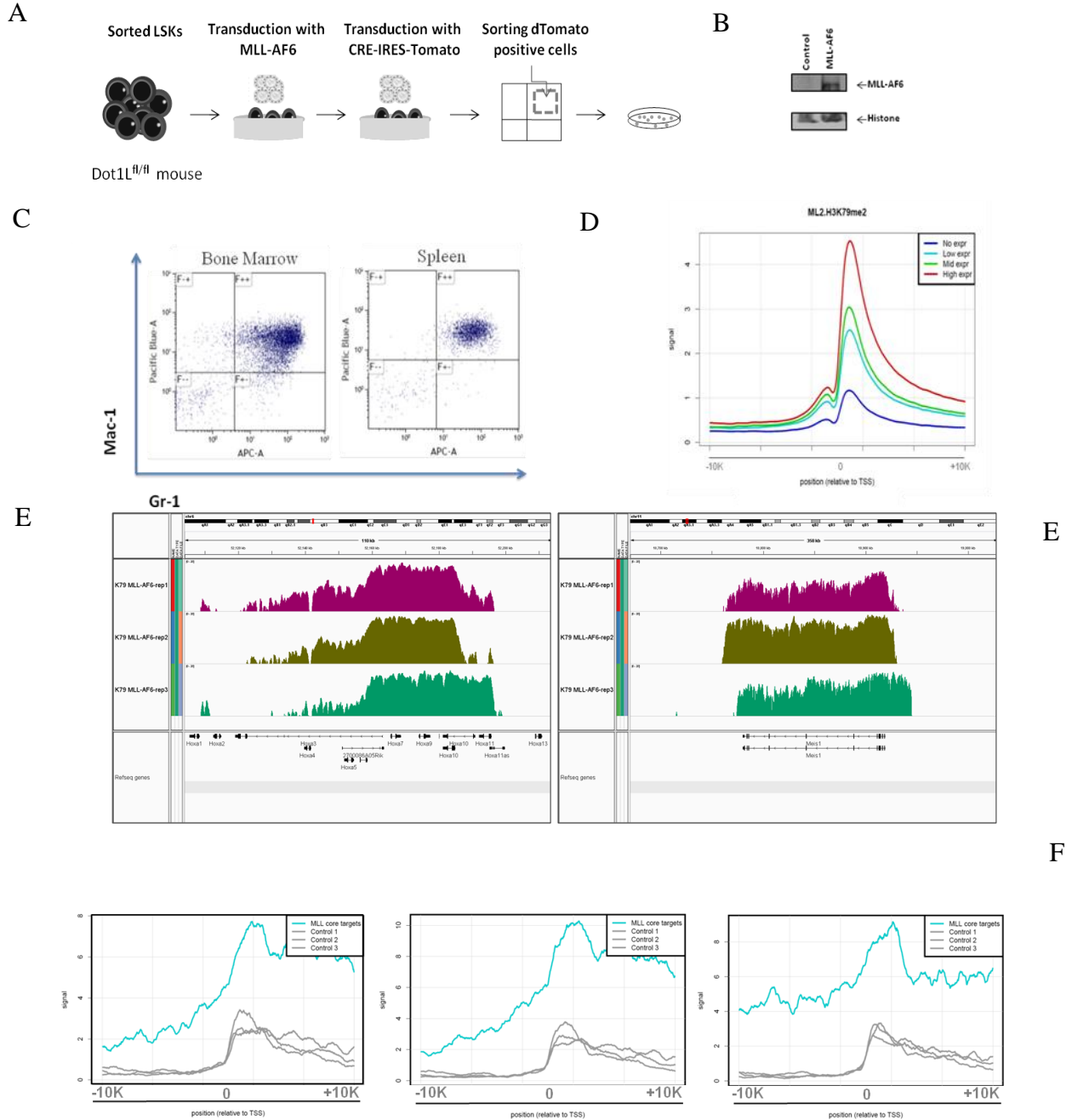
Figure 4-1 H3K79 methylation in MLL-AF6 transformed cells.

(A) Schematic depiction of experimental design. (B) Immunoblotting showing the MLL-AF6 fusion protein in control compared to MLL-AF6 expressing cells. Histone H3 is shown as the loading control. (C) Immnostaining of cells from the bone marrow or spleen of a representative moribund MLL-AF6 leukemic mouse. Gr-1: mouse granulocyte cell surface marker; Mac-1: mouse macrophage cell surface marker. (D) H3K79 dimethylation directly correlates with expression levels in MLL-AF6 mouse leukemic cells: Mean H3K79 dimethylation levels of genes divided into 4 equally sized groups of different expression levels are plotted. (E) H3K79me2 profiles of select MLL-AF9 targets. (F) Level and distribution of H3K79me2 profiles around the TSS of MLL core targets (blue lines) compared to 3 sets of size matched randomly chosen highly expressed genes (grey lines).

In order to assess whether H3K79 methylation is required for MLL-AF6 mediated transformation, we transduced LSK cells from mice harboring homozygous floxed *Dot1l* alleles (*Dot1l*$^{fl/fl}$) or *Dot1l* wild type controls (*Dot1l*$^{+/+}$) with the retrovirus encoding MLL-AF6. Subsequently, the MLL-AF6 transformed cells were selected with neomycin and transduced with an MSCV-based retrovirus that expresses Cre recombinase and tdTomato (Cre-Mi-Tomato). TdTomato positive cells were sorted and plated in methylcellulose-based media supplemented with cytokines and replated every week for up to three weeks (Figure 4-1A). Controls were MLL-AF6 transformed *Dot1l*$^{+/+}$ LSKs subsequently transduced with Cre-Mi-Tomato or MLL-AF6 transformed *Dot1l*$^{fl/fl}$ LSK cells subsequently transduced with the MSCV-based retrovirus without the Cre-recombinase (Mi-Tomato). Immunoblot analysis demonstrated that H3K79me2 levels were significantly reduced in MLL-AF6 transformed Dot1l$^{fl/fl}$ bone marrow cells after *Cre* expression as compared to controls (Figure 4-2E).

Dot1l deletion inhibits MLL-AF6 mediated transformation

In order to characterize the effects of Dot1l loss on MLL-AF6 transformation we first performed colony forming assays. We found that *Dot1l* excision significantly diminished the clonogenic capacity of MLL-AF6 transformed cells in the first week (Figure 4-2A). In contrast to the dense and compact "blast-like" colonies observed in control vector transduced cells, colonies generated upon *Dot1l* deletion were mostly small and diffuse, and Wright Giemsa stained cytospins of these colonies showed features characteristic of monocytic differentiation (Figure 4-2B). Genotyping PCR of the *Cre* transduced colonies at week 1, 2 and 3 of replating showed a progressive emergence of the *un*-excised *Dot1l* allele, demonstrating eventual outgrowth of cells that had escaped deletion of *Dot1l*. (Figure 4-2C). These results indicate a strong selective pressure against *Dot1l* deleted cells. As we and others have previously published, we noted the lack of such strong selection in HoxA9-Meis1 transformed LSK cells, and individual HoxA9-Meis1 transformed *Dot1l* excised colonies could be picked and propagated for several weeks (data not shown).

These results demonstrate a selective requirement for *Dot1l* in MLL-AF6 transformed cells, but not all transformed cells.
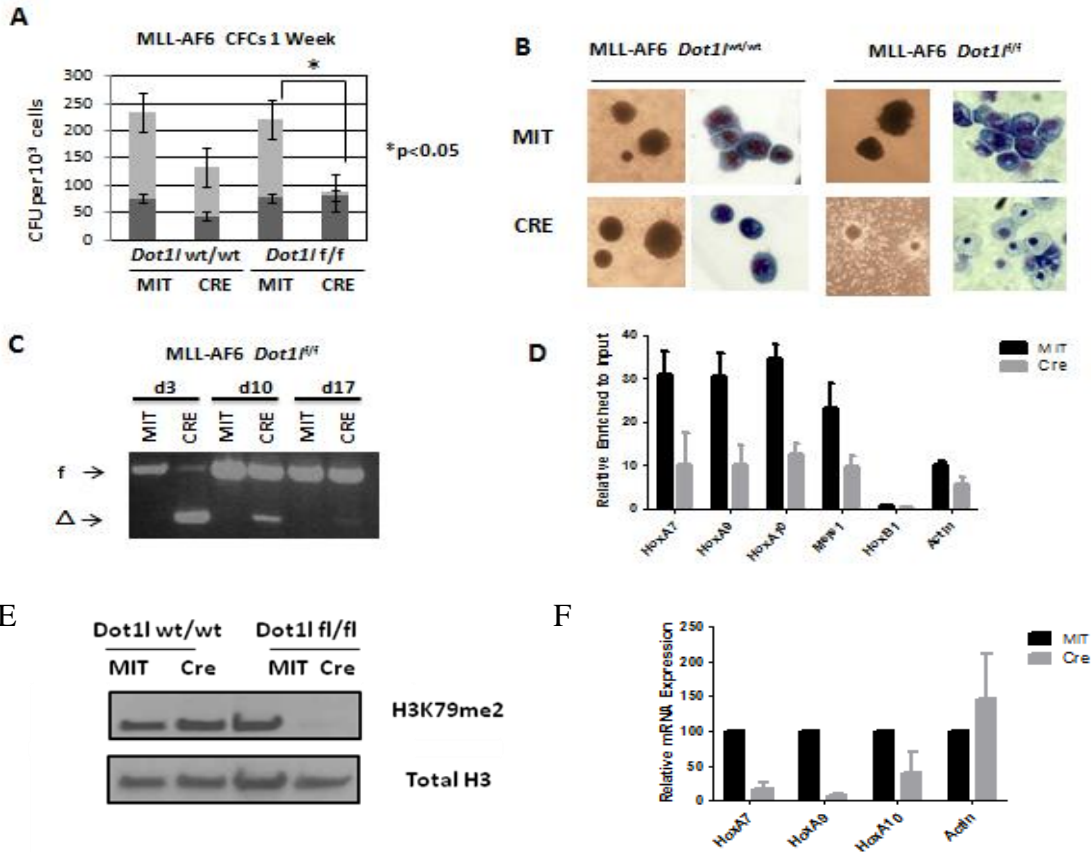
Figure 4-2 Dot1l deletion impairs the transforming capacity of MLL-AF6 transformed bone marrow cells.

(A). Differential colony counts from Dot1l-excised MLL-AF6 transformed cells 7 days after Cre transduction compared to vector expressing controls (n=3 independent experiments). (B). Morphological changes in colony and cell types upon Dot1l deletion in bone marrow cells immortalized by MLL-AF6 (colonies 10x; cell morphology: 40x)**.** (C). Genotyping of transduced bone marrow cells on day 3, day 10, and day 17 after transduction of Cre. f: floxed allele. Δ: deleted allele. (D). Enrichment of H3K79me2 normalized to input DNA on the chromatin locus of Hoxa/Meis1 gene promoters as assessed by q-RT-PCR is shown 6-9 days after Cre transduction, compared to MiTomato transduced cells cells. (n=2 independent experiments). (E)Western blot showing a marked decrease in H3K79me2 methylation 5 days after transduction with the Cre recombinase compared to control vector (Mi-Tomato) transduced cells. (F). Reverse transcription and q-RT-PCR 5 days after transduction with Cre-Mi-Tomato or MiTomato. Expression levels normalized to *Gapdh* and expressed relative to MiTomato-transduced cells (set to 100%) are shown. Error bars indicate the SEM (n=2 independent experiments).

Since aberrant H3K79 methylation at target chromatin is believed to result in inappropriate expression of MLL-fusion target genes, we sought to assess the effects of *Dot1l* deletion on H3K79me2 at select MLL-fusion target genes. Consistent with the ChIP-seq data from MLL-AF6 leukemias, we found high enrichment of H3K79me2 on the promoter proximal regions of the *Hoxa* cluster genes compared to input chromatin (Figure 4-2D dark bars). Cre-mediated excision of *Dot1l* from these MLL-AF6 transformed cells decreased H3K79me2 levels at the promoters of MLL-target genes and β-actin (Fig. 4-2D). Reduction in the levels of H3K79me2 resulted in a specific reduction in the transcript levels of MLL-targets genes *Hoxa9*, *Hoxa10* and *Meis1*, but not *β-actin* (Fig. 4-2F). This result demonstrates that similar to other MLL-fusion driven leukemias, continued expression of MLL-fusion target genes in MLL-AF6 leukemias requires continued activity of the Dot1l methyltransferase.

The Dotl1 inhibitor EPZ004777 selectively impairs proliferation of murine MLL-AF6 transformed cells

Since genetic inactivation of *Dot1l* severely impaired MLL-AF6 transformation, we sought to assess whether a specific small molecule inhibitor of Dot1l would similarly affect MLL-AF6 transformed cells. The specific small molecule Dot1l inhibitor EPZ004777 has been recently described to selectively impair the proliferation of several *MLL*-rearranged human cell lines although its impact on MLL-AF6 transformed cells has not yet been tested. We incubated MLL-AF6 transformed LSK cells with increasing concentrations (0.1μM to 10 μM) of EPZ004777 or DMSO vehicle control and assessed cell number over several days. MLL-AF9 transformed LSKs and HoxA9/Meis1 transformed LSKs served as positive and negative controls respectively. A dose-dependent reduction of H3K79me2 was seen in all the transformed cell populations by Western blotting after incubation with EPZ004777 (Figure 4-3A). As shown in Figure 4-3B, the expansion of MLL-AF6 as well as MLL-AF9 cells was dramatically impaired by EPZ004777, while the growth of HoxA9/Meis1 transformed cells was not significantly altered. Consistent with previous findings with human MLL-AF9 and MLL-AF4 leukemia cell lines, the effects on MLL-AF6

transformed primary murine hematopoietic progenitor cells only became apparent after 7 days. Nevertheless, when exposed to EPZ004777 for a longer time, MLL-AF6 transformed cells showed a dramatic decrease in cell number, while expansion of the HoxA9/Meis1 transformed cells was unaffected. We then used qRT-PCR to quantify expression levels of *Hoxa9, Hoxa10* and *Meis1* in cells exposed to EPZ004777. A decrease in *Hoxa9, Hoxa10* and *Meis1* transcript levels was observed in 3 days, with a significant drop at day 7 and day 10 after drug exposure (Figure 4-3C).

To assess the effect of EPZ004777 on the MLL-AF6 transformed cells in more detail, we analyzed changes in cell cycle and apoptosis upon exposure of the MLL-AF6 transformed cells to EPZ004777 by flow cytometry for DNA content and Annexin V staining. Dot1l inhibition reduced the number of actively proliferating MLL-AF6 cells, with a dramatic increase in the percentage of cells in the sub G1/G1 fractions after 4 days of incubation with 10 μM EPZ004777 (Figure 4-3D). These changes in the cell cycle were accompanied by an increase in the percentage of Annexin V positive cells, consistent with apoptotic cell death after EPZ004777 treatment (compared to DMSO control) (Figure 4-3E). These findings demonstrate that MLL-AF6 driven leukemias are selectively sensitive to pharmacologic inhibition of Dot1l.
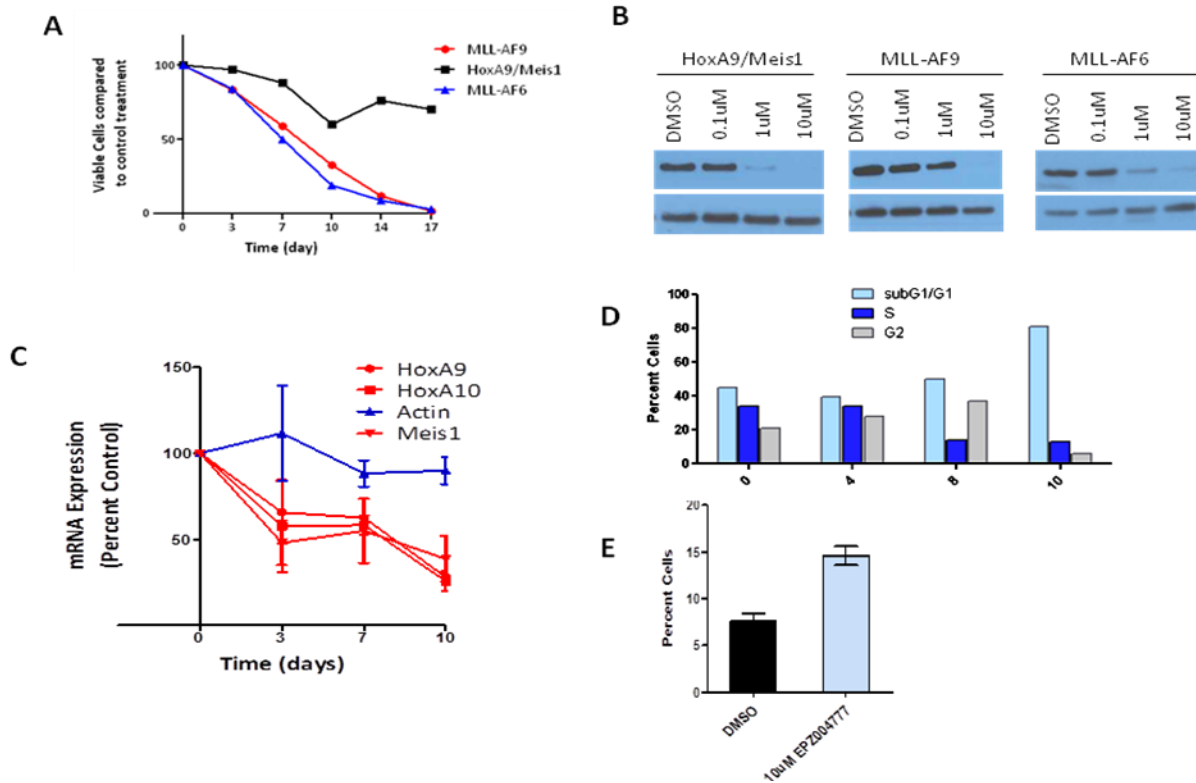
Figure 4-3 Selective inhibition of MLL-AF6 transformed cells by EPZ004777

(A) Growth kinetics of MLL-AF6, MLL-AF9, and HoxA9/Meis1a transformed murine bone marrow cells exposed to 10 uM of EPZ004777. Viable cells were counted and replated at equal cell numbers in fresh media with fresh compound every 3–4 days. Results were plotted as percentage of split-adjusted viable cells in the presence of 10uM EPZ004777 compared to DMSO vehicle control. Results are representative of three independent experiments. (B) Inhibition of cellular H3K79me2 levels in MLL-AF6, MLL-AF9 or Hoxa9-Meis1a transformed hematopoietic progenitor cells following 7 days of treatment with the indicated concentrations of EPZ004777 as measured by immunoblot analysis of extracted histones with an anti-H3K79me2 antibody. (C) Time course of *HoxA9* and *Meis1* mRNA expression in MLL-AF6 transformed cells over 10 days of incubation with 10 uM EPZ004777 as measured by quantitative real-time PCR. Expression levels were normalized to *Gapdh* and expressed relative to those at day 0 (set to 100%). Error bars indicate the SEM (n=3 independent experiments). (D) Cell cycle changes (BrdU/7-AAD flow cytometry) in MLL-AF6 transformed bone marrow cells after being treated with 10 uM EPZ004777 for 0, 4, 8, or 10 days. Similar results were obtained in 2 independent experiments. (E) Annexin V staining in MLL-AF6 transformed bone marrow cells 10 days after treatment with 10uM EPZ004777 or DMSO control (n = 2 independent experiments). Error bars represent standard error of the mean (SEM).

Detection of the elevated H3K79me2 at MLL-fusion target genes in a human MLL-AF6 positive cell line

In order to determine whether human leukemia cells bearing the MLL-AF6 fusion gene also display high H3K79me2 on MLL-fusion target genes, we performed genome-wide ChIP-seq for H3K79me2 on the human MLL-AF6 positive cell line ML2, with the *MLL*-germline cell line HL60 and the MLL-AF9 positive cell line MOLM-13 as negative and positive controls respectively. Similar to the MLL-AF6 murine leukemias, ML2 cells showed very high levels of H3K79 dimethylation on the *HoxA* gene cluster, similar to the MLL-AF9 positive MOLM-13 cell line whereas HL60 cells display low to undetectable levels of enrichment of this modification at the same locus (Figure 4-4A). H3K79me2 levels at other MLL-target genes such as *MEF2C* were similarly high in ML2 and MOLM-13 as compared to HL60. Of note, unlike MOLM-13 cells, the ML2 cell line did not display high H3K79 methylation on the *MEIS1* locus, consistent with a previous report (16). A recent study has published microarray data from patients bearing a number of MLL patient samples, which include 11 patients with the MLL-AF6 fusion gene (95). We performed an integrative analysis of gene expression from these MLL-AF6 patients with our ChIP-seq data from the ML2 cell line. Expectedly, when analyzed on a global scale, the levels of H3K79 dimethylation in ML2 positively correlated with the level of transcript expression in these patients (Figure 4-1D). In the ML2 cell line, MLL-fusion core targets showed significantly higher levels of H3K79me2 as compared to 3 randomly chosen size-matched sets of highly expressed genes (Figure 4-4B). A recent study identified the direct binding targets of the MLL-AF6 fusion protein using ChIP-Chip in the human t(6;11)(q27;q23) positive ML2 cell line. We observed that mean H3K79me2 levels at these 24 MLL-AF6 target genes was markedly higher than even the MLL-fusion core target genes (Figure 4-4B). These findings demonstrate that similar to murine leukemias, the human MLL-AF6 positive cell line ML2 harbors elevated H3K79me2 on MLL-fusion target genes.
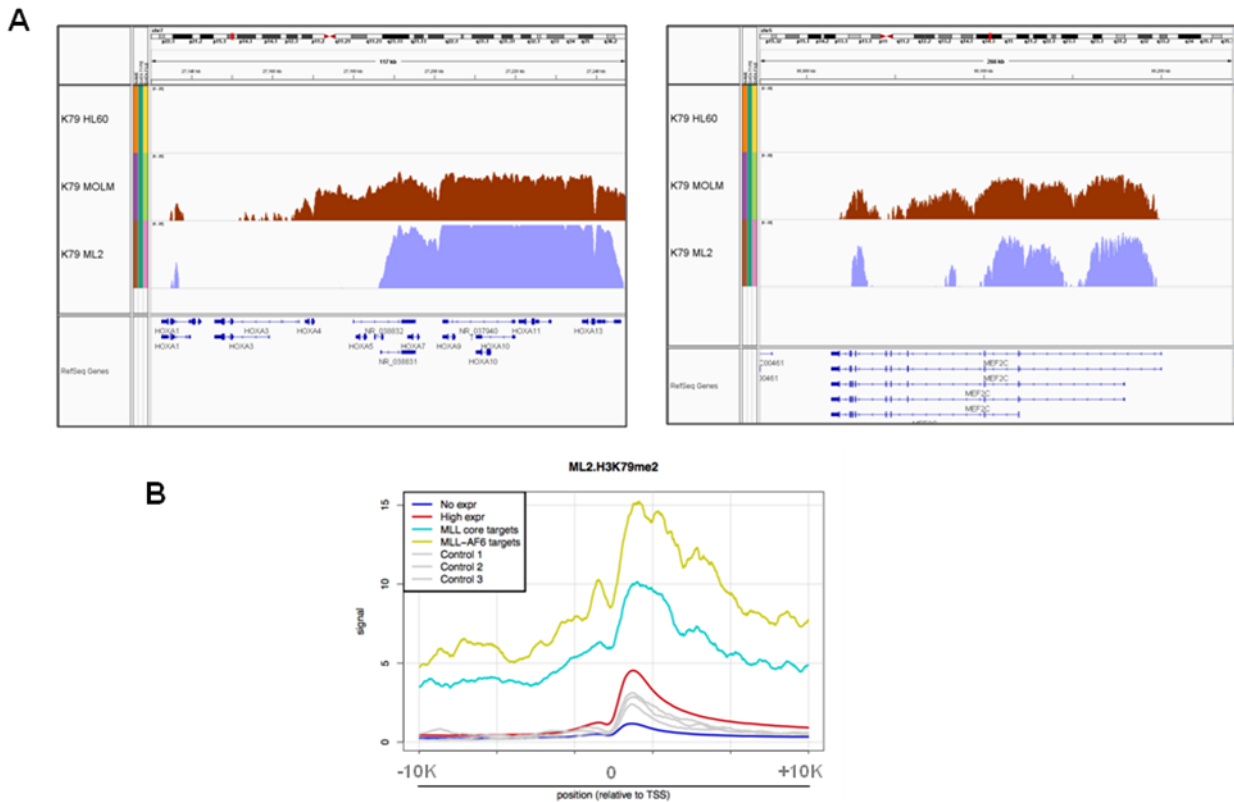
Figure 4-4 Abnormal H3K79me2 on MLL targets in the ML2 cell line.

(A) H3K79me2 profiles of select MLL-targets genes in MLL non-rearranged HL60 cells, MLL-AF9 positive MOLM 13 cells and the MLL-AF6 positive ML2 cell line. (B) Level and distribution of H3K79me2 profiles around the TSS of MLL core targets (blue line) and MLL-AF6 direct targets (gold line) compared to non-targets (grey lines). Genes with high levels of expression are depicted with the red line and genes with no expression are marked with the blue line. Grey lines indicate H3K79me2 on 3 randomly chosen sets of highly expressed genes.

The Dot1l inhibitor EPZ004777 impairs proliferation of the t(6;11) positive cell line ML2

In order to determine the effects of small molecule inhibition of DOT1L in human leukemia cells, we assessed whether the DOT1L inhibitor EPZ0004777 affected the proliferation, differentiation or survival of the ML2 cell line with HL60 and MOLM13 as negative and positive controls respectively. The ML2 cell line showed sensitivity to EPZ004777, with a significant reduction in cell numbers starting from day 10 after drug exposure (Figure 4-5A). Despite the fact that H3K79me2 was significantly diminished upon
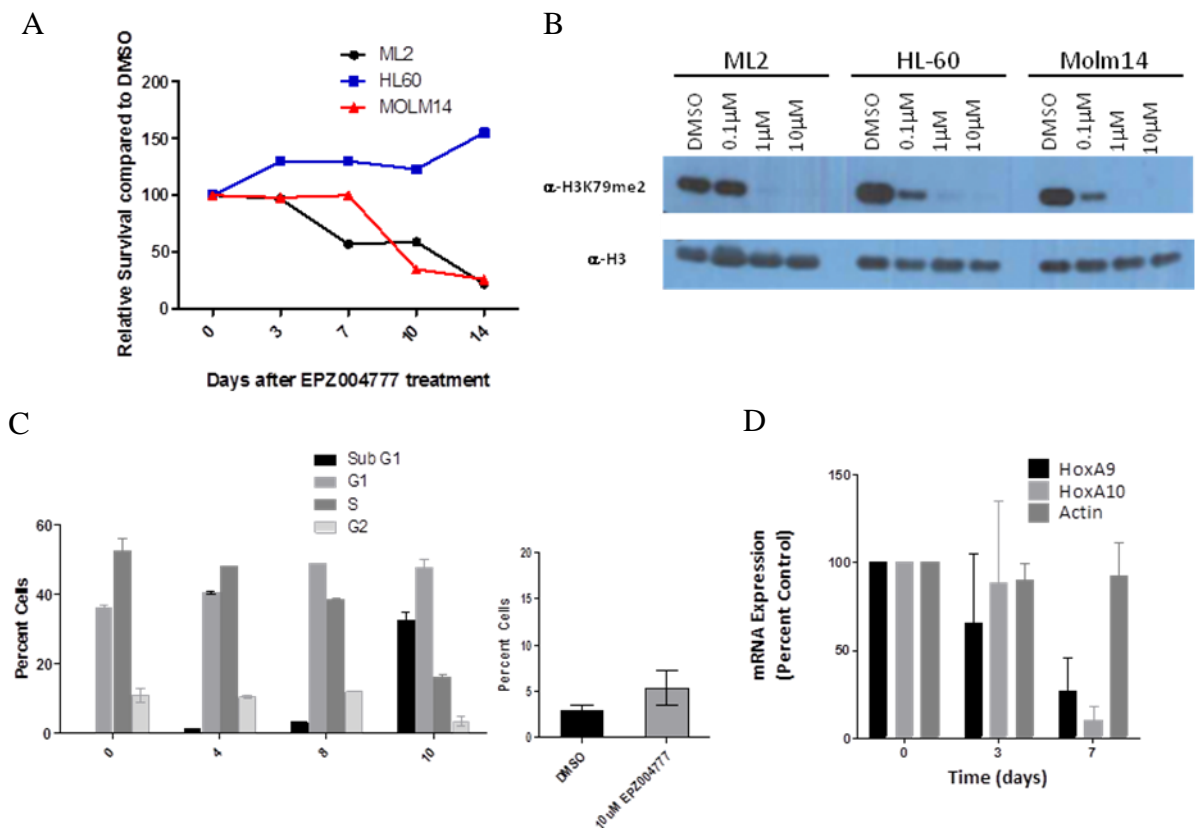
Figure 4-5 Selective inhibition of the ML2 cell line by EPZ004777.

(A) Effect of EPZ004777 on the proliferation of leukemia cell lines bearing an MLL-AF6 (ML2) or MLL-AF9 (MOLM-13) fusion, or a cell line lacking an MLL rearrangement (HL60). Cell lines were maintained in the presence of increasing concentrations of EPZ004777 0.1, 1 and 10 μM. (B) Immunoblots showing the levels of H3K79me2 upon exposure of the different cell lines to indicated concentrations of EPZ004777 or DMSO carrier controls. (C) Cell cycle changes (Hoechst staining) in ML2 cell line upon treatment with 10 μM EPZ004777 for 0, 4, 8, or 10 days. Similar results were obtained in 2 independent experiments each having two technical replicates. (D) Percentage of Annexin V positive cells plotted 10 days after treatment with 10 μM of EPZ004777 or DMSO control.

exposure to EPZ004777 in all the 3 tested cell lines (Figure 4-5B), only MOLM-13 and ML2 showed

significant sensitivity to EPZ004777 further supporting the selectivity of this small molecule for *MLL*-

rearranged cell lines. Exposure of ML2 cells to EPZ004777 resulted in a progressive reduction in cells

entering the S-phase starting from 3 days after drug exposure with an accumulation in the subG1/G1

phase (Figure 4-5C left panel). EPZ004777 treatment also led to a modest but statistically insignificant

increase in the percentage of Annexin V positive cells, indicating that in contrast to cell-cycle changes, the effects of EPZ00477 on apoptosis of ML2 cells was not as profound (Figure 4-5C right panel). Moreover, the expression of MLL-fusion target genes such as *HOXA9* and *HOXA10* was significantly downregulated starting from day 7 after exposure of the ML2 cells to EPZ004777 (Figure 4-5D). Taken together, results from the murine and human MLL-AF6 positive leukemia cells indicate that MLL-AF6 driven leukemias may show sensitivity to pharmacologic DOT1L inhibition.

Discussion

MLL-AF6 rearrangement is one of the most common MLL fusion events in human AML patients and MLL-AF6 fusions are associated with a significantly poor prognosis compared to most other common MLL-fusions (94, 95). Despite the clinical importance, there have been few studies assessing the mechanisms underlying MLL-AF6 leukemia. In this study we make the surprising observation that both mouse and human MLL-AF6 leukemia cells harbor abnormally high H3K79 methylation on MLL-target genes, strongly indicating aberrant DOT1L activity in these leukemias. We further show that inactivating Dot1l using a conditional knockout model or by using a Dot1l specific small-molecule inhibitor reduces H3K79 methylation on MLL-target genes and dramatically impairs the transforming ability of the MLL-AF6 fusion gene. The human MLL-AF6 positive cell line ML2 also reflects our findings in the murine models, suggesting that DOT1L may play a critical role in human MLL-AF6 leukemia.

It has been hypothesized that MLL fusions may recruit the DOT1L complex or transcriptional elongation complexes such as SEC or AEP onto MLL-fusion target loci, resulting in their constitutive and aberrant activation in MLL rearranged leukemia. However, the AF6 protein in its non-rearranged form is a cytoplasmic protein localized primarily at adherens junctions and binds to actin filaments (97) , and AF6 has not been co-purified in any of the described transcriptional elongation complexes or DOT1L complex.

70

Therefore, the targeting of these protein complexes on MLL-fusion loci in MLL-AF6 transformed cells is unexpected and it is surprising to discover the involvement of Dot1l and H3K79 methylation in MLL-AF6 leukemias.

It has been shown that the homo-dimerization domain of AF6 is necessary and sufficient for bone marrow transformation by MLL-AF6 fusion (96). In addition, it has been reported that other predominantly cytoplasmic MLL fusion partners such as GAS7, AF1p, and SEPT6 also possess oligomerization domains and an MLL N-terminal artificial homodimer can immortalize mouse bone marrow cells *in vitro*. Moreover, one unique MLL rearrangement without any MLL fusion partner, the MLL N-terminal partial tandem duplications (MLL-PTD), occurs in about 4-7% human AML and is associated with poor prognosis. Therefore, it is conceivable that the oligomerization of MLL N-terminus itself may change the conformation of MLL protein complex, creating docking sites for transcriptional activating factors and/or excluding interaction with transcriptional silencing factors. It will be of great interest to determine whether abnormal H3K79 methylation profile exists in MLL-PTD patients, and whether transformation by MLL N-terminal artificial homodimer is dependent on H3K79 methylation.

Although further studies are needed to reveal the mechanisms of DOT1L recruitment by MLL fusion proteins, our observation that MLL-AF6 leukemias are dependent on aberrant DOT1L activity are of high clinical relevance. We and others have previously demonstrated that transformation mediated by other oncogenes such as Hoxa9 and Meis1, E2A-PBX, and E2A-HLF is insensitive to Dot1l inhibition (25, 56, 57). In addition, Daigle et al. has recently shown that *MLL* wildtype human leukemia cell lines are insensitive to pharmacologically inhibition of DOT1L (85). These results strongly suggest that the recruitment of DOT1L is a molecular mechanism that is specific to certain, but not all hematological malignancies.

In summary, our studies discussed above indicate that several MLL fusions – independent of the normal sub-cellular localization of the fusion partner – may directly or indirectly recruit the DOT1L complex for constitutive activation of the MLL transcriptional program. This potentially shared mechanism of transformation could prove to be an attractive therapeutic target in the MLL leukemias. The results showing that MLL-AF6 mediated transformation is dependent upon Dot1l and can be inhibited using small molecule inhibitors could help inform future clinical trials with clinically effective DOT1L inhibitors.

Material and Methods

Generation of Transformed Murine Cells and Leukemia

The MSCV-neo *MLL-AF6* construct consists of amino acids 35 to 347 comprising the AF6 N-terminal conserved region (NCR) cloned in the MSCV-neo 5' MLL construct and has been described before (96). The Mi-Tomato plasmid was a kind gift from Hassan Jumaa (Max Planck Institute, Frieburg). cDNA for the *Cre* recombinase was sub-cloned into the Mi-Tomato plasmid to generate the Cre-Mi-Tomato construct. Retroviral supernatants were collected from 293-T cells separately transfected with the aforementioned plasmids using standard protocols and used for retroviral spin infections. Sorted Lin$^-$Sca-1$^+$cKit$^+$ (LSK) cells from mouse bone marrow cells were transduced with the *MLL-AF6* retrovirus and expanded for 2 weeks in methylcellulose M3234 (Stem Cell Technologies) supplemented with cytokines (6ng/ml IL3, 10ng/ml IL6 and 20ng/ml SCF) and 1mg/ml of G418. After 2 weeks of selection in G418, MLL-AF6 transformed cells were either transplanted into B6/129 syngeneic sublethally irradiated (600 rad) recipients at 10^6 cells/mouse to generate leukemia in mice, or transduced with either Cre-Mi-Tomato or the empty Mi-Tomato control vector *in vitro* to assess the effects of Cre-mediated Dot1l inactivation in colony forming assays.

Histone extraction and Chromatin IP-sequencing (ChIP-Seq)

Histones were extracted by overnight acid extraction using the protocol outlined on the Abcam website (www.abcam.com). Western blotting was done with standard procedures using a 10 % Bis-Tris Gel (Nupage, Invitrogen, Carlsbad, CA, USA) and transferred onto PVDF membranes. The MLL-AF6 fusion protein was detected from nuclear extracts from 293T cells transiently transfected with MLL-AF6 using an anti-MLL antibody A300-086A recognizing the N-terminal portion of MLL (Bethyl Laboratories, Montgomery, Texas, USA) with the anti-total H3 antibody ab1791 (Abcam, Cambridge, MA) as the loading control. For assessment of H3K79 methylation, the anti-H3K79me2 antibody ab3594 and anti-total H3 antibody ab1791 (both from Abcam, Cambridge, MA) were used. Secondary antibodies used were sheep anti-mouse ECL horseradish peroxidase linked NA931V and donkey anti-rabbit ECL horseradish peroxidase linked NA934V (GE healthcare UK limited, Little Chalfont Buckinghamshire, UK). ChIP was performed as previously described (Krivtsov et al., 2008; Bernt et al., 2011). Briefly, crosslinking was performed with 1% formaldehyde, and the cells were lysed in SDS buffer. DNA was fragmented by sonication. ChIP for H3K79me2 was performed using anti-H3K79me2 antibody ab3594 on human leukemia cell line ML2, MOLM14, and HL60, and three primary mouse MLL-AF6 leukemia cells. Eluted DNA fragments were analyzed by qPCR, or barcoded with NEBNext DNA library preparation kit (NEB, Ipswich, MA) and subjected to sequencing on Illumina HiSeq 2000 platform. Reads were aligned to either mouse genome assembly mm9 or human genome assembly hg19 using Bowtie (98) . Genome wide ChIP-Seq data was visualized using the integrated genome viewer (IGV) version 2.1 (99).

Mutant mice

Dot1l conditional knockout mice in which the active site of *Dot1l* (Exon5) is flanked by *LoxP* sites were generated in our laboratory and have been described previously (25) . Bone marrow cells from 7-10 week old mice in *Dot1l* $^{+/+}$ or *Dot1l*$^{f/f}$ backgrounds were used for transformation assays and subsequent biochemical experiments.

Cell lines

The MLL-AF6 positive ML2 cell line (obtained from DSMZ) and the cell lines HL60 and MOLM14 were grown in RPMI 10% FBS supplemented with 2mM L-glutamine and penicillin/streptomycin.

Colony forming assays

Colony forming cell (CFC) assays were performed by plating 1000 tdTomato positive cells per ml of cytokine-supplemented methylcellulose M3234 (6ng/ml IL3, 10ng/ml IL6 and 20ng/ml SCF). On day 6-7 after plating, colonies were scored using the Nikon Eclipse TS100 inverted microscope (Nikon, Tokyo, Japan). Since almost all colonies were either compact and hypercellular (blast-like) or small and diffuse (consistent with differentiation) under these conditions, colonies were classified into these two categories. Cells from pooled colony aggregates were then used for biochemical assays or replated for testing their secondary replating potential at the same concentration. Cell morphology was assessed by spinning 50,000 cells onto glass slides (500 rpm for 10 min) using the Shandon Cytospin 4 cytofuge (Thermo Scientific, Waltham, MA). Pictures of colonies and Wright-Giemsa stained cytospin preparations were taken using the Nikon Eclipse E400 microscope (Nikon, Tokyo, Japan) and a SPOT RT color digital camera (Diagnostic Instruments, Sterling Heights, MI, USA).

Real-Time PCR

Total RNA was isolated using Trizol (Invitrogen, Carlsbad, CA, USA) according to the manufacturer's instruction. cDNA was generated using the tetro cDNA synthesis kit (Bioline, Taunton, MA, USA) using oligo-dT primers. Real-time PCR was performed using pre-validated Taqman probes (Applied Biosystems) on the ABI 7700 Sequence Detection System (Applied Biosystems). Primer and probe information will be provided upon request. Average C_t values were normalized to the housekeeping gene GAPDH.

Cell cycle and apoptosis assays

Bone marrow cell transformed with MLL-AF6 were plated in 12-well plates at a density of 2×10^5 cells/ml and incubated with 10 μM EPZ004777 (Epizyme, Cambridge, MA, USA) or DMSO vehicle control in a

final volume of 1 ml for up to 10 days. Every 3-4 days, fresh media with inhibitor was replaced. Cell cycle analysis was performed after 30 mins of BrdU labeling using BrdU-APC/7AAD kit from BD-Pharmingen (San Jose, CA, USA) on day 0, day 4, day 8, and day10. Data was acquired on a 4-color Becton-Dickinson FACSCalibur flow cytometer and analyzed using BD FACSDiva software (San Jose, CA, USA) and Modfit LT (Verity Software House, Topsham, ME, USA). Annexin V apoptosis assays were performed on day 10. Cells incubated with 10uM EPZ004777 or DMSO vehicle control were washed in PBS, resuspended in Ca/HEPES buffer (10 mM HEPES, pH7.4; 140 mM NaCl; 2.5 mM CaCl2) and incubated with Annexin V-PE (BioVision Inc., Mountain View, CA) for 20 mins. Data was acquired on a 4-color Becton-Dickinson FACSCalibur flow cytometer and analyzed using BD FACSDiva. Human leukemia cell line HL60, ML2, and MOLM14 were plated in 12-well plates at a density of $2{\times}10^5$ cells/ml and incubated with 10 µM EPZ004777 (Epizyme, Cambridge, MA, USA) or DMSO vehicle control in a final volume of 1 ml for up to 10 days. Every 3-4 days, fresh media with inhibitor was replaced. For cell cycle analysis, cells were fixed and permeablized with buffer (1x PBS; 0.5% Triton X100; 1% Formaldehyde) for 5 mins, and then stained with 1µg/ml Hoechst 33342 (Invitrogen, Carlsbad, CA) in staining buffer (1x PBS; 2% FBS) for 30 mins on day 0, day 4, day 8, and day10. Data was acquired on the BD LSRII and analyzed using Modfit LT (Verity Software House, Topsham, ME, USA). Annexin V apoptosis assays were performed on day 10. Cells incubated with 10uM EPZ004777 or DMSO vehicle control were washed in PBS, resuspended in Ca/HEPES buffer (10 mM HEPES, pH7.4; 140 mM NaCl; 2.5 mM CaCl2) and incubated with Annexin V-APC (BD pharmingen, San Jose, CA, USA) for 20 mins. Data was acquired on the BD LSRII and analyzed using FlowJo software (TreeStar Inc., CA).

Chapter 5

The Interaction between Dot1l and Af10 Is Required for H3K79 Dimethylation and MLL Leukemogenesis

Addendum:

This work was done in collaboration with Aniruddha Deshpande.

Aniruddha Deshpande, Liying Chen, and Scott Armstrong designed the experiments. Aniruddha Deshpande made the Af10 knockout mice and performed genetic experiments with MLL-AF9 and MLL-AF6 leukemia model. Liying Chen characterized the effect of Af10 deletion on the H3K79 methylation pattern and chromatin structure, and performed genetic experiments with MLL-AF10 and CALM-AF10 leukemia models.

Introduction

Post-translational modification of histones provides an important regulatory platform for gene transcription. It has become increasingly apparent that the misregulation of histone modification, which is caused by the deregulation of factors that write, remove and/or read modifications, actively contributes to human cancer. DOT1L is the sole H3K79 methylase in yeast, mouse, and human (47-49). There has been accumulating evidence indicating that deregulation of DOT1L and H3K79 methylation is involved in the development of *MLL*-rearranged leukemia (25, 55-57, 100).

In previous chapters, we characterized DOT1L complex and validated the clinical relevance of inhibiting the DOT1L complex in leukemias bearing *MLL* translocations. In particular, our proteomic study of DOT1L complex in leukemia cells suggested that AF10 is a key component of DOT1L complex. Suppression of Af10 leads to a global reduction of H3K79 dimethylation and impaired survival of leukemia cells (Chapter 2). AF10 is a putative transcription factor with a C-terminal DOT1L binding motif designated the OM-LZ domain and N-terminal PHD fingers with unknown function. It was first cloned as fusion partners of *MLL* and *CALM* in human acute leukemia (70, 87). Recently, several other AF10 fusion partners, including NAP1L1, HNRNPH1, and DDX3X, have been identified in human early T-cell precursor ALL and T-ALL (101, 102). The fact that all the fusion proteins retain the DOT1L binding OM-LZ domain and the suppression of *AF10* leads to decrease of H3K79 methylation level (Chapter 2) also indicates that AF10 may serve a crucial role in DOT1L complex function in normal development and disease progression.

Here we hypothesize that the AF10-DOT1L interaction may be of therapeutic interest for *MLL*-rearranged leukemias. In this chapter, we use a conditional *Af10* knock-out mouse model to study the role of *Af10* in the epigenetic activation of gene expression and in leukemia development. Our results revealed the function of Af10, a key Dot1l complex component, is required for global H3K79 di-methylation and the

maintenance of the open chromatin structure of MLL-target genes. In addition, with genetic approaches, we confirmed that the Dot1l-AF10 interaction is required in the maintenance of *MLL*-rearranged leukemia.

Results

We generated conditional knockout mice in which the Dot1l-interacting octapeptide-motif leucine zipper (OM-LZ) domain of *Af10* was flanked by *LoxP* sites. Deletion of the *Af10*^{OM-LZ} domain with the Cre recombinase is predicted to abrogate the Af10-Dot1l interaction (Figure 5-1A). It is an ideal system to study the role of Af10-Dot1l complex in H3K79 methylation and leukemogenesis by MLL fusion proteins.

First we checked whether loss of Af10 indeed affects H3K79 methylation in leukemia cells. We immortalized bone marrow cells from *Af10*^{f/f} or *Dot1l*^{f/f} mice using Hoxa9/Meis1a, and subsequently transduced cells with Cre or empty vector MIT/MIY, sorted Tomato⁺ or YFP⁺ cells and grew them in methylcellulose-based culture medium. We picked single cell colonies from the methylcellulose dishes, confirmed the deletion by genotyping, and expanded them in methylcellulose culture for two more weeks. Western blot of extracted histones from these single cell clones showed that complete deletion of *Af10* led to a dramatic reduction of H3K79me2, very like deletion of *Dot1l* did (Figure 5-1C). Interestingly, loss of *Dot1l* seems to have less effect on H3K79me1 level (Figure 5-1C). However, it is not possible to make a strong conclusion about changes on H3K79me1 from the western blot. Therefore, I submitted the purified histones from *Af10* or *Dot1l* floxed cells and *Af10* or *Dot1l* excised cells to liquid-chromatography-mass spectrometry (LC-MS) to compare the relative abundance of H3K79me0/1/2/3 with or without *AF10/Dot1l*. Consistent with previously published data (56), the mass spectrometry showed both H3K79 mono- and di-methylation were abrogated in *Dot1l* knockout cells. In agreement with our western blot, mass spectrometry confirmed that H3K79 dimethylation was abrogated in *Af10* knockout cells. Strikingly,

it is revealed by mass spectrometry that H3K79 monomethylation is still retained in *Af10* knockout cells (Figure 5-1D). Therefore, we conclude that Af10 is required for di-methylation but not mono-methylation of H3K79.

A

B Experiment Design

C

D
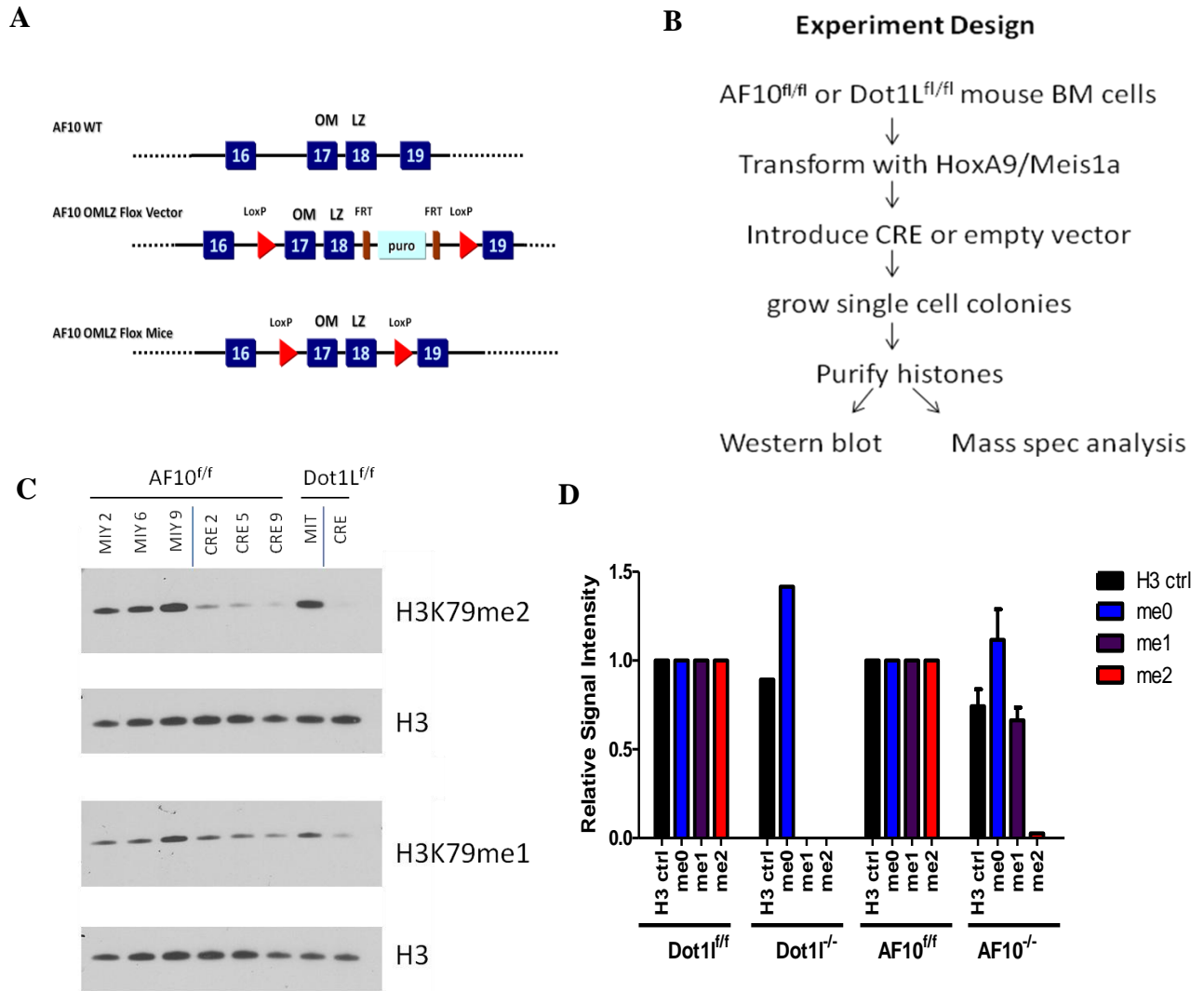
Figure 5-1 Generation of Af10$^{f/f}$ mice and abrogation of H3K79me2 in Hoxa9/Meis1-transformed Af10$^{-/-}$ mouse bone marrow cells.

(A) Schematic representation of Af10 wildtype allele, targeting vector, and floxed allele. Boxes with numbers inside indicate exons. OM-LZ: Octapeptide Motif-Leucine Zipper. (B) Schematic representation of generation of Af10 and Dot1l deleted Hoxa9/Meis1 transformed cell clones. Bone marrow cells from Af10$^{f/f}$ or Dot1l$^{f/f}$ mice were immortalized by retroviral transduction of Hoxa9/Meis1, and then transduced with either empty vector MIT/MIY or Cre. (C) Western blot showing loss of H3K79me2 but not H3K79me1 in transformed Af10$^{-/-}$ bone marrow cells. Western blot was done with histone extraction from signal cell clones with complete deletion of Af10 or Dot1l. (D) H3K79 non-, mono-, di-methylation profile in Dot1l and Af10 deleted cell lines shown by mass spec. (n=2)

We have shown that Dot1l and H3K79 dimethylation is required for transformation by MLL-AF9 (25), MLL-AF10, CALM-AF10 (100), and MLL-AF6 (Chapter 4). Using our *Af10^{OM-LZ}* knockout mouse model, we confirmed that disruption of Dot1l-Af10 interaction can abrogate H3K79 di-methylation. We then sought to study whether Af10 is required for bone marrow transformation by oncogenic fusions *in vitro* and the development of *MLL*-rearranged leukemias *in vivo*. Using MLL-AF9 and MLL-AF6 encoding retroviruses, we established immortalized blast-colony forming cultures from mouse bone marrow cells bearing *Af10^{f/f}* alleles. Deletion of *Af10* with Cre-recombinase dramatically reduced H3K79me2 on the MLL-target genes *Hoxa5-10* and *Meis1*, leading to downregulation of these genes. We performed colony-forming cell (CFC) assays from MLL-AF9 transformed cells in the presence or absence of the *Af10* allele. In the first week, *Af10* deletion profoundly impaired the blast-colony forming potential of MLL-AF9 as well as MLL-AF6 transformed LSKs and the only clones that could serially replate in subsequent passages had escaped *Af10* excision. *Af10* deleted colonies were very small and spread-out and showed morphological features of terminal myeloid differentiation (Figure 5-2). In contrast, HoxA9/Meis1 transformed LSK cells expanded normally in the absence of *Af10.* These results phenotypically mirror deletion of *Dot1l* and demonstrated that *Af10*, much like *Dot1l*, is critical for the *in vitro* transforming activity of *MLL-AF9* and *MLL-AF6* fusion gene, but does not generally inhibit cellular proliferation. It is conceivable that Dot1l and H3K79 methylation is required for the overexpression of MLL target genes including Hoxa9 and Meis1a, and as an important partner of Dot1l, Af10 is also required for MLL-AF6 and MLL-AF9 mediated transformation and works upstream of Hoxa9 and Meis1a.

80
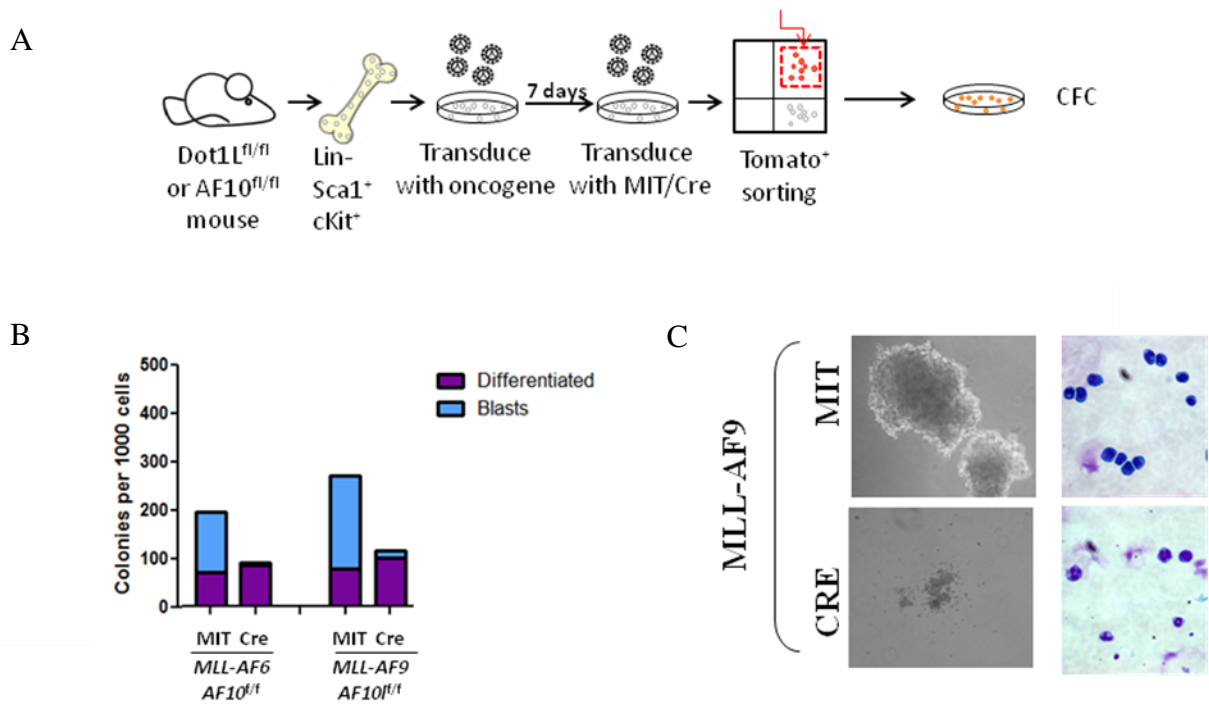
Figure 5-2   Loss of AF10 decreased colony forming potential of MLL-AF6 and MLL-AF9 transformed bone marrow cells, similar to loss of Dot1l.

(A) Schematic depiction of experimental design. (B) Blast and differentiated colony count of AF10–deleted MLL-AF6 or MLL-AF9 transformed cells in methylcellulose-based culture 10 days after transduction with Cre in comparison to MIT vector control. Result is representative of 3 independent experiments. (C) Morphological changes in colony and cell types upon AF10 deletion in bone marrow cells immortalized by MLL-AF9 (colonies 10x; cell morphology: 40x).

We then sought to investigate the potential role of the $Af10^{OM-LZ}$ domain in the *in vivo* leukemogenic activity of MLL-AF9. We generated primary MLL-AF9 leukemias from $Af10^{f/f}$ mouse bone marrow. Deletion of the $Af10^{OM-LZ}$ domain in cells explanted from the MLL-AF9 primary leukemias led to a significant increase in the disease latency in secondary recipient mice (Figure 5-3B). Microarray analysis showed that a vast majority of MLL-AF9 target genes were significantly downregulated in $Af10^{-/-}$ as compared to $Af10^{f/f}$ wildtype MLL-AF9 leukemias (Figure 5-3C-D). However, the $Af10^{OM-LZ}$ deleted cells could still eventually cause leukemia. This is intriguing given that $Af10^{OM-LZ}$ deletion, similar to Dot1l deletion, leads to a significant reduction in H3K79 dimethylation as well as MLL-target gene expression. A more detailed analysis of H3K79 methylation using mass spectrometry revealed that global levels of

81

H3K79 mono-methylation were largely unchanged in $Af10^{OM-LZ}$ deleted cells, and global levels of H3K79 dimethylation was diminished by 90%. The residual H3K79 dimethylation level, which was not detectable in *in vitro* transformed $Af10^{-/-}$ cells, may be caused by *in vivo* selection favoring cells with relatively high H3K79 dimethylation in the absence of Af10. One possible explanation of $Af10^{-/-}$ MLL-AF9 leukemia would be that the residual MLL-AF9 target gene expression seen in $Af10^{OM-LZ}$ deleted cells may be maintained by H3K79 monomethylation or residual H3K79 dimethylation, and though very little, is enough for maintaining the leukemia. Another possibility is that other oncogenic genes, like other Homeobox genes, may be activated to compensate the loss of MLL target gene expression in the process of *in vivo* leukemogenesis.
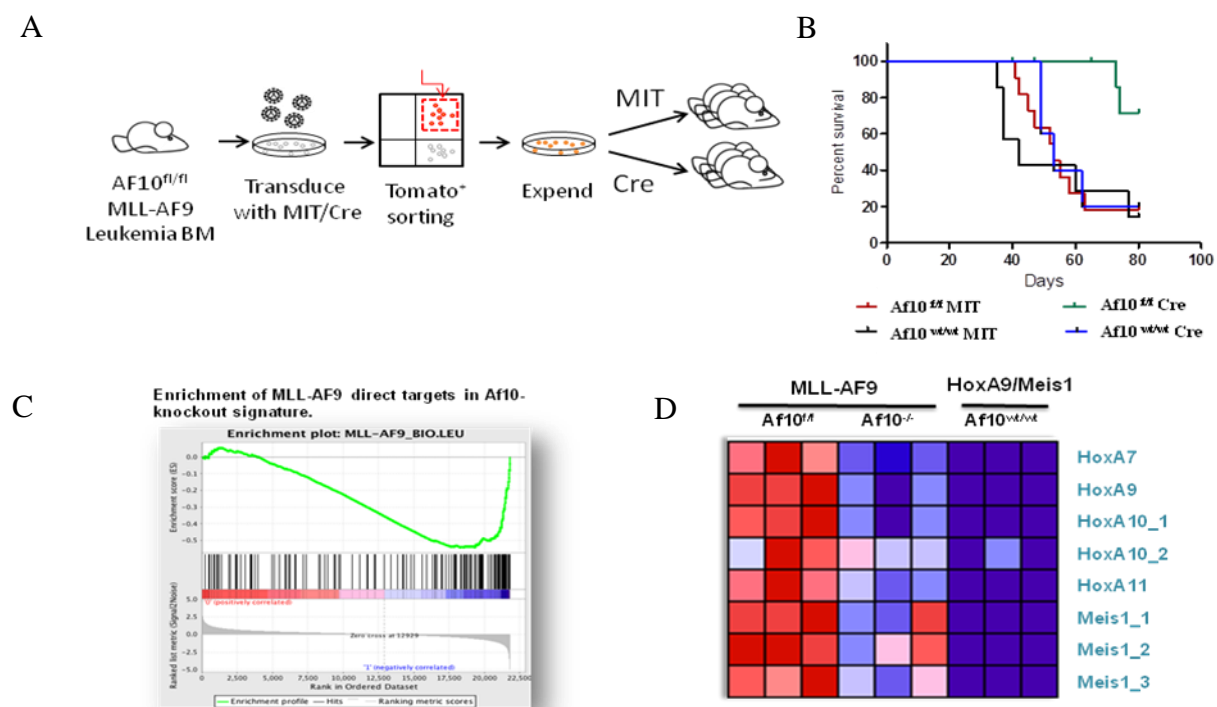
Figure 5-3 *AF10* deletion prolonged survival of secondary MLL-AF9 leukemia *in vivo*

(A) Schematic depiction of experiment to study the role of AF10 in MLL-AF9 leukemia maintenance. (B) Survival curves for secondary recipient mice that received $3X10^5$ MLL-AF9 leukemia cells with or without $AF10^{OM-LZ}$ deletion. (C) Gene set enrichment analysis showing enrichment of MLL-AF9 direct targets in "Af10-knockout" signature (D) Heat map showing MLL target expression in MLL-AF9 leukemia with or without $AF10^{OM-LZ}$ deletion. Expression in Hoxa9/Meis1 leukemia is a negative control. Names of probe sets used in expression array are shown.

As stated in Chapter 3, Dot1l has proven to be required for MLL-AF10 and CALM-AF10 mediated transformation of bone marrow cells. Here we want to answer the question whether wildtype Af10 is required for fusion oncogene-mediated transformation if the fusion retained OM-LZ domain of Af10. Therefore, I transduced bone marrow cells from $Af10^{f/f}$ mice with MLL-AF10 and CALM-AF10, and subsequently transduced cells with Cre or MIT, sorted Tomato$^+$ cells on day 3, and grew them in methylcellulose-based culture. Interestingly, the colony forming potential of MLL-AF10 and CALM-AF10 cells is not affected by loss of endogenous $Af10$ (Figure 5-4). There is no significant difference in the percentage of blast-like colony and there is no morphological difference between $Af10$ excised and $Af10$ floxed cells (Figure 5-4B). Moreover, I picked 8 single cell colonies from the Cre-transduced dishes and 4 single cell colonies from the MIT-transduced dishes on day 9 after transduction with Cre or MIT. Most of the Cre clones and the MIT clones can maintain proliferation for more than 4 weeks in methylcellulose culture. Genotyping showed that all the Cre-transduced single cell clones have clear homozygous Af10 deletion (Figure 5-4), and surprisingly, these Af10$^{-/-}$ single cell clones have almost no H3K79me2 as shown by Western blot (Figure 5-4D).
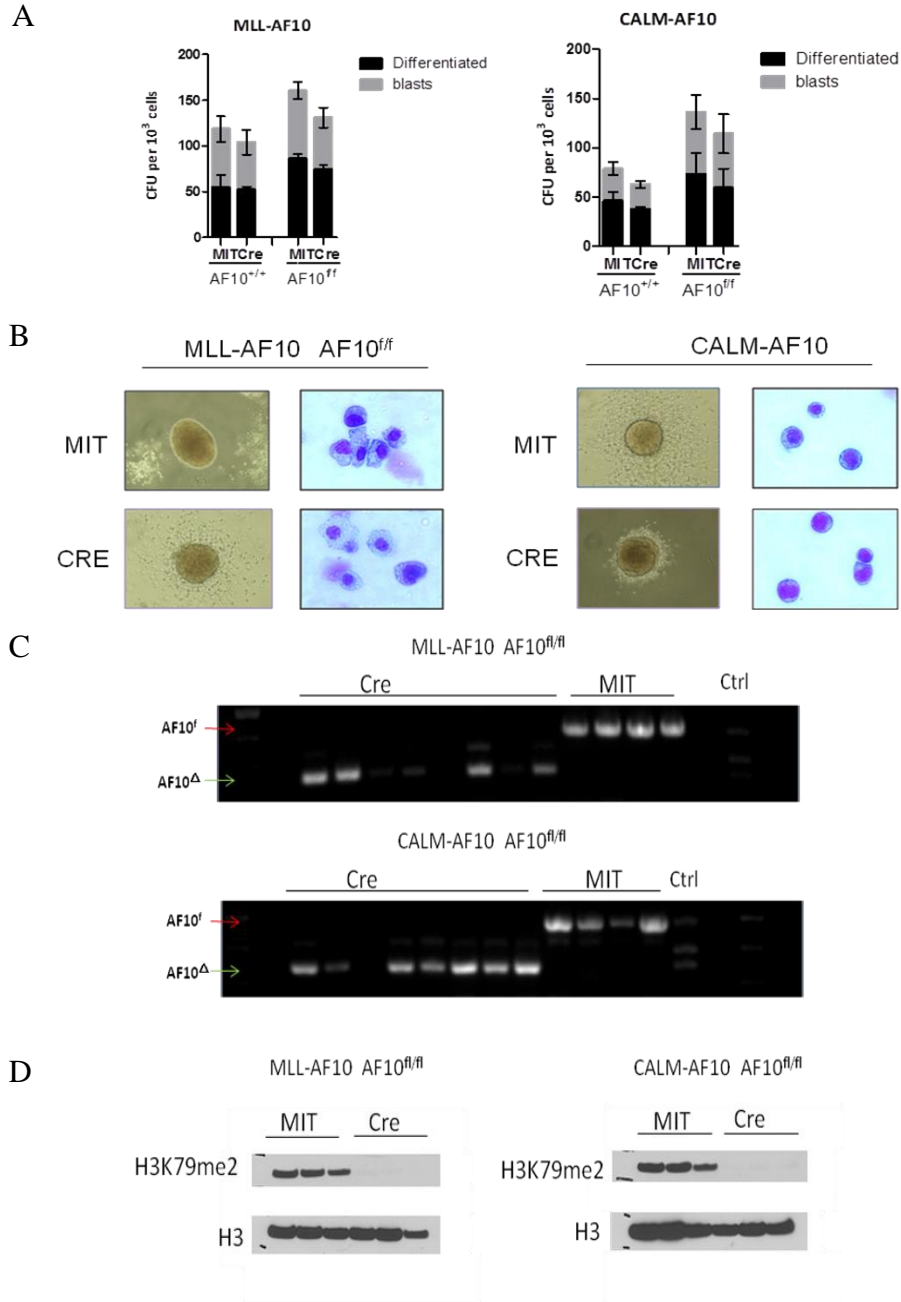
Figure 5-4 AF10 is dispensable for bone marrow transformation by MLL-AF10 as well as CALM-AF10.

(A) Blast and differentiated colony count of *AF10*–deleted MLL-AF10 (left panel) and CALM-AF10 (right panel) transformed cells in methylcellulose 10 days after transduction with Cre in comparison to controls (n=3 independent experiments). (B) Morphology (10X image of colony morphology in methylcellulose, 40X image of Wright-Giemsa stain) of established MLL-AF10 and CALM-AF10 *AF10$^{f/f}$* leukemia cells 10 days after transduction with Cre or MIT. (C) Bone marrow cells from *AF10$^{f/f}$* mice were immortalized by MLL-AF10 or CALM-AF10, and then transduced with MIT or Cre. Single cell clones were picked and genomic status of AF10 was confirmed by PCR. f: floxed allele. △: deleted allele. WT: wildtype allele. (D) Western blot was performed with histone extraction from three different Cre clones and three different MIT clones (as control). Left panel: MLL-AF10. Right panel: CALM-AF10.

To understand why MLL-AF9 leukemia is affected by loss of $AF10^{OM-LZ}$, but MLL-AF10 leukemia is not affected by loss of $AF10^{OM-LZ}$ and how MLL-AF10 or CALM-AF10 cells survive with a global reduction of H3K79me2, I performed ChIP-qPCR from in vitro transformed cells on day 9 after transduction with Cre. First, I compared the change of H3K79me2 on the promoter regions of MLL target genes (*Hoxa7, Hoxa9, Hoxa10*, and *Meis1*) and housekeeping genes (*β-Actin* as an example) and silent genes (*Hoxb1* as an example) in MLL-AF9 transformed cells after *AF10* deletion versus after *Dot1l* deletion. As shown in Figure 5-5, *Dot1l* deletion, as well as *AF10* deletion, led to a significant reduction of H3K79me2 on promoters of MLL target genes and housekeeping genes. Next, I compared the effects of loss of AF10 on the H3K79me2 levels on the promoter regions of MLL target genes and housekeeping genes in MLL-AF10 transformed cells versus MLL-AF9 transformed cells. As shown in Figure 5-5, in MLL-AF9 transformed cells, loss of AF10 resulted in reduction of H3K79me2 level on both MLL target genes and housekeeping genes, while in MLL-AF10 transformed cells, loss of AF10 only resulted in reduction of H3K79me2 level on housekeeping genes, but not MLL target gene *Hoxa7, Hoxa9, Hoxa10*, and *Meis1*. These MLL target genes are leukemia-promoting oncogenes whose overexpression is sufficient to transform bone marrow cells. The fact that although being globally decreased after loss of AF10, H3K79me2 level is maintained on the small number of MLL target genes in MLL-AF10 leukemia may explain why MLL-AF10 leukemia can survive loss of endogenous AF10. It also suggested that the OM-LZ domain of AF10 is necessary and sufficient for Dot1l-catalyzed H3K79 methylation in MLL targets. The AF10 OM-LZ domain and H3K79 methylation does have an important role in MLL-AF10 and CALM-AF10 transformation; however, MLL-AF10 and CALM-AF10 transformed $AF10^{OM-LZ}$ deleted cells could be "rescued" by the AF10 OM-LZ domain in the respective fusion protein.
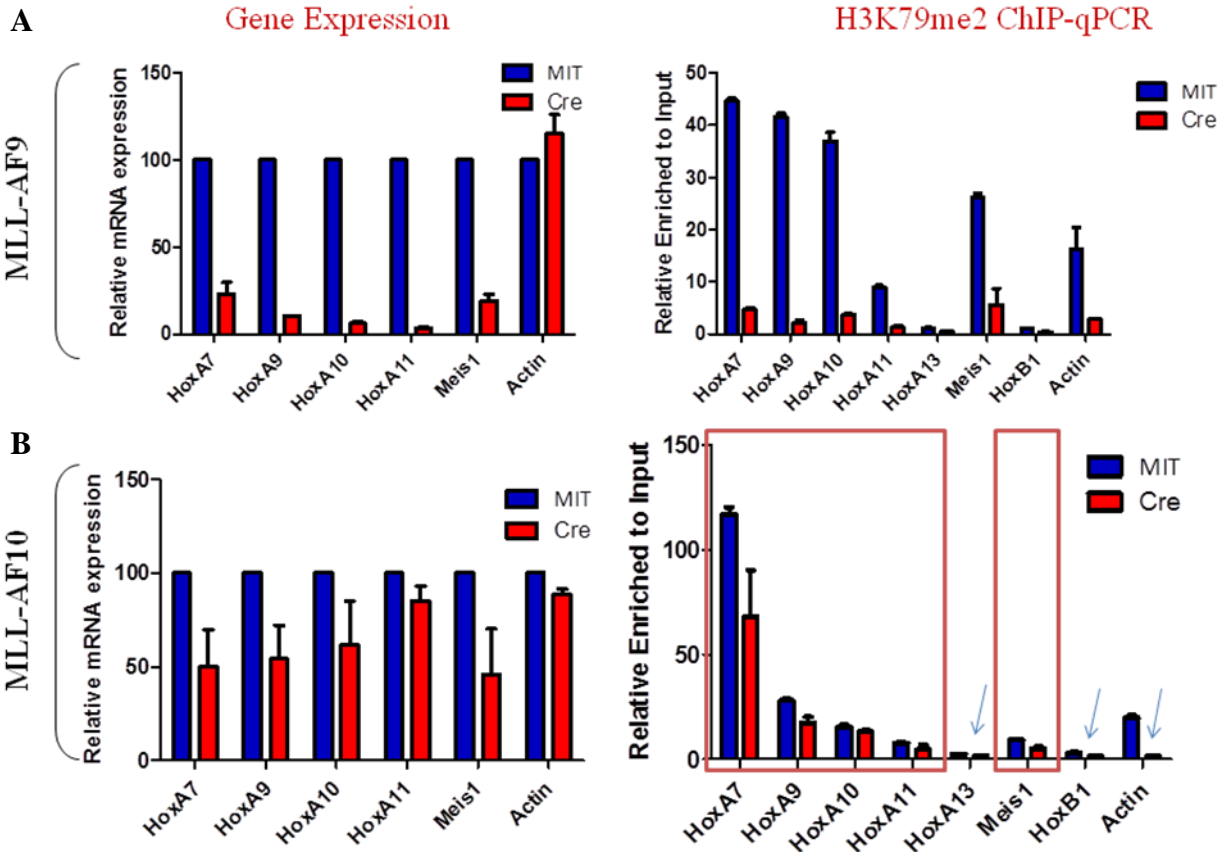
Figure 5-5 H3K79me2 ChIP-qPCR from in vitro transformed cells on day 9 after transduction with Cre.

(A) Loss of H3K79me2 after deletion of AF10 in MLL-AF9 transformed bone marrow cells. (B) H3K79me2 is selectively maintained on the promoters of MLL target genes after deletion of AF10 in MLL-AF10 transformed bone marrow cells.

Given that Af10 is required for global H3K79 dimethylation and the expression of MLL-AF9 target genes specifically, we sought to explore how $Af10^{OM-LZ}$ deletion would affect the chromatin structure of different gene loci. The chromatin structure was determined by a nuclease accessibility assay, in which the DNA in euchromatin or "open" chromatin region is digested by the nuclease but DNA in heterochromatin or "close" chromatin region is not. In $Af10^{f/f}$ cells, MLL target loci and housekeeping gene loci displayed "open" structure with high accessibility, while a silent gene Hoxb1 has low accessibility. Interestingly, upon Af10 OMLZ deletion, housekeeping genes still displayed high accessibility while all of the tested MLL-target genes become less accessible (Figure 5-6).
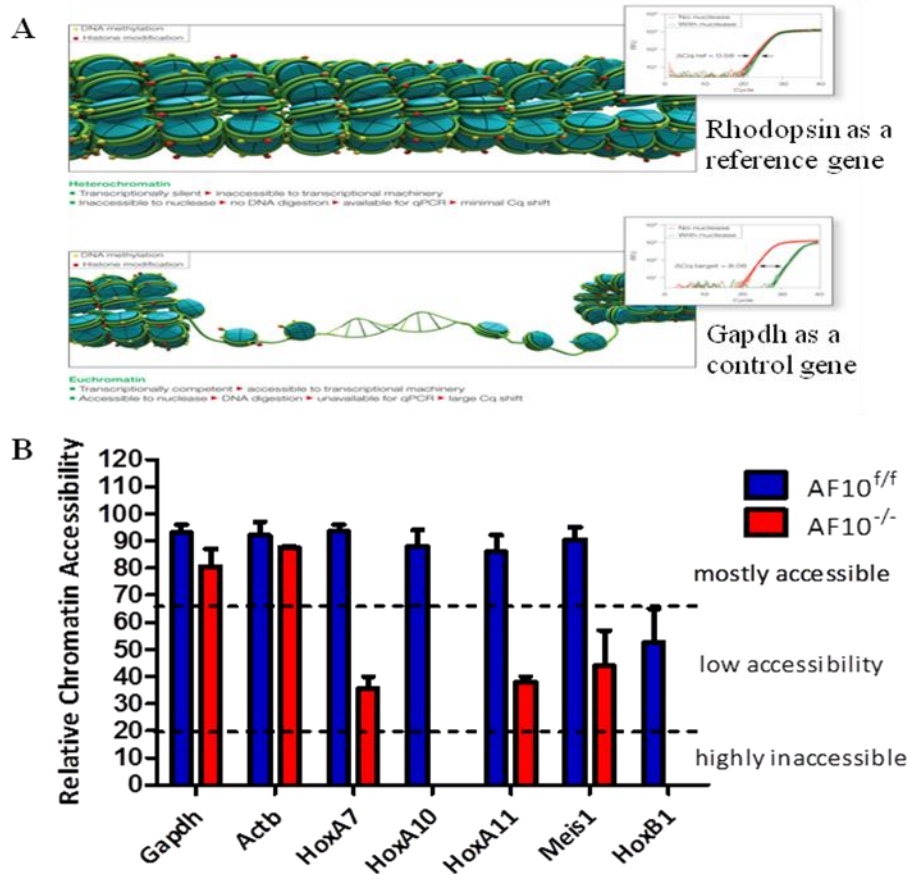
Figure 5-6 Loss of AF10 decreased the chromatin accessibility of MLL-target genes specifically.

(A) Schematic representation of nuclease accessibility assay to study chromatin structure. (B) The relative chromatin accessibility with and without AF10 deletion is calculated using *Rhodopsin* as a reference gene.

Discussion

The results presented here demonstrated that *Af10* plays an important role in the conversion of H3K79 monomethylation to dimethylation. When Af10-Dot1l interaction was abrogated by genetic deletion of Af10 OM-LZ domain in our knockout mouse model, global H3K79 dimethylation disappeared, while H3K79 monomethylation was largely unchanged. Recently, our lab has reported that aberrant H3K79 dimethylation on MLL target loci controls the MLL-fusion associated leukemogenic transcription program (25). Here we showed that MLL-fusion associated leukemogenic transcription program was suppressed in our AF10[OM-LZ] deleted MLL-AF9 leukemia. Moreover, we demonstrated a strong dependence of *MLL* rearranged leukemia cells on the Af10-Dot1l complex *in vitro* and *in vivo*. Deletion

of endogenous $Af10^{OM-LZ}$ affected *in vitro* bone marrow transformation by MLL-AF9 and MLL-AF6 and prolonged the survival of mice with MLL-AF9 leukemia *in vivo*, phenotypically mirroring the loss of Dot1l. In addition, the AF10 OM-LZ domain in MLL-AF10 or CALM-AF10 fusion protein can maintain H3K79 dimethylation in highly specific fusion targets and support *in vitro* bone marrow transformation despite the loss of endogenous $Af10^{OM-LZ}$ and global H3K79 dimethylation, supporting the important role of AF10-DOT1L interaction in the installation of H3K79 dimethylation and oncogenic transformation.

We have previously discovered highly abnormal H3K79me2 pattern at MLL target loci in MLL-AF9 leukemia as well as MLL-AF6 leukemia, which was unique with respect to other actively transcribed loci within the same cell. This epigenetic lesion in MLL target loci may explain a specific and nonphysiological dependence of the MLL fusion-driven leukemogenic transcription program on H3K79 methylation. Our lab has recently shown that deletion of endogenous Dot1l abrogates global H3K79 methylation in MLL-AF9 but only the expression of MLL-AF9 target genes is affected, suggesting that H3K79 methylation is not uniformly involved in maintaining transcription. In this study, we demonstrated that genetic disruption of Af10-Dot1l interaction abrogated global H3K79 dimethylation but not H3K79 monomethylation. Our microarray data comparing the transcription program in $Af10^{f/f}$ and $Af10^{-/-}$ MLL-AF9 cells demonstrated that H3K79 dimethylation is required specifically for the expression of MLL target genes but is dispensable for transcription of non-MLL-target loci which normally are also associated with H3K79 dimethylation. Interestingly, our results of nuclease accessibility assay revealed that deletion of $AF10^{OM-LZ}$ domain in MLL-AF9 leukemia led to specific chromatin compaction in MLL target loci but not in house-keeping genes like *Gapdh* or *β-Actin*, suggesting a link between aberrant H3K79 dimethylation and open chromatin structure. It is thus of tremendous interest to determine the temporal order of aberrant H3K79 dimethylation, the opening of chromatin structure, and transcriptional activation at MLL target genes during transformation by MLL fusions. This may be assessed by

monitoring the dynamic changes of chromatin status, H3K79me2 level, and RNA synthesis at various time points after inducing the expression of MLL-AF9 in hematopoietic progenitors.

It has been shown that Dot1l is a nonprocessive enzyme and it adds methyl groups to H3 lysine 79 one at a time. In yeast, lower concentration of induced Dot1l expression and expression of partially active Dot1l will affect the levels of H3K79me2 and H3K79me3 more than the level of H3K79me1. In addition, the conversion of H3K79me1 to H3K79me2 and H3K79me3 requires a complex epigenetic network involving prior mono-ubiquitination of histone H2B. Therefore, Af10-Dot1l interaction may affect the transition between H3K79 mono- to di-methylation by three mutually non-exclusive mechanisms. The first possibility is that Af10-Dot1l interaction stabilizes Dot1l protein and prevents it from degradation. The second possibility is that Af10 is required for targeting Dot1l to chromatin, thus increasing the enzyme concentration in the microenvironment. The third possibility is that Af10-Dot1l is required for the optimal enzymatic activity of Dot1l. Our preliminary result showed that Af10 deletion in mouse fibroblasts affects the nuclear localization but not the protein stability of ectopically expressed FLAG-DOT1L-GFP (data not shown). To test whether Af10 functions by targeting Dot1l to chromatin, I tried to determine the binding patterns of endogenous Af10 and Dot1l and compare them with the binding pattern of H3K4me2/3 and H3K79me2/3. However, my initial ChIP-seq experiments failed due to lack of good antibodies against endogenous Af10 or Dot1l. Future directions will be to generate better antibodies against Af10 and Dot1l for studying the mechanism of the installation and propagation of H3K79 methylation by Dot1l, and to do an *in vitro* enzymatic activity assay to determine whether AF10 affects the enzymatic activity of DOT1L.

It has been demonstrated by us as well as by others that the normal balance of H3K4 methylation and H3K79 methylation is destroyed in *MLL*-rearranged leukemia (12, 25, 93). In mammalian chromatin, H3K4 methylation and H3K79 methylation are two parallel marks that coexist in actively transcribed

genes and may share a requirement for the PAF elongation complex and H2B ubiquitylation. *MLL* rearrangement affects the H3K4 methylation function by genetic inactivation of one MLL allele, but the H3K79 methyltransferase DOT1L is recruited to MLL-fusion target loci, resulting in much more extensive H3K79 methylation in MLL targets. Although the mechanisms for the involvement of DOT1L-mediated H3K79 methylation in transcriptional activation are not clear, our study here again confirms that *MLL*-rearranged leukemia is addicted to the epigenetic lesion and suggests another strategy to suppress the H3K79 methylation in MLL-rearranged leukemia.

In summary, our findings demonstrated that the Af10-Dot1l interaction plays an important role in H3K79 dimethylation and MLL-fusion leukemogenesis, suggesting that the AF10-DOT1L interaction may serve as an attractive therapeutic target in *MLL*-rearranged leukemias. Proof-of-concept experiments will be needed to assess the effectiveness of pharmaceutically targeting Af10-Dot1l interaction in MLL-rearranged leukemia. Further directions will be to address how Af10 affects the transition between H3K79 mono- and di-methylation and how dimethylation affects gene transcription.

Materials and Methods

Mutant Mice

Mice engineered to harbour *LoxP* sites flanking the OM-LZ domain of *AF10* were generated in our laboratory by Dr. Anirrudha Deshpande. Bone marrow cells from 7-10 week old mice in *AF10* wild-type or homozygous floxed (*AF10*$^{f/f}$) backgrounds were used for transformation assays and subsequent biochemical experiments.

Generation of Transformed Murine Cells and Leukemia

The MSCV based MLL-AF9-IRES-GFP, HoxA9-IRES-GFP, and Meis1a-PGK-Puromycin, FLAG-CALM-AF10-IRES-GFP, FLAG-MLL-AF10-IRES-GFP, MLL-AF6-neo constructs were described in Chapter 3 and Chapter 4. The MSCV-IRES-Tomato (MiTomato, or MIT) plasmid was a kind gift from the lab of Hassan Jumaa (Max Planck Institute, Freiburg). The cDNA for Cre recombinase was sub-cloned into the MIT plasmid to generate the MSCV-Cre-IRES-Tomato (Cre-MiTomato, or Cre) construct. Retroviral supernatants were collected from 293-T cells separately transfected with the plasmids using standard protocols and used for retroviral spin infections. Sorted Lin$^-$Sca$^-$1$^+$cKit$^+$ (LSK) cells from mouse bone marrow were used for retroviral transduction experiments. The LSK cells were transduced with viruses carrying MLL-AF10, CALM-AF10, MLL-AF9, MLL-AF6 or HoxA9 and Meis1, and expanded for 2-5 days in methylcellulose M3234 (StemCell Technologies, Vancouver, Canada) supplemented with cytokines (6ng/ml IL3, 10ng/ml IL6 and 20ng/ml SCF). Transformed cells were then transduced with Cre or MIT and expanded in methylcellulose M3234 supplemented with cytokines. After two days, GFP$^+$Tomato$^+$ cells were sorted for in vitro colony forming assays, or sorted and transplanted into B6/129 syngeneic sublethally irradiated (550 rad) recipients at 5×10^5 cells/mouse. For secondary transplants, whole-bone marrow from leukemic mice was isolated and transduced with Cre or MIT on the same day;

GFP$^+$Tomato$^+$ cells were sorted in two days, and transplanted into sublethally irradiated (550 rad) B6/129 syngeneic recipients at 5×10^5 cells/mouse for generation of secondary MLL-AF9 leukemia.

Colony Forming Assays

Colony forming cell (CFC) assays were performed by plating 1000 cells per ml of methylcellulose M3234 supplemented with cytokines (6ng/ml IL3, 10ng/ml IL6 and 20ng/ml SCF). On day 6-7 after plating, colonies were scored using a Nikon Eclipse TS100 microscope (Nikon, Tokyo, Japan) and classified into two categories - compact and hypercellular blast-like colonies or small and diffuse differentiated-type colonies. Colonies were then pooled and used for biochemical assays or replated for assessment of secondary replating potential at the same concentration. Cytospin preparations were performed from 50-100,000 cells. Pictures of colonies and Wright-Giemsa stained cytospin preparations were taken using a Nikon Eclipse E400 microscope (Nikon, Tokyo, Japan) and a SPOT RT color digital camera (Diagnostic Instruments, Sterling Heights, MI, USA).

Western Blotting

Histone purification was performed with triton extraction (1×PBS, 0.5% TritonX100 and 2 mM phenylmethylsulfonylfluoride) followed by acid extraction with 0.2 N HCl as previously described (25). Proteins were separated on a 10% Bis-Tris gel (Nupage, Invitrogen, Carlsbad, CA, USA), and transferred onto PVDF membranes. The following antibodies were used for detection: anti-H3K79me2 antibody ab3594 (Abcam, Cambridge, MA, USA), anti-total H3 antibody ab1791 (Abcam, Cambridge, MA, USA); secondary antibodies used: sheep anti-mouse ECL horseradish peroxidase linked NA931V and donkey anti-rabbit ECL horseradish peroxidase linked NA934V (GE healthcare UK limited, Little Chalfont Buckinghamshire, UK).

Mass Spectrometry

Histone was extracted from 10^8 cells with triton extraction (1×PBS, 0.5% TritonX100 and 2 mM phenylmethylsulfonylfluoride) followed by acid extraction with 0.2 N HCl as previously described (25). Histone extract was separated by 10% SDS-PAGE gel and stained with comassie stain. Histone bands were cut out and trypsinized and subjected to LC-MS analysis. The abundance of different form of H3K79 modifications in *Dot1l*$^{f/f}$ or *Af10*$^{f/f}$ cells was set to 1 and the relative abundance of different modifications in *Dot1l*$^{-/-}$ or *Af10*$^{-/-}$ celles was compared to that in *Dot1l*$^{f/f}$ or *Af10*$^{f/f}$ cells, respectively. The intensity of the following digested peptides were plotted: Control H3 peptide sequence is YRPGTVALR; H3K79me0 represents unmodified (EIAQDFK) H3K79 peptide; H3K79me1 represents monomethyl (EIAQDFKTDLR) H3K79 peptide; H3K79me2 represents dimethyl (EIAQDFKTDLR) H3K79 peptides. H3K79 trimethylation was rare and below the sensitivity of mass spectrometric detection.

Reverse transcription and Real Time PCR

Total RNA was isolated using Trizol (Invitrogen, Carlsbad, CA, USA) according to the manufacturer's instruction. The resultant cDNA was generated using the Tetro cDNA synthesis kit (Bioline, Taunton, MA, USA). Real time PCR was performed using Taqman probes (Applied Biosystems) on the ABI 7700 Sequence Detection System (Applied Biosystems). Expression levels (average values and standard deviations of triplicate determinations) were normalized to housekeeping gene Gapdh. All experiments were performed with technical duplicates from three individual experiments.

After two rounds of plating cells were harvested and subjected to Chromatin immunoprecipitation (ChIP). Chromatin immunoprecipitation was performed similarly as described (25). Briefly, cells were fixed in PBS 1% formalin (v/v) with gentle rotation for 10 minutes at room temperature. Fixation was stopped by the addition of glycine (125 mM final concentration). Fixed cells were washed twice in ice-cold PBS, resuspended in SDS lysis buffer (1% SDS, 10 mM EDTA, 50 mM Tris-HCl, pH 8.1). Chromatin was sheared by sonication to about 100-500bp fragments using bioruptor (diagenode, Denville, NJ) and

diluted ten folds with dilution buffer (0.01% SDS, 1.1% Triton-X100, 1.2 mM EDTA, 16.7 mM Tris-HCl, pH 8.1,167 mM NaCl). Antibodies against specific histone modifications or Dynabeads M280 streptavidin beads (Invitrogen) was used to precipitate DNA fragments associated with modified histones. Precipitates were washed sequentially with ice cold low salt wash (0.1% SDS, 1% Triton-X-100, 2mM EDTA, 20mM Tris-HCl, pH8.1, 150mM NaCl), high salt wash (0.1% SDS, 1% Triton-X-100, 2mM EDTA, 20mM Tris-HCl, pH 8.1, 500mM NaCl), LiCl wash (0.25M LiCl, 1% IGEPAL CA-630, 1% deoxycholic acid, 1mM EDTA, 10mM Tris-HCl, pH 8.1) and TE wash (1mM EDTA, 10mM Tris-HCl, pH 8.1) and eluted in elution buffer (1% SDS, 0.1 M NaHCO3). All buffers except for elution buffer were supplemented with protease inhibitor (Complete mini protease inhibitor cocktail tablets, Roche, Indianapolis, IN). Eluted DNA fragments were analyzed by quantitative PCR using promoter specific primers for Hoxa7 (forward: CTCTTCTGTTTCCCATCCTGGT; reverse: GGCAATATCCGGGATCCACT), Hoxa9 (forward: GGAATAGGAGGAAAAAACAGAAGAGG; reverse: TGTATGAACCGCTCTGGTATCCTT), Hoxa10 (forward: CCTTTTTGGTCGACTCGCTC; reverse: CAACACCAGCCTCGCCTCT), Meis1a (forward: TCACCACGTTGACAACCTCG; reverse: GCTTTCTGCCACTCCAGCTG), Hoxb1 (forward: GGGACTGCCAAACTCTGGC; reverse: CATGTGATCTCTCCCAGGCC) and β-Actin (forward: GGGAACCAGACGCTACGATC; reverse: TTGGACAAAGACCCAGAGGC). Chromatin immunoprecipitation for H3K79me2 and H3K79me1 was performed as above using rabbit polyclonal antibodies from abcam (Cambridge, MA): ab3594 and ab2886, respectively. For ChIP sequencing, ChIP DNA libraries were made following Illumina ChIP-seq library preparation kit and subjected to Solexa sequencing (Illumina).

RNA amplification and gene expression array

RNA was isolated from $1x10^5$ sorted GFP$^+$/YFP$^+$ cells using Trizol (Invitrogen, Carlsbad, CA). RNA was amplified using the Nugen Ovation Pico WTA system (Nugen, San Carlos, CA), and labeled using the Nugen EncoreTM Biotin Module. 5 µg of amplified and labeled DNA was hybridized to Affymetrix 430 2.A murine microarrays. GenePattern (Reich et al., 2006) release 3.2.3 was used to normalize the raw

microarray data using RMA algorithm, preprocess the normalized data using default parameters and find differentially expressed probe sets.

Nuclease accessibility assay

Nuclease accessibility assay was performed with EpiQ chromatin analysis kit (Bio-Rad, 172-5400) following instructures from the manufacturer. In brief, leukemia cells with or without Af10 deletion were processed in two treatment groups: undigested and digested. The undigested group was not digested with the EpiQ nuclease, the digested group was treated with limited EpiQ nuclease digestion according to the kit instruction. The genomic DNA samples for both groups were isolated and subjected to quantitative PCR. Primers for qPCR are: Hoxa7 (forward: TTTCCGGGGCAATTCCATTGTGAAG; reverse: CAGATCCCGCGGCTTCACCTTTCTA); Hoxa9 (forward: CAATGTCCAGTGTTCCTCCCGGGTTA; reverse: TTGCTGAGGGGTCACCTCGCCTAGT); Hoxa10 (forward: CGGCCTTTGAGCCATAGGTG TCAGG; reverse: TGGCGAAGGGAGCAGATAGCCCTTT); Hoxa11 (forward: TTACACCGGCGATTACGTGCTTTCG; reverse: TCCACTGCAGCTGCCTCTTTGAAGC); Hoxa13 (forward: GGGAGCTAGAGCTGGCGCAGAGGAC; reverse: AGCCGCATGGAGAAGACCCCAGTG; Meis1 (forward: ATTTGTGTGCATGTGCCCTGGGTGT; reverse: CGCCGTGCGTGTGTAAAGTGTG TGT); Gapdh (forward: CCAGCACAGATGGAGCGGAAAGAGG; reverse: CCTAGTCCCTGCGCCG GTACATTCA); β-Actin (forward: CCACAAGGGCGGAGGCTATTCCTGT; reverse: ACAGCGGCCACTCGAGCCATAAAAG); Hoxb1 (forward: TCGCTCTCAGATGGATGGGCTCAG; reverse: TGGGGGAGACACCCTCTTGCCCTAC). qPCR results for all samples were normalized to an internal control, a fragment of an unexpressed gene Rhodopsin according to the kid instruction. Nuclease accessibility index was calculated as the ratio between the undigested sample and the digested sample at the same time point.

Chapter 6

Conclusions and Perspectives

The DOT1L-AF10 complex is a promising therapeutic target in MLL-rearranged leukemia

Rearrangements of the *Mixed-Lineage Leukemia* (*MLL*) gene are found in > 70% of infant leukemia, ~ 10% of adult *de novo* acute myeloid leukemia, and many cases of secondary acute leukemias. The diversity of MLL fusion partners poses a challenge to developing a unified mechanistic model for *MLL*-rearranged leukemias. However, gene expression signatures of *MLL* rearranged leukemias are remarkably similar, with high expression of MLL targets such as *HOXA* loci and *MEIS1*, which can be reliably used to distinguish leukemias with *MLL* rearrangements from other subtypes. We showed that *MLL* rearranged leukemias with nuclear fusion partners and with cytoplasmic fusion partners both have aberrantly high methylation at histone H3K79 in MLL target genes. This epigenetic lesion may be involved in driving the gene expression signatures in *MLL* rearranged leukemias. We further demonstrated that Dot1l is essential for the leukemogenesis of several MLL- and CALM-fusion driven leukemias with dismal outcome, such as MLL-AF10, MLL-AF6, and CALM-AF10. Our results with genetic and pharmacological approaches support the notion of inhibiting H3K79 methylation by DOT1L as a new therapeutic strategy for MLL-rearranged leukemia.

We further showed that Af10, a key component of Dot1l complex, is required for global H3K79 dimethylation but not H3K79 monomethylation. Using an *Af10^{OM-LZ}* knockout mouse model, we demonstrated that genetic disruption of Af10-Dot1l interaction abrogated *in vitro* bone marrow transformation by MLL-AF9 and MLL-AF6, and resulted in prolonged survival of mice injected with *Af10^{OM-LZ}* deleted MLL-AF9 leukemic cells compared to mice injected with *Af10^{OM-LZ}* floxed MLL-AF9 leukemic cells. Nuclease accessibility assay and microarray revealed that deletion of *Af10^{OM-LZ}* led to chromatin compaction and downregulation of gene expression in highly selective MLL target loci, without affecting the chromatin structure and gene expression in the majority of the genome. Our results reveal the AF10-DOT1L interaction as an attractive therapeutic target in *MLL*-rearranged leukemias.

97

Identifying new dependence in genetically-defined cancer cells for the design of targeted therapy

The term "targeted cancer therapy" describes various approaches that aim to block the growth of cancer cells based on specific molecular characteristics of the cancer, rather than by general inhibition of cell division. One of the first definitive experiments that showed that targeted therapy would reverse the malignant phenotype of tumor cells was the treatment of Human Epidermal Growth Factor Receptor2 (HER2)-transformed cells with anti-HER2 monoclonal antibody *in vitro* and *in vivo* in 1985 (103). Since then, more and more targeted therapies have been validated by pre-clinical experiments and been used in clinical applications, including Tyrosine kinase inhibitor Gleevec for BCR-ABL rearranged chronic myeloid leukemia (1) and BRAF inhibitor Zelboraf for BRAF mutated melanoma (104), both of which are examples of successful targeted cancer therapy.

Targeted cancer therapies benefit patients by increasing "therapeutic index", or to put it another way, by maximizing therapeutic efficacy and minimizing toxicity. One critical first step in the design of targeted cancer therapy is the identification of molecular "Achilles' Heels" of genetically-defined cancer cells. Recent cancer genomic discovery efforts, such as whole genome sequencing, continue to reveal genetic mutations in various types of human cancer. Some of the mutations are driver mutations, which actively drive oncogenesis by promoting cell division and/or blocking cell differentiation and cell death, while some of the mutations are passenger mutations, which are not critical to the development of cancer but may be involved in the progression of the specific disease. Previously, the effort of discovering targets has been focused on identifying oncogene mutations that drive the oncogenesis directly. Targeted therapies have been established for BRAF mutated melanoma, BCR-ABL rearranged CML, HER2 positive breast cancer by inhibiting the hyperactive oncogenic proteins that turn on cell division through signaling pathways. This type of targeted therapy usually possesses an enormous therapeutic window because it inhibits the oncogene on which cancer cells are dependent but normal cells are not. However,

98

this type of targeted therapy design sometimes faces limitations regarding the druggability of the specific oncogene and the issue of drug resistance.

Interestingly, our research revealed that some non-oncogenes also have the potential to be great therapeutic targets for genotype-specific cancers. Normal cells are not affected by the suppression of the non-oncogenes due to functional redundancy of homologous genes or compensation by other pathways. However, specific oncogenic mutation may depend on these non-oncogenes to drive cancer cell division or to turn off cancer cell differentiation and apoptosis. In this case, the oncogene mutation creates a new co-dependence on specific non-oncogenes in the development of cancer. Targeting these special non-oncogenes will kill the genotype-specific cancer cells while sparing normal cells.

MLL-rearranged leukemias are driven by the oncogenic MLL-fusion proteins, which are not ideal targets for drug development due to the diversity of MLL fusion partners and the importance of MLL in normal cells. Our results demonstrated that MLL-rearranged leukemias depend on the function of DOT1L, which can serve as an alternative drug target. Based on the cancer genome sequencing data, the gene encoding DOT1L is relatively quiet. Although not an oncoprotein, DOT1L is specifically hijacked to MLL-fusion targets in MLL-rearranged leukemic cells and drives the expression of the oncogenic target genes. Loss of DOT1L selectively killed MLL-fusion transformed bone marrow cells but had no effect on HoxA9/Meis1 transformed cells. In addition, genetic deletion of DOT1L led to a selective silencing of MLL-fusion target genes without inhibiting general transcription. Furthermore, preclinical studies have shown that DOT1L inhibitor has a great efficacy in treating MLL-rearranged leukemia and it is well tolerated in mice (105), suggesting a huge therapeutic window of DOT1L inhibitors for patients with MLL-rearranged leukemias.

Recently, William Hahn's group published another study describing the co-dependence between the oncogene KRAS and a non-oncogene TBK1 (106). KRAS mutation is a common driver mutation in pancreatic cancer and is very difficult to target because of high gene mutation rate and frequent drug resistance. TBK1 is an essential KRAS partner. It is a non-oncogene and is dispensable for normal cells. Through genome-wide shRNA screen, Hahn's group discovered that KRAS-mutated cancers are specifically sensitive to the suppression of TBK1, suggesting TBK1 as a new therapeutic target for KRAS-mutated cancers. Together, the two studies support the use of non-oncogene as targets for patient-specific therapy.

The idea of co-dependence between specific oncogene and non-oncogene may open up a much broader class of protein targets for new therapy. As long as the efficacy and toxicity is well monitored, not only oncogenes can serve as drug targets, non-oncogenes can also serve as therapy targets for cancer based on patient-specific molecular features. In the near future, the joint efforts in high-throughput sequencing, chemical genomic screening and bioinformatics will build connection between genotype-specific cancer and potential targets and contribute to the development of personalized targeted cancer therapy.

H3K79 methylation inhibitors show promise in personalized medicine for patients with MLL-rearranged leukemia.

The preclinical result of optimized DOT1L inhibitor showed promise for personalized medicine for patients with MLL-rearranged leukemia (105). Based on this, the first-in-human clinical trial of DOT1L inhibitor is ongoing. Although we believe that targeting DOT1L enzymatic activity domain will be an important therapeutic approach in MLL-rearranged leukemia, single agent therapy is virtually never curative. Our results support an alternative approach to inhibit H3K79 methylation. Besides targeting the enzymatic active domain of DOT1L, targeting the protein-protein interaction between DOT1L and the

OM-LZ domain of AF10 can also suppress H3K79 dimethylation and inhibit the growth of MLL-rearranged leukemia. With advances in pharmacology and biochemistry, designing small-molecule inhibitors to target protein-protein interaction has now become very feasible. An epigenetic drug JQ1, which targets the interaction between bromodomain and acetylated histone H4 thus inhibiting c-Myc activation, has proven effective in treating human multiple myeloma in preclinical animal studies (107). Given the involvement of aberrant H3K79 dimethylation in MLL-rearranged leukemia and the requirement of AF10-DOT1L interaction for H3K79 dimethylation, I envision that small-molecule inhibitors targeting AF10-DOT1L interaction combined with the DOT1L enzymatic domain inhibitor or with differentiating and/or apoptosis agents may yield better therapy.

In the past decade, the successful use of epigenetic drugs in clinical and preclinical studies has lighted up cancer research. In this thesis, I focused on one type of epigenetics-- chromatin modifications. However based on a broad definition of epigenetics, every program that maintain a heritable change of cell state without altering DNA sequence can be called as epigenetics. It includes DNA methylation, histone modification, small RNA-mediated silencing, and many other mechanisms that we have not yet understood clearly. The scientific curiosity and the hope of benefiting patients will continue to drive me and millions of other scientists to study cancer epigenetics and targeted therapy.

Concluding remarks

To conclude, our studies presented here contribute to a growing body of cancer epigenetic studies. Cancer, as a cell state, is influenced by the epigenetic program that determines how chromatins are packaged and how the genome gets expressed. Growing evidence supports that targeting epigenetic modifiers may correct the deregulated epigenetic program in cancer, and set the cell state back to normal. We are glad to see the first-in-human clinical trial of DOT1L inhibitor is underway. It is our hope that continued

advances in our understanding of *MLL* leukemia mechanism and in the development of more effective epigenetic drugs will eventually make an impact in the treatment of this dismal disease.

List of References

1.   Sawyers C. Targeted cancer therapy. Nature. 2004 Nov 18;432(7015):294-7. PubMed PMID: 15549090.

2.   Krivtsov AV, Armstrong SA. MLL translocations, histone modifications and leukaemia stem-cell development. Nat Rev Cancer. 2007 Nov;7(11):823-33. PubMed PMID: 17957188. Epub 2007/10/25. eng.

3.   Biondi A, Cimino G, Pieters R, Pui CH. Biological and therapeutic aspects of infant leukemia. Blood. 2000 Jul 1;96(1):24-33. PubMed PMID: 10891426.

4.   Huret JL, Dessen P, Bernheim A. An atlas of chromosomes in hematological malignancies. Example: 11q23 and MLL partners. Leukemia : official journal of the Leukemia Society of America, Leukemia Research Fund, UK. 2001 Jun;15(6):987-9. PubMed PMID: 11417488.

5.   Meyer C, Kowarz E, Hofmann J, Renneville A, Zuna J, Trka J, et al. New insights to the MLL recombinome of acute leukemias. Leukemia : official journal of the Leukemia Society of America, Leukemia Research Fund, UK. 2009 Aug;23(8):1490-9. PubMed PMID: 19262598.

6.   Bernt KM, Armstrong SA. Targeting epigenetic programs in MLL-rearranged leukemias. Hematology / the Education Program of the American Society of Hematology American Society of Hematology Education Program. 2011;2011:354-60. PubMed PMID: 22160057.

7.   Chen CS, Sorensen PH, Domer PH, Reaman GH, Korsmeyer SJ, Heerema NA, et al. Molecular rearrangements on chromosome 11q23 predominate in infant acute lymphoblastic

leukemia and are associated with specific biologic variables and poor outcome. Blood. 1993 May 1;81(9):2386-93. PubMed PMID: 8481519.

8.   Krivtsov AV, Twomey D, Feng Z, Stubbs MC, Wang Y, Faber J, et al. Transformation from committed progenitor to leukaemia stem cell initiated by MLL-AF9. Nature. 2006 Aug 17;442(7104):818-22. PubMed PMID: 16862118. Epub 2006/07/25. eng.

9.   So CW, Karsunky H, Passegue E, Cozzio A, Weissman IL, Cleary ML. MLL-GAS7 transforms multipotent hematopoietic progenitors and induces mixed lineage leukemias in mice. Cancer cell. 2003 Feb;3(2):161-71. PubMed PMID: 12620410.

10.   Corral J, Lavenir I, Impey H, Warren AJ, Forster A, Larson TA, et al. An Mll-AF9 fusion gene made by homologous recombination causes acute leukemia in chimeric mice: a method to create fusion oncogenes. Cell. 1996 Jun 14;85(6):853-61. PubMed PMID: 8681380. Epub 1996/06/14. eng.

11.   Collins EC, Pannell R, Simpson EM, Forster A, Rabbitts TH. Inter-chromosomal recombination of Mll and Af9 genes mediated by cre-loxP in mouse development. EMBO reports. 2000 Aug;1(2):127-32. PubMed PMID: 11265751. Pubmed Central PMCID: 1084253.

12.   Krivtsov AV, Feng Z, Lemieux ME, Faber J, Vempati S, Sinha AU, et al. H3K79 methylation profiles define murine and human MLL-AF4 leukemias. Cancer Cell. 2008 Nov 4;14(5):355-68. PubMed PMID: 18977325. Pubmed Central PMCID: 2591932. Epub 2008/11/04. eng.

13.   Shilatifard A. Chromatin modifications by methylation and ubiquitination: implications in the regulation of gene expression. Annu Rev Biochem. 2006;75:243-69. PubMed PMID: 16756492. Epub 2006/06/08. eng.

14.   Yu BD, Hess JL, Horning SE, Brown GA, Korsmeyer SJ. Altered Hox expression and segmental identity in Mll-mutant mice. Nature. 1995 Nov 30;378(6556):505-8. PubMed PMID: 7477409. Epub 1995/11/30. eng.

15.   Mohan M, Herz HM, Takahashi YH, Lin C, Lai KC, Zhang Y, et al. Linking H3K79 trimethylation to Wnt signaling through a novel Dot1-containing complex (DotCom). Genes Dev. 2010 Mar 15;24(6):574-89. PubMed PMID: 20203130. Pubmed Central PMCID: 2841335. Epub 2010/03/06. eng.

16.   Yokoyama A, Lin M, Naresh A, Kitabayashi I, Cleary ML. A higher-order complex containing AF4 and ENL family proteins with P-TEFb facilitates oncogenic and physiologic MLL-dependent transcription. Cancer Cell. 2010 Feb 17;17(2):198-212. PubMed PMID: 20153263. Pubmed Central PMCID: 2824033. Epub 2010/02/16. eng.

17.   Lin C, Smith ER, Takahashi H, Lai KC, Martin-Brown S, Florens L, et al. AFF4, a component of the ELL/P-TEFb elongation complex and a shared subunit of MLL chimeras, can link transcription elongation to leukemia. Molecular cell. 2010 Feb 12;37(3):429-37. PubMed PMID: 20159561. Pubmed Central PMCID: 2872029.

18.   So CW, Lin M, Ayton PM, Chen EH, Cleary ML. Dimerization contributes to oncogenic activation of MLL chimeras in acute leukemias. Cancer cell. 2003 Aug;4(2):99-110. PubMed PMID: 12957285.

19.   So CW, Cleary ML. Common mechanism for oncogenic activation of MLL by forkhead family proteins. Blood. 2003 Jan 15;101(2):633-9. PubMed PMID: 12393557.

20.   Wang J, Iwasaki H, Krivtsov A, Febbo PG, Thorner AR, Ernst P, et al. Conditional MLL-CBP targets GMP and models therapy-related myeloproliferative disease. The EMBO journal. 2005 Jan 26;24(2):368-81. PubMed PMID: 15635450. Pubmed Central PMCID: 545811.

21.   Ohnishi H, Taki T, Yoshino H, Takita J, Ida K, Ishii M, et al. A complex t(1;22;11)(q44;q13;q23) translocation causing MLL-p300 fusion gene in therapy-related acute myeloid leukemia. European journal of haematology. 2008 Dec;81(6):475-80. PubMed PMID: 18778367.

22.   Armstrong SA, Staunton JE, Silverman LB, Pieters R, den Boer ML, Minden MD, et al. MLL translocations specify a distinct gene expression profile that distinguishes a unique leukemia. Nature genetics. 2002 Jan;30(1):41-7. PubMed PMID: 11731795.

23.   Argiropoulos B, Humphries RK. Hox genes in hematopoiesis and leukemogenesis. Oncogene. 2007 Oct 15;26(47):6766-76. PubMed PMID: 17934484.

24.   Kroon E, Krosl J, Thorsteinsdottir U, Baban S, Buchberg AM, Sauvageau G. Hoxa9 transforms primary bone marrow cells through specific collaboration with Meis1a but not Pbx1b. The EMBO journal. 1998 Jul 1;17(13):3714-25. PubMed PMID: 9649441. Pubmed Central PMCID: 1170707.

25.   Bernt KM, Zhu N, Sinha AU, Vempati S, Faber J, Krivtsov AV, et al. MLL-rearranged leukemia is dependent on aberrant H3K79 methylation by DOT1L. Cancer Cell. 2011 Jul 12;20(1):66-78. PubMed PMID: 21741597. Epub 2011/07/12. eng.

26.   Zhang W, Xia X, Reisenauer MR, Hemenway CS, Kone BC. Dot1a-AF9 complex mediates histone H3 Lys-79 hypermethylation and repression of ENaCalpha in an aldosterone-sensitive manner. The Journal of biological chemistry. 2006 Jun 30;281(26):18059-68. PubMed PMID: 16636056. Pubmed Central PMCID: 3015183.

27.   Bitoun E, Oliver PL, Davies KE. The mixed-lineage leukemia fusion partner AF4 stimulates RNA polymerase II transcriptional elongation and mediates coordinated chromatin remodeling. Human molecular genetics. 2007 Jan 1;16(1):92-106. PubMed PMID: 17135274.

28.   Mueller D, Bach C, Zeisig D, Garcia-Cuellar MP, Monroe S, Sreekumar A, et al. A role for the MLL fusion partner ENL in transcriptional elongation and chromatin modification. Blood. 2007 Dec 15;110(13):4445-54. PubMed PMID: 17855633. Pubmed Central PMCID: 2234781.

29.   Okada Y, Feng Q, Lin Y, Jiang Q, Li Y, Coffield VM, et al. hDOT1L links histone methylation to leukemogenesis. Cell. 2005 Apr 22;121(2):167-78. PubMed PMID: 15851025. Epub 2005/04/27. eng.

30.   Zhang Y, Rowley JD. Chromatin structural elements and chromosomal translocations in leukemia. DNA repair. 2006 Sep 8;5(9-10):1282-97. PubMed PMID: 16893685.

31.   Forster A, Pannell R, Drynan L, Cano F, Chan N, Codrington R, et al. Chromosomal translocation engineering to recapitulate primary events of human cancer. Cold Spring Harbor symposia on quantitative biology. 2005;70:275-82. PubMed PMID: 16869763.

32.   Chen W, Li Q, Hudson WA, Kumar A, Kirchhof N, Kersey JH. A murine Mll-AF4 knock-in model results in lymphoid and myeloid deregulation and hematologic malignancy. Blood. 2006 Jul 15;108(2):669-77. PubMed PMID: 16551973. Pubmed Central PMCID: 1895483.

33.   Zeisig BB, Garcia-Cuellar MP, Winkler TH, Slany RK. The oncoprotein MLL-ENL disturbs hematopoietic lineage determination and transforms a biphenotypic lymphoid/myeloid cell. Oncogene. 2003 Mar 20;22(11):1629-37. PubMed PMID: 12642866.

34.   Barabe F, Kennedy JA, Hope KJ, Dick JE. Modeling the initiation and progression of human acute leukemia in mice. Science. 2007 Apr 27;316(5824):600-4. PubMed PMID: 17463288.

35.	Huntly BJ, Shigematsu H, Deguchi K, Lee BH, Mizuno S, Duclos N, et al. MOZ-TIF2, but not BCR-ABL, confers properties of leukemic stem cells to committed murine hematopoietic progenitors. Cancer cell. 2004 Dec;6(6):587-96. PubMed PMID: 15607963.

36.	Strahl BD, Allis CD. The language of covalent histone modifications. Nature. 2000 Jan 6;403(6765):41-5. PubMed PMID: 10638745.

37.	Martin C, Zhang Y. The diverse functions of histone lysine methylation. Nature reviews Molecular cell biology. 2005 Nov;6(11):838-49. PubMed PMID: 16261189.

38.	Kouzarides T. Chromatin modifications and their function. Cell. 2007 Feb 23;128(4):693-705. PubMed PMID: 17320507.

39.	Deguchi K, Ayton PM, Carapeti M, Kutok JL, Snyder CS, Williams IR, et al. MOZ-TIF2-induced acute myeloid leukemia requires the MOZ nucleosome binding motif and TIF2-mediated recruitment of CBP. Cancer cell. 2003 Mar;3(3):259-71. PubMed PMID: 12676584.

40.	Wang GG, Cai L, Pasillas MP, Kamps MP. NUP98-NSD1 links H3K36 methylation to Hox-A gene activation and leukaemogenesis. Nature cell biology. 2007 Jul;9(7):804-12. PubMed PMID: 17589499.

41.	Issa JP, Kantarjian HM, Kirkpatrick P. Azacitidine. Nature reviews Drug discovery. 2005 Apr;4(4):275-6. PubMed PMID: 15861567.

42.	Gore SD, Jones C, Kirkpatrick P. Decitabine. Nature reviews Drug discovery. 2006 Nov;5(11):891-2. PubMed PMID: 17117522.

43.	Marks PA. The clinical development of histone deacetylase inhibitors as targeted anticancer drugs. Expert opinion on investigational drugs. 2010 Sep;19(9):1049-66. PubMed PMID: 20687783.

44.	Boumber Y, Issa JP. Epigenetics in cancer: what's the future? Oncology. 2011 Mar;25(3):220-6, 8. PubMed PMID: 21548464.

45.	Nguyen AT, Zhang Y. The diverse functions of Dot1 and H3K79 methylation. Genes & development. 2011 Jul 1;25(13):1345-58. PubMed PMID: 21724828. Pubmed Central PMCID: 3134078.

46.	Frederiks F, Tzouros M, Oudgenoeg G, van Welsem T, Fornerod M, Krijgsveld J, et al. Nonprocessive methylation by Dot1 leads to functional redundancy of histone H3K79 methylation states. Nature structural & molecular biology. 2008 Jun;15(6):550-7. PubMed PMID: 18511943.

47.	van Leeuwen F, Gafken PR, Gottschling DE. Dot1p modulates silencing in yeast by methylation of the nucleosome core. Cell. 2002 Jun 14;109(6):745-56. PubMed PMID: 12086673.

48.	Shanower GA, Muller M, Blanton JL, Honti V, Gyurkovics H, Schedl P. Characterization of the grappa gene, the Drosophila histone H3 lysine 79 methyltransferase. Genetics. 2005 Jan;169(1):173-84. PubMed PMID: 15371351. Pubmed Central PMCID: 1448877.

49.	Jones B, Su H, Bhat A, Lei H, Bajko J, Hevi S, et al. The histone H3K79 methyltransferase Dot1L is essential for mammalian development and heterochromatin structure. PLoS genetics. 2008;4(9):e1000190. PubMed PMID: 18787701. Pubmed Central PMCID: 2527135.

50.	Min J, Feng Q, Li Z, Zhang Y, Xu RM. Structure of the catalytic domain of human DOT1L, a non-SET domain nucleosomal histone methyltransferase. Cell. 2003 Mar 7;112(5):711-23. PubMed PMID: 12628190.

51.   Sawada K, Yang Z, Horton JR, Collins RE, Zhang X, Cheng X. Structure of the conserved core of the yeast Dot1p, a nucleosomal histone H3 lysine 79 methyltransferase. The Journal of biological chemistry. 2004 Oct 8;279(41):43296-306. PubMed PMID: 15292170. Pubmed Central PMCID: 2688786.

52.   Ng HH, Feng Q, Wang H, Erdjument-Bromage H, Tempst P, Zhang Y, et al. Lysine methylation within the globular domain of histone H3 by Dot1 is important for telomeric silencing and Sir protein association. Genes & development. 2002 Jun 15;16(12):1518-27. PubMed PMID: 12080090. Pubmed Central PMCID: 186335.

53.   Okada Y, Jiang Q, Lemieux M, Jeannotte L, Su L, Zhang Y. Leukaemic transformation by CALM-AF10 involves upregulation of Hoxa5 by hDOT1L. Nat Cell Biol. 2006 Sep;8(9):1017-24. PubMed PMID: 16921363. Epub 2006/08/22. eng.

54.   Reisenauer MR, Anderson M, Huang L, Zhang Z, Zhou Q, Kone BC, et al. AF17 competes with AF9 for binding to Dot1a to up-regulate transcription of epithelial Na+ channel alpha. The Journal of biological chemistry. 2009 Dec 18;284(51):35659-69. PubMed PMID: 19864429. Pubmed Central PMCID: 2790997.

55.   Nguyen AT, Taranova O, He J, Zhang Y. DOT1L, the H3K79 methyltransferase, is required for MLL-AF9-mediated leukemogenesis. Blood. 2011 Jun 23;117(25):6912-22. PubMed PMID: 21521783. Pubmed Central PMCID: 3128482. Epub 2011/04/28. eng.

56.   Chang MJ, Wu H, Achille NJ, Reisenauer MR, Chou CW, Zeleznik-Le NJ, et al. Histone H3 lysine 79 methyltransferase Dot1 is required for immortalization by MLL oncogenes. Cancer research. 2010 Dec 15;70(24):10234-42. PubMed PMID: 21159644. Pubmed Central PMCID: 3040779. Epub 2010/12/17. eng.

57.   Jo SY, Granowicz EM, Maillard I, Thomas D, Hess JL. Requirement for Dot1l in murine postnatal hematopoiesis and leukemogenesis by MLL translocation. Blood. 2011 May

5;117(18):4759-68. PubMed PMID: 21398221. Pubmed Central PMCID: 3100687. Epub 2011/03/15. eng.

58.   Smith E, Lin C, Shilatifard A. The super elongation complex (SEC) and MLL in development and disease. Genes & development. 2011 Apr 1;25(7):661-72. PubMed PMID: 21460034. Pubmed Central PMCID: 3070929.

59.   Kim J, Cantor AB, Orkin SH, Wang J. Use of in vivo biotinylation to study protein-protein and protein-DNA interactions in mouse embryonic stem cells. Nat Protoc. 2009;4(4):506-17. PubMed PMID: 19325547. Epub 2009/03/28. eng.

60.   Wang J, Cantor AB, Orkin SH. Tandem affinity purification of protein complexes in mouse embryonic stem cells using in vivo biotinylation. Curr Protoc Stem Cell Biol. 2009 Mar;Chapter 1:Unit1B 5. PubMed PMID: 19306258. Pubmed Central PMCID: 2782545. Epub 2009/03/24. eng.

61.   Schwieger M, Schuler A, Forster M, Engelmann A, Arnold MA, Delwel R, et al. Homing and invasiveness of MLL/ENL leukemic cells is regulated by MEF2C. Blood. 2009 Sep 17;114(12):2476-88. PubMed PMID: 19584403. Epub 2009/07/09. eng.

62.   Zhang Z, Huang L, Reisenauer MR, Wu H, Chen L, Zhang Y, et al. Widely expressed Af17 is likely not required for embryogenesis, hematopoiesis, and animal survival. Genesis. 2010 Dec;48(12):693-706. PubMed PMID: 21170927. Pubmed Central PMCID: 3069500.

63.   Chen L, Wu H, Pochynyuk OM, Reisenauer MR, Zhang Z, Huang L, et al. Af17 deficiency increases sodium excretion and decreases blood pressure. Journal of the American Society of Nephrology : JASN. 2011 Jun;22(6):1076-86. PubMed PMID: 21546577. Pubmed Central PMCID: 3103727.

64.   Shevchenko A, Wilm M, Vorm O, Mann M. Mass spectrometric sequencing of proteins silver-stained polyacrylamide gels. Analytical chemistry. 1996 Mar 1;68(5):850-8. PubMed PMID: 8779443.

65.   Peng J, Gygi SP. Proteomics: the move to mixtures. Journal of mass spectrometry : JMS. 2001 Oct;36(10):1083-91. PubMed PMID: 11747101.

66.   Yates JR, 3rd, Eng JK, McCormack AL, Schieltz D. Method to correlate tandem mass spectra of modified peptides to amino acid sequences in the protein database. Analytical chemistry. 1995 Apr 15;67(8):1426-36. PubMed PMID: 7741214.

67.   Chaplin T, Bernard O, Beverloo HB, Saha V, Hagemeijer A, Berger R, et al. The t(10;11) translocation in acute myeloid leukemia (M5) consistently fuses the leucine zipper motif of AF10 onto the HRX gene. Blood. 1995 Sep 15;86(6):2073-6. PubMed PMID: 7662954. Epub 1995/09/15. eng.

68.   Beverloo HB, Le Coniat M, Wijsman J, Lillington DM, Bernard O, de Klein A, et al. Breakpoint heterogeneity in t(10;11) translocation in AML-M4/M5 resulting in fusion of AF10 and MLL is resolved by fluorescent in situ hybridization analysis. Cancer research. 1995 Oct 1;55(19):4220-4. PubMed PMID: 7671224. Epub 1995/10/01. eng.

69.   Bohlander SK, Muschinsky V, Schrader K, Siebert R, Schlegelberger B, Harder L, et al. Molecular analysis of the CALM/AF10 fusion: identical rearrangements in acute myeloid leukemia, acute lymphoblastic leukemia and malignant lymphoma patients. Leukemia : official journal of the Leukemia Society of America, Leukemia Research Fund, UK. 2000 Jan;14(1):93-9. PubMed PMID: 10637482. Epub 2000/01/19. eng.

70.   Dreyling MH, Schrader K, Fonatsch C, Schlegelberger B, Haase D, Schoch C, et al. MLL and CALM are fused to AF10 in morphologically distinct subsets of acute leukemia with

translocation t(10;11): both rearrangements are associated with a poor prognosis. Blood. 1998 Jun 15;91(12):4662-7. PubMed PMID: 9616163. Epub 1998/06/17. eng.

71.   Yagi H, Deguchi K, Aono A, Tani Y, Kishimoto T, Komori T. Growth disturbance in fetal liver hematopoiesis of Mll-mutant mice. Blood. 1998 Jul 1;92(1):108-17. PubMed PMID: 9639506. Epub 1998/06/25. eng.

72.   Milne TA, Kim J, Wang GG, Stadler SC, Basrur V, Whitcomb SJ, et al. Multiple interactions recruit MLL1 and MLL1 fusion proteins to the HOXA9 locus in leukemogenesis. Molecular cell. 2010 Jun 25;38(6):853-63. PubMed PMID: 20541448. Pubmed Central PMCID: 2902588. Epub 2010/06/15. eng.

73.   Yokoyama A, Cleary ML. Menin critically links MLL proteins with LEDGF on cancer-associated target genes. Cancer cell. 2008 Jul 8;14(1):36-46. PubMed PMID: 18598942. Pubmed Central PMCID: 2692591. Epub 2008/07/05. eng.

74.   Thiel AT, Blessington P, Zou T, Feather D, Wu X, Yan J, et al. MLL-AF9-induced leukemogenesis requires coexpression of the wild-type Mll allele. Cancer cell. 2010 Feb 17;17(2):148-59. PubMed PMID: 20159607. Pubmed Central PMCID: 2830208. Epub 2010/02/18. eng.

75.   Milne TA, Briggs SD, Brock HW, Martin ME, Gibbs D, Allis CD, et al. MLL targets SET domain methyltransferase activity to Hox gene promoters. Molecular cell. 2002 Nov;10(5):1107-17. PubMed PMID: 12453418. Epub 2002/11/28. eng.

76.   Nakamura T, Mori T, Tada S, Krajewski W, Rozovskaia T, Wassell R, et al. ALL-1 is a histone methyltransferase that assembles a supercomplex of proteins involved in transcriptional regulation. Molecular cell. 2002 Nov;10(5):1119-28. PubMed PMID: 12453419. Epub 2002/11/28. eng.

77. Tebar F, Bohlander SK, Sorkin A. Clathrin assembly lymphoid myeloid leukemia (CALM) protein: localization in endocytic-coated pits, interactions with clathrin, and the impact of overexpression on clathrin-mediated traffic. Mol Biol Cell. 1999 Aug;10(8):2687-702. PubMed PMID: 10436022. Pubmed Central PMCID: 25500. Epub 1999/08/06. eng.

78. Klebig ML, Wall MD, Potter MD, Rowe EL, Carpenter DA, Rinchik EM. Mutations in the clathrin-assembly gene Picalm are responsible for the hematopoietic and iron metabolism abnormalities in fit1 mice. Proceedings of the National Academy of Sciences of the United States of America. 2003 Jul 8;100(14):8360-5. PubMed PMID: 12832620. Pubmed Central PMCID: 166234. Epub 2003/07/02. eng.

79. Deshpande AJ, Rouhi A, Lin Y, Stadler C, Greif PA, Arseni N, et al. The clathrin-binding domain of CALM and the OM-LZ domain of AF10 are sufficient to induce acute myeloid leukemia in mice. Leukemia : official journal of the Leukemia Society of America, Leukemia Research Fund, UK. 2011 Nov;25(11):1718-27. PubMed PMID: 21681188. Epub 2011/06/18. eng.

80. Chaplin T, Ayton P, Bernard OA, Saha V, Della Valle V, Hillion J, et al. A novel class of zinc finger/leucine zipper genes identified from the molecular cloning of the t(10;11) translocation in acute leukemia. Blood. 1995 Mar 15;85(6):1435-41. PubMed PMID: 7888665. Epub 1995/03/15. eng.

81. Feng Q, Wang H, Ng HH, Erdjument-Bromage H, Tempst P, Struhl K, et al. Methylation of H3-lysine 79 is mediated by a new family of HMTases without a SET domain. Curr Biol. 2002 Jun 25;12(12):1052-8. PubMed PMID: 12123582. Epub 2002/07/19. eng.

82. Steger DJ, Lefterova MI, Ying L, Stonestrom AJ, Schupp M, Zhuo D, et al. DOT1L/KMT4 recruitment and H3K79 methylation are ubiquitously coupled with gene transcription in mammalian cells. Molecular and cellular biology. 2008 Apr;28(8):2825-39. PubMed PMID: 18285465. Pubmed Central PMCID: 2293113. Epub 2008/02/21. eng.

83.   Caudell D, Zhang Z, Chung YJ, Aplan PD. Expression of a CALM-AF10 fusion gene leads to Hoxa cluster overexpression and acute leukemia in transgenic mice. Cancer research. 2007 Sep 1;67(17):8022-31. PubMed PMID: 17804713. Pubmed Central PMCID: 1986634. Epub 2007/09/07. eng.

84.   Dik WA, Brahim W, Braun C, Asnafi V, Dastugue N, Bernard OA, et al. CALM-AF10+ T-ALL expression profiles are characterized by overexpression of HOXA and BMI1 oncogenes. Leukemia : official journal of the Leukemia Society of America, Leukemia Research Fund, UK. 2005 Nov;19(11):1948-57. PubMed PMID: 16107895. Epub 2005/08/19. eng.

85.   Daigle SR, Olhava EJ, Therkelsen CA, Majer CR, Sneeringer CJ, Song J, et al. Selective killing of mixed lineage leukemia cells by a potent small-molecule DOT1L inhibitor. Cancer cell. 2011 Jul 12;20(1):53-65. PubMed PMID: 21741596. Epub 2011/07/12. eng.

86.   Thompson CB. Attacking cancer at its root. Cell. 2009 Sep 18;138(6):1051-4. PubMed PMID: 19766556. Epub 2009/09/22. eng.

87.   Dreyling MH, Martinez-Climent JA, Zheng M, Mao J, Rowley JD, Bohlander SK. The t(10;11)(p13;q14) in the U937 cell line results in the fusion of the AF10 gene and CALM, encoding a new member of the AP-3 clathrin assembly protein family. Proceedings of the National Academy of Sciences of the United States of America. 1996 May 14;93(10):4804-9. PubMed PMID: 8643484. Pubmed Central PMCID: 39360. Epub 1996/05/14. eng.

88.   Deshpande AJ, Cusan M, Rawat VP, Reuter H, Krause A, Pott C, et al. Acute myeloid leukemia is propagated by a leukemic stem cell with lymphoid characteristics in a mouse model of CALM/AF10-positive leukemia. Cancer Cell. 2006 Nov;10(5):363-74. PubMed PMID: 17097559.

89.   DiMartino JF, Ayton PM, Chen EH, Naftzger CC, Young BD, Cleary ML. The AF10 leucine zipper is required for leukemic transformation of myeloid progenitors by MLL-AF10. Blood. 2002 May 15;99(10):3780-5. PubMed PMID: 11986236. Epub 2002/05/03. eng.

90.   Mulaw MA, Krause AJ, Deshpande AJ, Krause LF, Rouhi A, La Starza R, et al. CALM/AF10-positive leukemias show upregulation of genes involved in chromatin assembly and DNA repair processes and of genes adjacent to the breakpoint at 10p12. Leukemia : official journal of the Leukemia Society of America, Leukemia Research Fund, UK. 2011 Nov 8. PubMed PMID: 22064352. Epub 2011/11/09. Eng.

91.   Lin YH, Kakadia PM, Chen Y, Li YQ, Deshpande AJ, Buske C, et al. Global reduction of the epigenetic H3K79 methylation mark and increased chromosomal instability in CALM-AF10-positive leukemias. Blood. 2009 Jul 16;114(3):651-8. PubMed PMID: 19443658. Epub 2009/05/16. eng.

92.   Muntean AG, Hess JL. The Pathogenesis of Mixed-Lineage Leukemia. Annual Review of Pathology: Mechanisms of Disease. 2012;7(1):null.

93.   Guenther MG, Lawton LN, Rozovskaia T, Frampton GM, Levine SS, Volkert TL, et al. Aberrant chromatin at genes encoding stem cell regulators in human mixed-lineage leukemia. Genes & development. 2008 Dec 15;22(24):3403-8. PubMed PMID: 19141473. Pubmed Central PMCID: 2607073.

94.   Balgobind BV, Raimondi SC, Harbott J, Zimmermann M, Alonzo TA, Auvrignon A, et al. Novel prognostic subgroups in childhood 11q23/MLL-rearranged acute myeloid leukemia: results of an international retrospective study. Blood. 2009 Sep 17;114(12):2489-96. PubMed PMID: 19528532. Pubmed Central PMCID: 2927031.

95.   Pigazzi M, Masetti R, Bresolin S, Beghin A, Di Meglio A, Gelain S, et al. MLL partner genes drive distinct gene expression profiles and genomic alterations in pediatric acute myeloid

leukemia: an AIEOP study. Leukemia : official journal of the Leukemia Society of America, Leukemia Research Fund, UK. 2011 Mar;25(3):560-3. PubMed PMID: 21331072.

96.   Liedtke M, Ayton PM, Somervaille TC, Smith KS, Cleary ML. Self-association mediated by the Ras association 1 domain of AF6 activates the oncogenic potential of MLL-AF6. Blood. 2010 Jul 8;116(1):63-70. PubMed PMID: 20395419. Pubmed Central PMCID: 2904581.

97.   Takahashi K, Nakanishi H, Miyahara M, Mandai K, Satoh K, Satoh A, et al. Nectin/PRR: an immunoglobulin-like cell adhesion molecule recruited to cadherin-based adherens junctions through interaction with Afadin, a PDZ domain-containing protein. The Journal of cell biology. 1999 May 3;145(3):539-49. PubMed PMID: 10225955. Pubmed Central PMCID: 2185068.

98.   Langmead B, Trapnell C, Pop M, Salzberg SL. Ultrafast and memory-efficient alignment of short DNA sequences to the human genome. Genome Biol. 2009;10(3):R25. PubMed PMID: 19261174. Pubmed Central PMCID: 2690996. Epub 2009/03/06. eng.

99.   Thorvaldsdottir H, Robinson JT, Mesirov JP. Integrative Genomics Viewer (IGV): high-performance genomics data visualization and exploration. Brief Bioinform. 2012 Apr 19. PubMed PMID: 22517427. Epub 2012/04/21. Eng.

100.   Chen L, Deshpande A, Banka D, Bernt KM, Dias S, Buske C, et al. Abrogation of MLL-AF10 and CALM-AF10 mediated transformation through genetic inactivation or pharmacological inhibition of the H3K79 methyltransferase Dot1l. Leukemia : official journal of the Leukemia Society of America, Leukemia Research Fund, UK. 2012 Nov 9. PubMed PMID: 23138183.

101.   Zhang J, Ding L, Holmfeldt L, Wu G, Heatley SL, Payne-Turner D, et al. The genetic basis of early T-cell precursor acute lymphoblastic leukaemia. Nature. 2012 Jan 12;481(7380):157-63. PubMed PMID: 22237106. Pubmed Central PMCID: 3267575.

102.   Brandimarte L PV, Giacomo DD, Gorello P, Matteucci C, Giordan M, et al. MLLT10 Gene Promiscuity Unravels Involvement of RNA Processing Genes in Pediatric T-Acute Lymphoblastic Leukemia. Blood (ASH Annual Meeting Abstract 1431). 2012;120(21).

103.   Drebin JA, Link VC, Stern DF, Weinberg RA, Greene MI. Down-modulation of an oncogene protein product and reversion of the transformed phenotype by monoclonal antibodies. Cell. 1985 Jul;41(3):697-706. PubMed PMID: 2860972.

104.   Morita H, Nagai R. Vemurafenib in melanoma with BRAF V600E mutation. The New England journal of medicine. 2011 Oct 13;365(15):1448; author reply 50. PubMed PMID: 21995398.

105.   Pollock RM, Daigle SR, Therkelsen CA, Basavapathruni A, Jin L, Allain CJ, et al. Preclinical Characterization of a Potent, Selective Inhibitor of the Protein Methyltransferase DOT1L for Use in the Treatment of MLL-Rearranged Leukemia. Blood (ASH Annual Meeting Abstract 2379) 2012;120.

106.   Barbie DA, Tamayo P, Boehm JS, Kim SY, Moody SE, Dunn IF, et al. Systematic RNA interference reveals that oncogenic KRAS-driven cancers require TBK1. Nature. 2009 Nov 5;462(7269):108-12. PubMed PMID: 19847166. Pubmed Central PMCID: 2783335.

107.   Delmore JE, Issa GC, Lemieux ME, Rahl PB, Shi J, Jacobs HM, et al. BET bromodomain inhibition as a therapeutic strategy to target c-Myc. Cell. 2011 Sep 16;146(6):904-17. PubMed PMID: 21889194. Pubmed Central PMCID: 3187920.